Bulletin of the Geological Survey of Japan, vol. 71 (4), p. 355–393, 2020

Article

Oxygen isotope analysis of Mesozoic radiolarites using SIMS

Maximilien BÔLE[1, 2, 3*], IKEDA Masayuki[2, 3], Peter O. BAUMGARTNER[1], HORI S. Rie[4], Anne-Sophie BOUVIER[1] and Duje KUKOČ[1, 5]

Maximilien BÔLE, IKEDA Masayuki, Peter O. BAUMGARTNER, HORI S. Rie, Anne-Sophie BOUVIER and Duje KUKOČ (2020) Oxygen isotope analysis of Mesozoic radiolarites using SIMS. *Bulletin of the Geological Survey of Japan*, vol. 71(4), p. 355–393, 8 figs, 3 tables, 2 appendicies.

Abstract: The oxygen isotope ($\delta^{18}O$) analysis of carbonate fossils is widely applied for palaeoceanographic analysis, whereas that of siliceous fossils is only limited partly due to technical constraints and uncertain fractionation factors. Here we used a secondary ion mass spectrometer (SIMS) for $\delta^{18}O$ of radiolarian silica, precipitated inside radiolarian molds in Mesozoic radiolarites from Japan, Italy, Switzerland and Romania in order to examine its potential for palaeoceanographic proxy. 507 measurements of the isotopic oxygen signature relative to the Vienna Standard Mean Ocean Water ($\delta^{18}O_{VSMOW}$) of 53 chert samples range between 19.8 to 35.3 ‰ overlapping with that of modern and Cenozoic radiolarian tests in the equatorial Pacific. Relatively large intra-chert variability supports that $\delta^{18}O$ of the Mesozoic radiolarian tests are not perfectly homogenized within a chert bed during the diagenetic segregation. The temporal changes in the $\delta^{18}O$ values of radiolarians ($\delta^{18}O_{radiolarians}$) show an Early-Middle Triassic slight positive excursion, a Late Triassic high plateau, an Early Jurassic negative excursion with up to 8 ‰ , a Middle Jurassic slight positive excursion, and a few light values for the Cretaceous despite of their low resolution. A comparison of $\delta^{18}O$ between radiolarian molds, conodont apatite, and the low magnesium calcium shells show overall similar secular variations during the Triassic, but different trends was observed during the Early Jurassic. Because our data is low-resolution, further cross check of $\delta^{18}O_{radiolarians}$ is necessary to use as a proxy for paleoceanography.

Keywords: $\delta^{18}O$, Mesozoic, radiolarites, radiolarians, SIMS

1. Introduction

One of the most widely used palaeoceanographic techniques is the oxygen isotope ($\delta^{18}O$) analysis of carbonate shells which reflects past environmental changes, such as temperature, ice sheet volume, and precipitation/evaporation ratio (e.g., Emiliani, 1955; Shackleton and Kennett, 1975). However, a significant caveat in the paleoceanographic analyses using carbonate shells is their scarcity or complete absence in some sediments for large sections of the globe and deep past, due to dissolution below carbonate compensation depth (CCD) and/or carbonate organism evolution in pelagic ocean after the Late Triassic. The most easily available archive of seawater $\delta^{18}O$ for such sediments is biogenic silica (BSi), such as diatoms, sponges, and radiolarians (e.g. Jaffrés *et al.*, 2007). At least, $\delta^{18}O$ values of opal have been recognized as a potential proxy of past seawater temperature and isotopic composition as referred for diatoms (Labeyrie, 1974; Mikkelsen *et al.*, 1978; Juillet-Leclerc and Labeyrie, 1987; Shemesh *et al.*, 1992, 2001; Schmidt *et al.*, 1997; Swann *et al.*, 2008; Swann and Leng, 2009; Maier *et al.*, 2013), even if this is still debated. In Southern Ocean cores, $\delta^{18}O$ values of diatoms and radiolarians show similar patterns with similar values from 43 ‰ to 45 ‰ for at least last 30 ky (cf. Abelmann *et al.*, 2015). Therefore, $\delta^{18}O_{radiolarians}$ might also be a potential proxy for paleoceanography.

Radiolarians dominated as BSi producers in Paleozoic and Mesozoic open ocean (Hein and Parrish, 1987), whereas siliceous sponges were and are today largely restricted to marginal settings, and diatoms became quantitatively important in the Cenozoic (Racki and Cordey, 2000; Kidder and Erwin, 2001). Radiolarites were deposited in

[1] Institute of Earth Sciences (ISTE), Faculty of Geoscience, Geopolis, University of Lausanne, 1015 Lausanne, Switzerland

[2] Department of Geosciences, Faculty of Sciences, Shizuoka University, 836 Ohya Suruga, Shizuoka 422-8529, Japan.

[3] Department of Earth and Planetary Science, Graduate School of Science, The University of Tokyo, 7-3-1 Hongo, Bunkyo-ku, Tokyo 113-0033 Japan

[4] Department of Earth Sciences, Faculty of Science, Ehime University, Bunkyo-cho 2-5, Matsuyama, Ehime 790-8577, Japan

[5] Croatian Geological Survey, Sachsova 2, Hr-10000 Zagreb, Croatia

[*] Corresponding author: M, BÔLE., Rue des Envers 13, 2400 Le Locle, Switzerland. Email: maximilien.bole@gmail.com

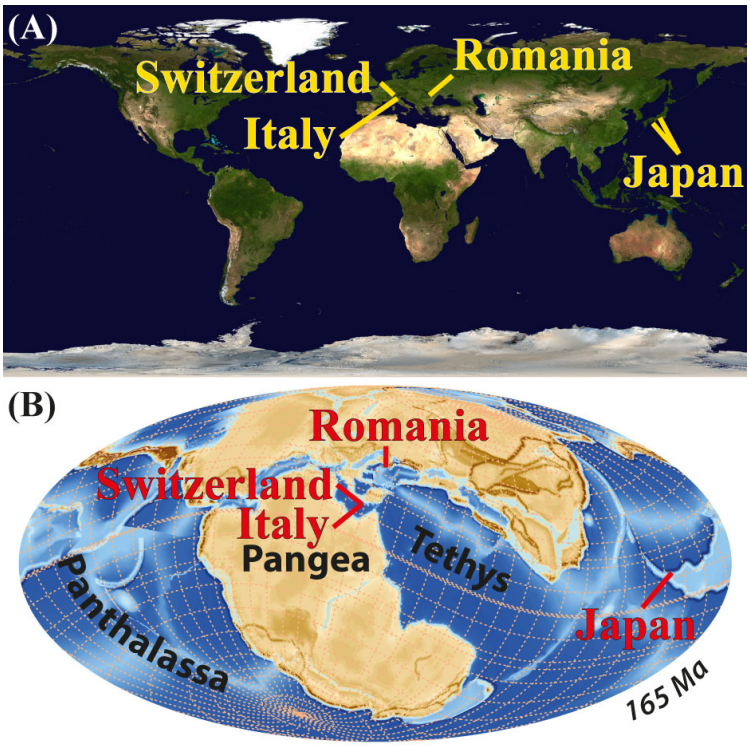

Fig. 1 Location of the studied sections (A) and their paleogeography during the Middle Jurassic (B). The Paleomap is from the Stampfli model developed at the University of Lausanne (Stampfli and Borel, 2002).

a broad low-latitude belt, and radiolarian-bearing siliceous mudstones also dominated in mid-latitudes (Baumgartner, 2013). Therefore, radiolarian $\delta^{18}O$ provides potentially important information for paleoceanography of the Paleozoic and Mesozoic.

Some evidence supports that radiolarian $\delta^{18}O$ may reflect environmental change (Knauth and Epstein, 1976; Wu *et al.*, 1997; Abelmann *et al.*, 2015). Although diagenetic isotopic fractionation of radiolarian test is still debated, even for Cenozoic (e.g. Fontorbe *et al.*, 2016), that for early Mesozoic bedded chert might be more simple system due to diagenetic segregation; This segregation results from the migration of silica from layers with low-Si content to layers with high-Si content during the transformation from opal-A to opal-CT (Isaacs, 1981; Tada, 1991). Thus, the cm-scale alternations of chert and shale might have limited migration of BSi within a chert-shale couplet. Contrary to this advantage, such diagenetic processes make extraction and picking of radiolarian molds without strong chemical procedures quite hard. To solve this disadvantage, secondary ion mass spectrometer (SIMS) is a powerful technique to measure the Mesozoic radiolarian molds on ~10 μm scale. Here we used SIMS for the Mesozoic radiolarian $\delta^{18}O$ to examine their paleoceanographic and diagenetic imprints.

2. Materials

We collected 55 chert samples from Mesozoic radiolarites in Japan, Italy, Switzerland and Romania (Fig. 1). Only fresh cherts were sampled to avoid alteration. The Triassic to Early Jurassic Panthalassan bedded cherts are distributed in the Inuyama Area from Japan (Kiso River sections; Nakaseko and Nishimura, 1979; Yao *et al.*, 1980; Mizutani and Koike, 1982; Hori, 1988; Sugiyama, 1997; Yao and Kuwahara, 1997; Carter and Hori, 2005; Ikeda and Tada, 2014). These bedded cherts consist of several tectonic imbricates outcropping along the Kiso River which were formed during the Jurassic accretion (Kimura and Hori, 1993). The Cretaceous Panthalassan radiolarites come from the Goshikikahama section (Okamura and Uto, 1982; Kodama *et al.*, 1983). We sampled Middle Jurassic Tethyan radiolarites from the Sogno section (Gaetani and Poliani, 1978; Baumgartner *et al.*, 1980; Kocher, 1981; Baumgartner, 1984; Baumgartner *et al.*, 1995; Ikeda *et al.*, 2016). Additional material (Pi01, Pe01, Ro01 and Ca01) are a Middle Jurassic radiolarite sample from the southern part of Switzerland (45°54′12″N, 8°59′55″E), a Late Permian radiolarian chert from Neo section, Japan (35°41′39″N, 136°39′25″E), a Middle Jurassic radiolarian chert from the Rarau synclinal of the Carpathian Mountain along a road going to Lagu Rosu, Romania (46°47′29″N, 25°47′32″E; Dumitrica, 1995) and a Berriasian diagenetic chert nodule from the Capriolo section in the Lombardian basin, Italy (45°38′40″N, 9°57′32″E; Weissert *et al.*, 1979; Channell *et al.*, 1987; Lini *et al.*, 1992; Föllmi *et al.*, 2012), respectively.

Bedded chert is composed of silica-rich chert layers interbedded with silica-poorer shale partings (Davis, 1918; Tada, 1991; Hori *et al.*, 1993). In radiolarian cherts, radiolarian silica can be easily distinguished from a stained matrix enclosing radiolarian molds often filled with nearly

Table 1 Raw, drift corrected, calibrated for our $\delta^{18}O_{VSMOW}$ least square mean and standard deviations on the UNIL-Q1 standard (in ‰; 2SD). The identic raw and drift corrected $\delta^{18}O_{VSMOW}$ suggests that there was no major instrumental drift during our sessions. Overall, the reproductivity of the UNIL-Q1 on the 269 measurements after calibration is 0.3 ‰ (2SD). The raw $\delta^{18}O_{VSMOW}$ of the PRIM123 session for Ki08C, Pi01 and Ca01 is in average 2.5 ‰ higher than the other session due to instrumental fractionation differences.

Session	Number of measurements	Raw $\delta^{18}O_{VSMOW}$ (‰)		Drift corrected $\delta^{18}O_{VSMOW}$ (‰)		Calibrated $\delta^{18}O_{VSMOW}$ (‰)	
		LSmean	LSstd	LSmean	LSstd	LSmean	LSstd
Prim123	48	6.5	0.3	6.5	0.3	9.8	0.3
Br2	47	4.4	0.5	4.4	0.5	9.8	0.5
Br3	31	4.5	0.4	4.4	0.4	9.8	0.3
Br4	52	3.8	0.3	3.8	0.3	9.8	0.3
Br6	28	3.7	0.3	3.7	0.3	9.8	0.3
Br7	63	3.9	0.3	3.9	0.3	9.8	0.3
All UNIL-Q1 measurements	269					9.8	0.3

pure microquartz and/or chalcedony (Bôle *et al.*, 2020). Most of these microquartz are early diagenetic products from opal-A precipitating in the pore space produced by radiolarian skeletons which are the target of this study.

3. Methods

Secondary ion mass spectrometer (SIMS) can achieve accurate in situ analyses of very small sample amount. The aim of in situ analyses in the infills radiolarian molds by SIMS is to measure the oxygen derived from their microquartz without contamination from clays or aeolian/detrital minerals present in the matrix. Microquartz infills in radiolarian molds, which are likely an early silica precipitation derived from biosilica, were analysed with a CAMECA IMS 1280HR at the University of Lausanne (e.g. Seitz *et al.*, 2016).

About 10 subsamples were mounted in each 1-inch micron-polished epoxy sample holder (Epofit resin) around an internal standard. An amorphous glass standard from the National Institute of Standard and Technology (NIST-610) was used for the initial three mounts with samples Ki08C, Pi01, and Ca01, to control instrumental drift in absence of a proper quartz standard. The quartz internal standard UNIL-Q1 (Seitz *et al.*, 2016) have been used for all mounts, including initial three samples reanalysed, to correct instrumental drift and mass fractionation. As instrumental mass fractionation on SIMS depend on minerals species (Marin *et al.*, 2010), data from chert samples are calibrated with UNIL-Q1. Before SIMS measurements, radiolarian molds and their microcrystalline quartz infill was carefully examined on each subsample on mount by optical and/or scanning electrons microscopy (SEM).

The $\delta^{18}O$ from 532 points of radiolarian molds was measured with a primary Cs+ ion beam intensity of ~2 nA, resulting in a beam diameter of ~10 µm. Electrical charges were compensated using an electron flood gun, with normal incidence and the conductivity of the sample surface was assured by a gold coating connected to electrical ground. ^{16}O and ^{18}O secondary ions, accelerated at 10 kV, were analyzed at a mass resolving power of 3000 and collected on Faraday cups (FC) multi-collection mode. The resistances of the L'2 and H'2 FC were set to 10^{10} Ω and 10^{11} Ω for the detection of ^{16}O and ^{18}O, respectively. FC were calibrated in the beginning of each session, using the calibration routine. Mass calibration was performed at the beginning of each session and every 12 h.

Each analysis took less than 4 minutes and consists of 20 cycles of 5 seconds starting with a presputtering time of 30 seconds to remove gold, stabilized the secondary ion emission allowing automatic centring of the secondary ion beam. This setting allowed an average reproducibility better than 0.3 ‰ (2 standard deviation, 2SD) on UNIL-Q1 (Seitz *et al.*, 2016; Table 1) at the beginning each session, and analytical standard deviation for each analysis lower than 0.3 ‰ (2SD). The analytical standard deviation expressed here is the standard deviation of each data from different analytical cycles. A minimum set of 4 analyses of UNIL-Q1 quartz standard (9.18 ± 0.14 ‰ (VSMOW); Seitz *et al.*, 2016), inserted in each mount, has been measured every 6-10 analyses for monitoring the instrument stability, and for accurately correcting the instrumental mass fractionation, as it can slightly differ from mount to mount. The data have been obtained in 10 different sessions for $\delta^{18}O$ measurements, over 11 months. The variation of the UNIL-Q1 quartz standard over the entire sessions is < 0.3‰ (2SD after the drift correction (Table 1).

The target locations were controlled by optical methods and SEM for each measurement to check that radiolarian molds were effectively hit. Analytical yield and standard deviation of each measurement were also used to check the validation. The analytical yield is the quantity of elements measured relative to the intensity of primary ion beam (cps/nA), and here we used relative analytical yield normalized

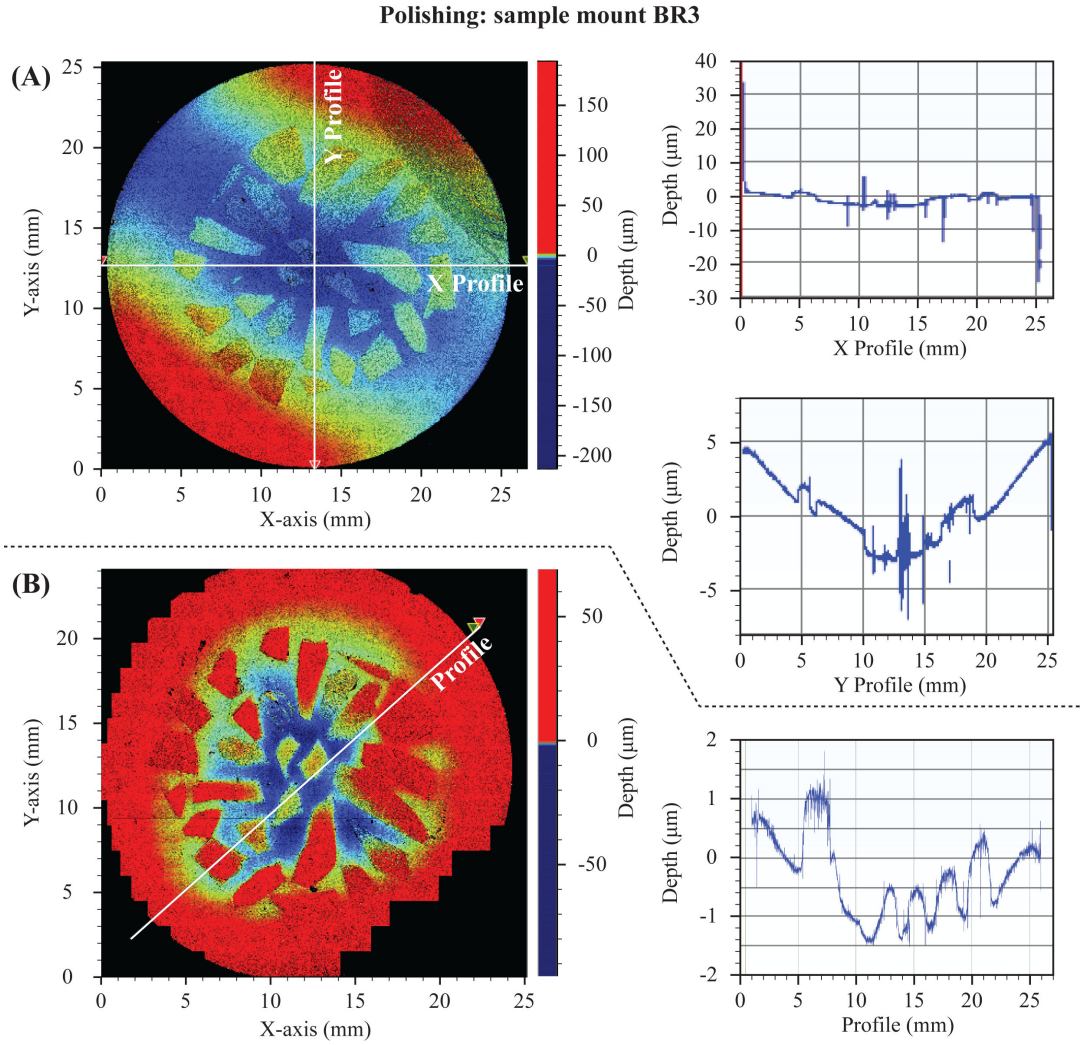

Fig.2 Topography of the sample mount BR3 after polishing. (A) Between the lower part of the rim and the centre of the sample mount, there is a difference of about 7.5 µm in depth. This difference was due to an internal tension triggered by a screw which initially hold the sample holder during the polishing. (B) After a second polishing without the screw, the topography of the rim is better and the difference between the rim and the center is reduced to 0.25 µm. The profiles on the right part are represented by white lines on the surface of the sample mount.

by that of internal standard UNIL-Q1. Different analytical yields result from the nature of the analysed material (mineral species and matrix effect) and from the topography of the analysed surface, which modifies the incident angle of the primary ion beams and thus the energy per surface of the primary ion beam. Therefore, the planarity of our sample mounts after polishing up to 0.25 µm was checked using white light profilometer (Brucker: Countour GT; Fig. 2) to have elevation differences of less than 1.5 µm between the standard and the samples. High analytical standard deviation depends on isotopic heterogeneities in the analysed minerals, but also on modifications of the instrumental mass fractionation which could be triggered by changes of the analytical conditions (topography, beam and analyser stability) or by the analyses of a mixture of silica, clay minerals and oxides. Overall, analytical yield similar to the one of our UNIL-Q1 standard (~ 7.9 cps/nA, but depends on sessions) and analytical standard deviation lower than 0.35 ‰ (2SD) are objective criterions to decide if a measurement should be accepted.

The drift correction was realized using a least square regression line weighted for incertitude (σ_i^2). For the calibration, the weighted δ^{18}O-mean ($\underline{\dot{x}}$) and standard deviation ($\dot{\sigma}_i$) for the internal standard was calculated also using the incertitude (Equation 1 and 2) to keep consistent data processing with the least square drift correction. The calibrated δ^{18}O for samples ($\delta^{18}O_{VSMOW}$ *Spl*), depend on each sample measurement ($\delta^{18}O$ $Spl_{measured}$) and are proportional to the measured least square δ^{18}O-mean and the true $\delta^{18}O_{VSMOW}$ from the internal standard ($\delta^{18}O$ $Std_{measured}$ and $\delta^{18}O_{VSMOW}$ *Std*, respectively) (Equation 3). The errors on the calibrated δ^{18}O (σ ($\delta^{18}O_{VSMOW}$ *Spl*)) were

obtained by error propagation (Equation 4). The weighted means and standard deviations (Table 2 and Appendix Table A1) were then calculated for each sample following equation 1 and 2. Conversion from VSMOW to VPDB was realized using the Equation 5 (Kim *et al.*, 2015). For comparison, $\delta^{18}O$ values relative to the Vienna Pee Dee Belemnite standard for low magnesium calcium shells ($\delta^{18}O_{VPDB}$ LMC) from Grossman (2012) were digitalized using PlotDigitizer (2.6.8).

Equation 1

$$\dot{\underline{x}} = \sum \left(\frac{1}{\sigma_i^2} \times x_i\right) / \left(\frac{1}{\sigma_i^2}\right)$$

Equation 2

$$\dot{\sigma_i} = \sqrt{\sum \left(\frac{1}{\sigma_i^2} \times (x_i - \dot{\underline{x}})^2\right) / \sum \left(\frac{1}{\sigma_i^2}\right) \times \frac{N}{N-1}}$$

Equation 3

$$\delta^{18}O_{VSMOW\ Spl} = x_i = \left(\left(\left(1 + \frac{\delta^{18}O\ Spl_{measured}}{1000}\right) \Big/ \frac{(1 + \delta^{18}O\ Std_{measured} / 1000)}{(1 + \delta^{18}O_{VSMOW\ Std} / 1000)}\right) - 1\right) \times 1000$$

Equation 4

$$\sigma\left(\delta^{18}O_{VSMOW\ Spl}\right) = \sqrt{\left(\frac{\partial F}{\partial V_1} \times dV_1\right)^2 + \left(\frac{\partial F}{\partial V_2} \times dV_2\right)^2 + \left(\frac{\partial F}{\partial V_3} \times dV_3\right)^2}$$

With $F = \delta^{18}O_{VSMOW\ Spl}$, $V_1 = \delta^{18}O\ Spl_{measured}$, $V_2 = \delta^{18}O\ Std_{measured}$ and $V_3 = \delta^{18}O_{VSMOW\ Std}$

Equation 5

$$\delta^{18}O_{VSMOW} = 1.0392 \times \delta^{18}O_{VPDB} + 30.92\ ‰$$

4. Results

Here we present some raw data from the SIMS to illustrate the measurements of single radiolarian molds and their validation. Raw results from repetitive measurements on some samples are also described to highlight reproducibility of our analyses. Finally, we present the $\delta^{18}O_{VSMOW}$ trends from our measurements through the Mesozoic.

4. 1 Quality 234 check of SIMS analyses

We validate the quality of the SIMS measurement by post-checking of analysed spots by optical and/or SEM, and relative analytical yield. Illustrating the necessity of the pre- and post-checking, some spherical zones on the Late Triassic Inuyama chert sample Ki48 (Fig. 3A and B) are difficult to be identified as radiolarian molds or epoxy, and have been measured with very low analytical yield (~3 % of the UNIL-Q1 yield) and very light $\delta^{18}O_{RAW}$ (uncalibrated $\delta^{18}O$) (<-30 ‰) (Appendix Table A2). The normal analytical yield and $\delta^{18}O_{RAW}$ of this sample (e.g. Fig. 3C) are ~97.8 % and ~25 ‰, respectively, with calibrated $\delta^{18}O_{VSMOW}$ of ~31.3 ‰.

The measurements of mixings of epoxy and radiolarian molds for some analytical spots have low analytical yields and light $\delta^{18}O_{RAW}$-values. Such value can be found in an Early Triassic siliceous mudstone sample Ki12s from Inuyama (e.g. Fig. 3E). The detection of potential analytical sites in this sample is particularly difficult due to scarcity of radiolarian molds. Alternatively, we also commonly observed quartz patches, which could be the result from radiolarian silica precipitation, aleatory distributed that we tried to analyse (Fig. 3D). The post checking of these patches was nearly impossible due to their small size (smaller or equal to the 10 μm beam size) and we exclude them because they have usually low analytical yield (<90 %). The measurement of one of these patches has however a relatively good yield (94.9 %) but an uncommon light $\delta^{18}O_{RAW}$ (2.8 ‰), corresponding to a calibrated $\delta^{18}O_{VSMOW}$ of 8.7 ‰ (Fig. 3D).

High analytical $\delta^{18}O$-yields were measured in the Middle Jurassic Sogno sample So29 (~130.2 %). SEM-EDX analyses demonstrate that the molds in this sample were filled with carbonates, and that the matrix is more siliceous (Fig. 4). This observation contrasts with the radiolarian molds being commonly more siliceous than the matrix, which contains clays (Fig. 5 and Fig. 6).

4. 2 Reproducibility of SIMS measurements for radiolarian $\delta^{18}O$

Three chert samples (Pi01, Ki08C, Ca01) have been initially measured in detail relative to the NIST-610 standard, and then together relative to UNIL-Q1 standard (Table 3). NIST-610 was used to correct instrumental drift, but not to calibrate $\delta^{18}O$ measurements because the instrument fractionation depends on matrix and structure of the material analysed, mainly chert in this study. Overall, reproducibility on the UNIL-Q1 standard was 0.3 ‰ for $\delta^{18}O$ over all SIMS sessions (Table 1).

In detail, $\delta^{18}O$-measurements on Pi01 (a Middle Jurassic radiolarite sample in the southern Switzerland) with NIST-610 were done during two sessions. Uncalibrated $\delta^{18}O$-results for Pi01 after drift correction for the first and second sequences are 28.2 ± 1.5 ‰ (10 points, 2SD) and 28.4 ± 5.1 ‰ (27 points, 2SD) with NIST-610 values at 10.4 ± 0.2 ‰ (5 points, 2SD) and 10.8 ± 0.4 ‰ (16 points, 2SD), respectively. $\delta^{18}O$-measurements on Ki08C (a Middle Triassic chert in Inuyama) and Ca01 (a diagenetic chert lacking radiolarian molds in the Cretaceous Maiolica Formation of the Lombardian basin) were measured relative to NIST-610 during single session. Uncalibrated $\delta^{18}O$-results for Ki08C after drift correction

Table 2 List of samples with their age, the number of measurements, their $\delta^{18}O$ least square mean (LS-mean) and their $\delta^{18}O$ least square standard deviation (LS std; 1SD). The $\delta^{18}O$ was average with a 10 Ma windows moving average (5 Ma step) and compared with $\delta^{18}O$ from low magnesium carbonate shells for tropical and temperate regions (Grossman, 2012).

Sample	Age (Ma)	Number of measurements	Results		Curves			
			$\delta^{18}O_{Vsmow}$ (‰)		$\delta^{18}O_{VSMOW}$ Radiolarian molds (‰)		$\delta^{18}O_{VPDB}$ LMC shells (‰)	
			This study		This study		Grossman, 2012	
			LS-mean	LS-std	Panthalassa	Tethys	Tropical	Temperate
					10 Ma moving average		4 Ma moving average	
Pe01	253.15	10	24.0	0.2	27.21		-3.0	
Ki09	250.30	9	29.3	0.4	28.15			
Ki01	248.00	10	30.9	1.4	28.57			
Ki02	247.80	6	30.8	1.0	28.60			
Ki03s	247.20	4	20.9	2.3	28.69			
Ki03s	247.20	5	23.9	1.1	28.69			
Ki03	247.20	10	30.4	0.7	28.69			
Ki04	246.60	9	31.3	0.9	28.79			
Ki06	245.25	6	31.9	1.2	29.00		-4.0	
Ki07	245.00	6	29.3	1.8	29.04		-4.1	
Ki08	244.90	10	30.6	1.0	29.06		-4.1	
Ki08	244.90	86	30.8	0.6	29.06		-4.1	
Ki58C	243.48	6	31.2	0.7	29.24		-4.3	
Ki57	241.00	9	26.8	1.8	29.56		-3.8	
Ki15	228.00	10	31.5	0.7	31.49		-2.5	
Ki51	219.00	6	31.9	0.3	31.35		-2.1	
Ki48	217.09	3	30.6	0.9	31.52		-2.1	
Ki46	210.27	10	32.6	1.6	32.55		-1.8	
Ki44	204.82	9	31.6	0.4	31.48		-1.7	
Ki43s	204.82	6	31.3	0.4	31.48		-1.7	
Ki39	201.50	9	31.4	0.5	31.48			
Ki40	201.50	10	31.7	0.6	31.48			
Ki41	201.50	10	31.4	0.8	31.48			
Ki42	201.50	10	31.4	0.5	31.48			
Ki35	185.62	9	30.0	0.4	28.92		-0.8	
Ki34s	184.37	1	30.8	0.0	28.66		-1.0	
Ki34s	184.37	8	25.8	1.4	28.66		-1.0	
Ki32	184.20	10	30.2	0.9	28.62		-1.1	
Ki24	182.00	6	30.8	0.7	28.22		-1.9	
Ki25	180.66	8	25.2	2.5	27.97		-2.4	
Ki22c1	178.00	9	27.0	1.2	26.90		-2.7	
Ki22c2	178.00	6	26.1	1.5	26.90		-2.7	
Ki21	178.00	10	27.2	1.1	26.90		-2.7	
Ki20	174.00	5	21.9	1.9	24.76		-2.3	
So07	169.50	6	32.5	0.8		33.53		0.3
So08	169.50	7	34.0	0.4		33.53		0.3
So09	169.30	6	34.3	0.4		33.54		0.3
So12	168.27	6	35.0	0.5		33.63		0.3
So13	168.13	9	34.3	0.4		33.64		0.3
So15	167.54	6	34.7	0.5		33.69		0.4
So17	166.89	9	32.7	2.6		33.75		0.5
So21	166.09	6	32.3	1.0		33.81		0.5
Ro01	166.00	6	30.9	0.8		33.82		0.5
So23	165.10	6	34.0	0.6		33.90		0.4
So25	164.31	9	35.3	0.3		34.06		0.3
Pi01	163.00	32	34.6	0.4		34.35		-0.1
So26	162.65	6	35.1	0.3		34.43		-0.2
So28	161.14	8	34.7	0.7		34.76		-0.4
So31	159.97	9	35.2	0.3		35.02		-0.5
Ca01	139.00	10	34.3	0.2		34.36		-0.3
Go68	131.70	6	26.5	0.6	26.49		-0.3	
Go73	97.95	9	28.5	1.0	24.09		-2.6	
Go74	97.59	10	19.8	0.7	24.09		-2.8	

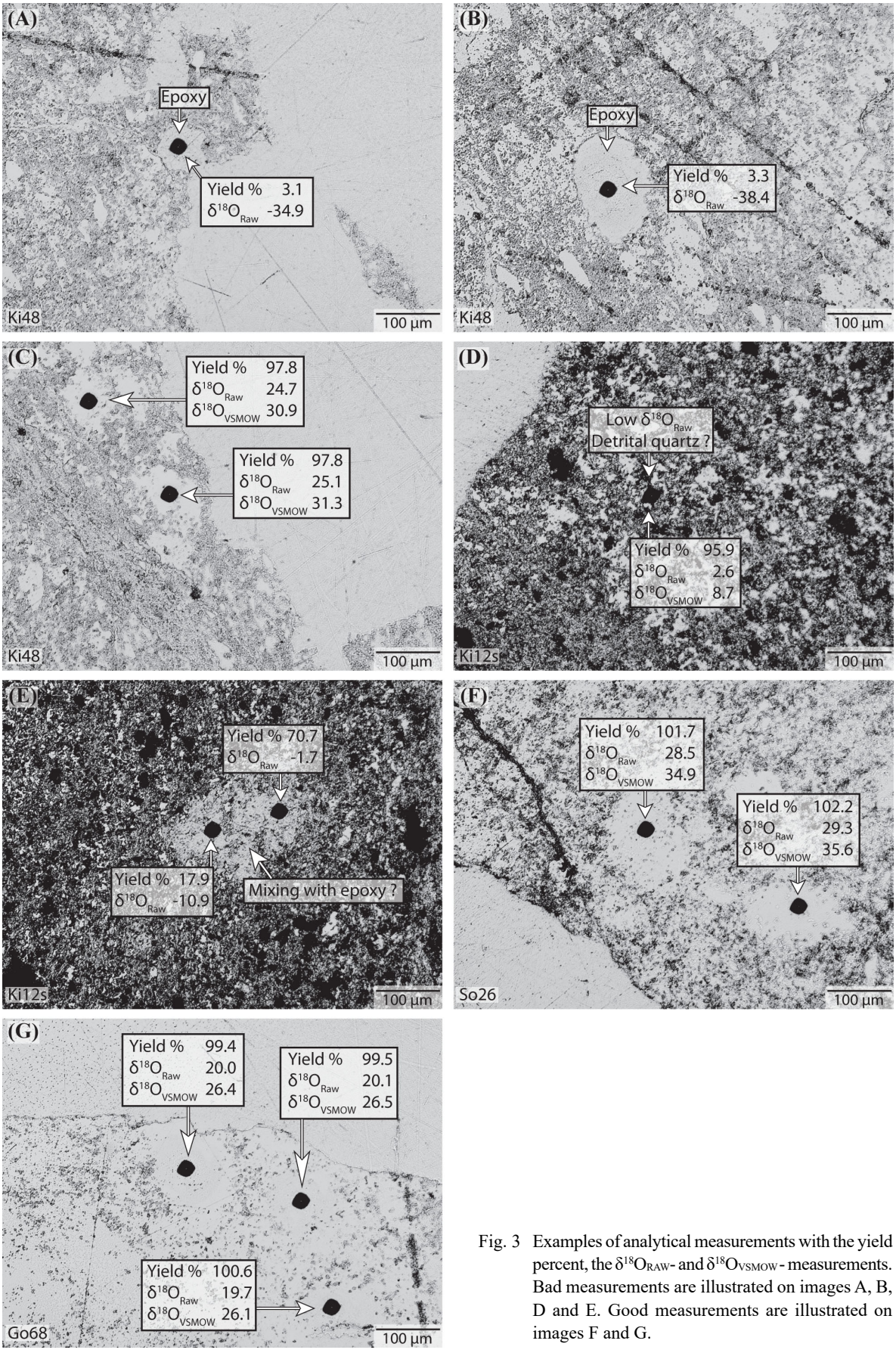

Fig. 3 Examples of analytical measurements with the yield percent, the $\delta^{18}O_{RAW}$- and $\delta^{18}O_{VSMOW}$- measurements. Bad measurements are illustrated on images A, B, D and E. Good measurements are illustrated on images F and G.

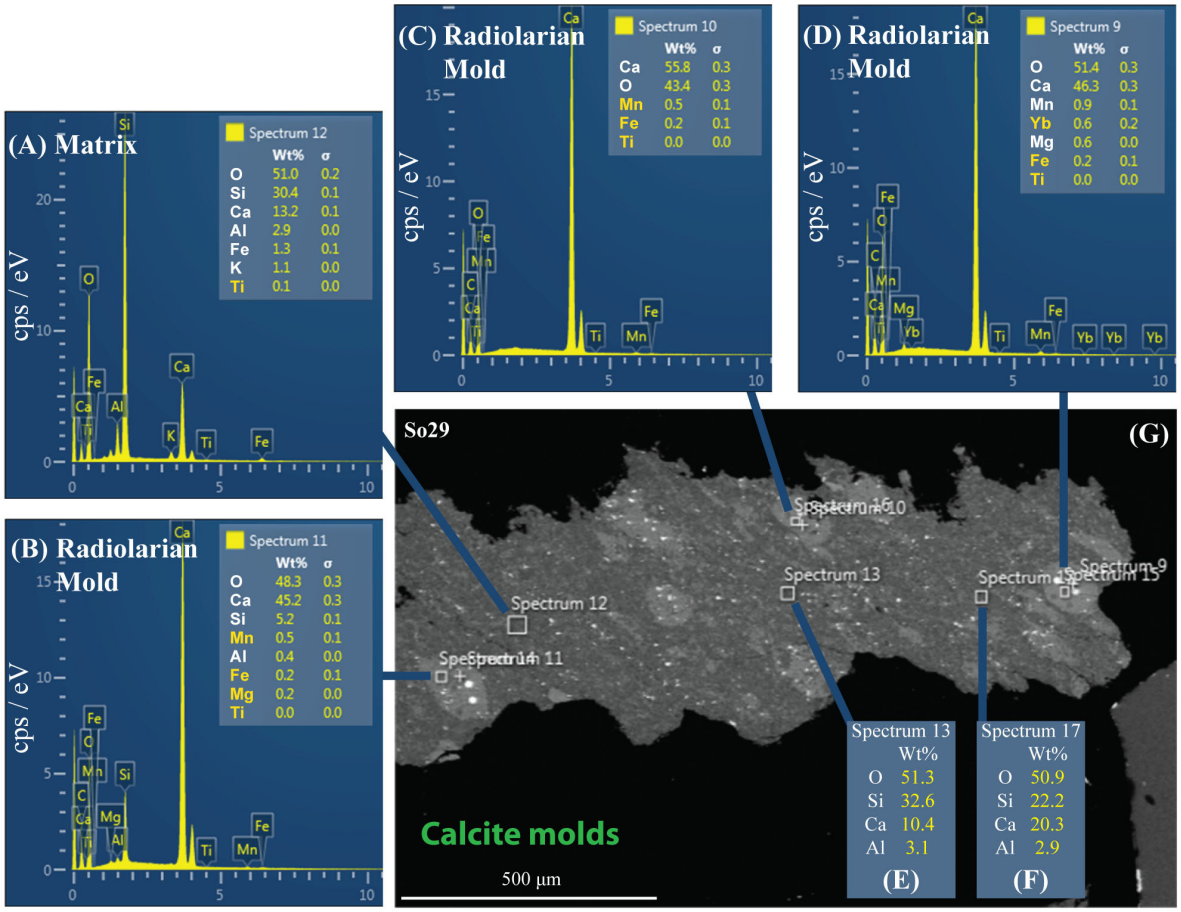

Fig. 4 EDX analyses of sample So29 with SEM. The EDX spectrums prove that the molds were filled with calcites in this sample (B, C and D) during diagenesis. The $\delta^{18}O$- and $\delta^{30}Si$-yields were respectively about 130.2 % and 11 % of the UNIL-Q1 quartz standard yield. The matrix is more siliceous but also included some carbonates (A, E, F). BSE image is show in (G).

are 25.4 ± 1.8 ‰ (27 points, 2SD) for radiolarians, 23.6 ± 1.2 ‰ (3 points, 2SD) for the matrix and 10.5± 0.4 ‰ (16 points, 2SD) for NIST-610. Uncalibrated $\delta^{18}O$-results for Ca01 after drift correction are 29.0 ± 1.6 ‰ (11 points, 2SD) for sample and 10.6 ± 0.2 ‰ (8 points, 2SD) for NIST-610.

The samples Pi01, Ca01 and Ki08C were then measured together during a single session relative to UNIL-Q1 (PRIM123) to calibrate oxygen isotopes correcting instrumental mass fractionation due to the mineralogy of samples (chemical composition and crystal structure). Uncalibrated $\delta^{18}O$-results after drift correction for this UNIL-Q1 session are 6.5 ± 0.3 ‰ (48 points, 2SD) for UNIL-Q1, 31.2 ± 0.7 ‰ (32 points, 2SD) for Pi01, 27.4 ± 1.2 ‰ (86 points, 2SD) for Ki08C, and 30.9 ± 0.4 ‰ (10 points, 2SD) for Ca01, respectively. Measurements of the base, middle and top of samples Ki08C are 27.3 ± 0.6 ‰ (4 points, 2SD), 27.9 ± 1 ‰ (28 points, 2SD) and 27.0 ± 1 ‰ (15 points, 2SD), respectively, with the average value of 27.4 ± 1.2 ‰ (86 points, 1SD).

Between the NIST-610 and the UNIL-Q1 sessions, we observed an $\delta^{18}O$-offset of ~2.4 ± 1.2 ‰ for the uncalibrated $\delta^{18}O$ of the samples Pi01, Ki08C and Ca01. However, the $\delta^{18}O$-results for Ki08C are systematically lighter of about 3.3 ± 0.9 ‰ (2SD) than the two other samples (Pi01 and Ca01). Moreover, it is interesting to note that UNIL-Q1 has an uncalibrated $\delta^{18}O$ of 6.5 ± 0.3 ‰ during the PRIM123 session whereas UNIL-Q1 has an average value of 4.0 ± 0.7 ‰ during the other session, and that correspond relatively well with the ~2.4 ± 1.2 ‰ offset detected (Table 2).

4. 3 Mesozoic $\delta^{18}O_{radiolarians}$ trends and fluctuations

Here, we present the $\delta^{18}O_{VSMOW}$ trends after having checked and calibrated our results (Fig. 7 and Fig. 8). The Early Triassic to Early Jurassic Panthalassan samples from the Inuyama area have least square means (LS-means) $\delta^{18}O_{VSMOW}$ range from 20.9 ‰ to 32.6 ‰. The Early to Middle Triassic LS-means $\delta^{18}O_{VSMOW}$ range from 20.9 ‰ to 31.9 ‰ with a slightly increasing trend. The Late Triassic LS-means $\delta^{18}O_{VSMOW}$ range has relatively low variation between 30.6 ‰ to 32.6 ‰. The Early Jurassic LS-means $\delta^{18}O_{VSMOW}$ range from 21.9 ‰ to 30.8 ‰ with a decreasing trend.

In the Middle Jurassic Lombardian basin of the Tethys, the LS-means $\delta^{18}O_{VSMOW}$ values are relatively high from

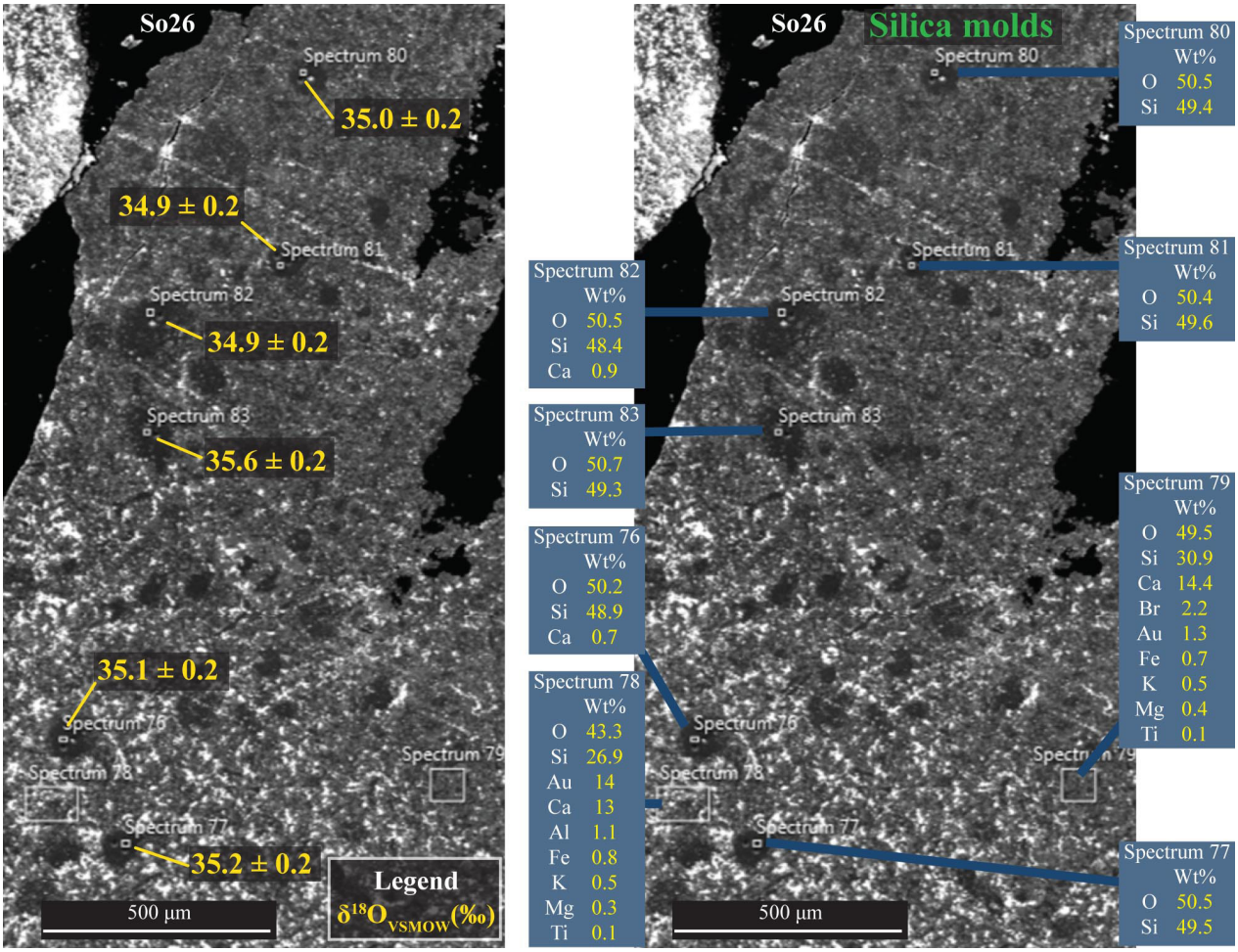

Fig. 5 Comparison between $\delta^{18}O_{VSMOW}$ and the chemical composition estimated by SEM-EDX spectrum in sample So26.

32.3 ‰ to 35.3 ‰. Our Middle Jurassic radiolarite sample from southern Switzerland (Pi01) has a LS-mean of 34.6 ‰, which is coherent with the other $\delta^{18}O$ range from the Sogno section in north Italy. A Berriasian diagenetic chert (Ca01) from the Lombardian basin has similar LS-means of 34.3 ‰. However, our Middle Jurassic Romanian sample (Ro01) has lighter $\delta^{18}O_{VSMOW}$ (30.9 ‰).

For the Cretaceous, the $\delta^{18}O_{VSMOW}$ values of the Goshikigahama samples are relatively light. A Hauterivian sample has a LS-mean 26.5 ‰, and two other Cenomanian samples have LS-means of 28.5 ‰ and 19.8 ‰.

5. Discussion

5. 1 Quality of the SIMS analysis

To evaluate quality of SIMS results, we examined analytical yields relative to UNIL-Q1 yield, in addition to optical check. We rejected analytical spots with low yield values, generally <90 %, potentially the measurement of a mixing with epoxy or other minerals. Even if the spot analysed of the Early Triassic Inuyama shale sample Ki12s on Fig. 3D was discarded after optical control, it is interesting to note that it has one of the best analytical yield (94.9 %) of the spots measured in Ki12s. In this sample, radiolarian molds are scarce, but quartz patches are common. The quartz patches are potentially precipitated radiolarian silica, but could be a diagenetic product. Its $\delta^{18}O_{RAW}$ is very light (2.8 ‰), corresponding to a calibrated $\delta^{18}O_{VSMOW}$ of 8.7 ‰. Such light value is common for igneous quartz (e.g. Seitz *et al.*, 2016), metamorphic quartz or eventually diagenetic quartz (cf. Bindeman, 2008), but not for radiolarian molds (e.g. Viswanathan and Mahabaleswar, 2014). We thus discarded this measurement.

The chemical composition of some excluded molds was also checked by SEM-EDX. SEM-EDX shows calcium as the first major element of the radiolarian molds in chert sample So29 from Sogno section (Fig. 4), and too high analytical $\delta^{18}O$-yields (~130.2 %) were measured in this sample. Therefore, the chemical composition of these radiolarian molds is necessary to be checked before interpretation of isotopic data. In total, 53 samples and 507 measurements passed our checking from the initial 55 samples and 532 measurements.

Calibration of our measurements requires to know the nature of our samples (mineralogy and chemical

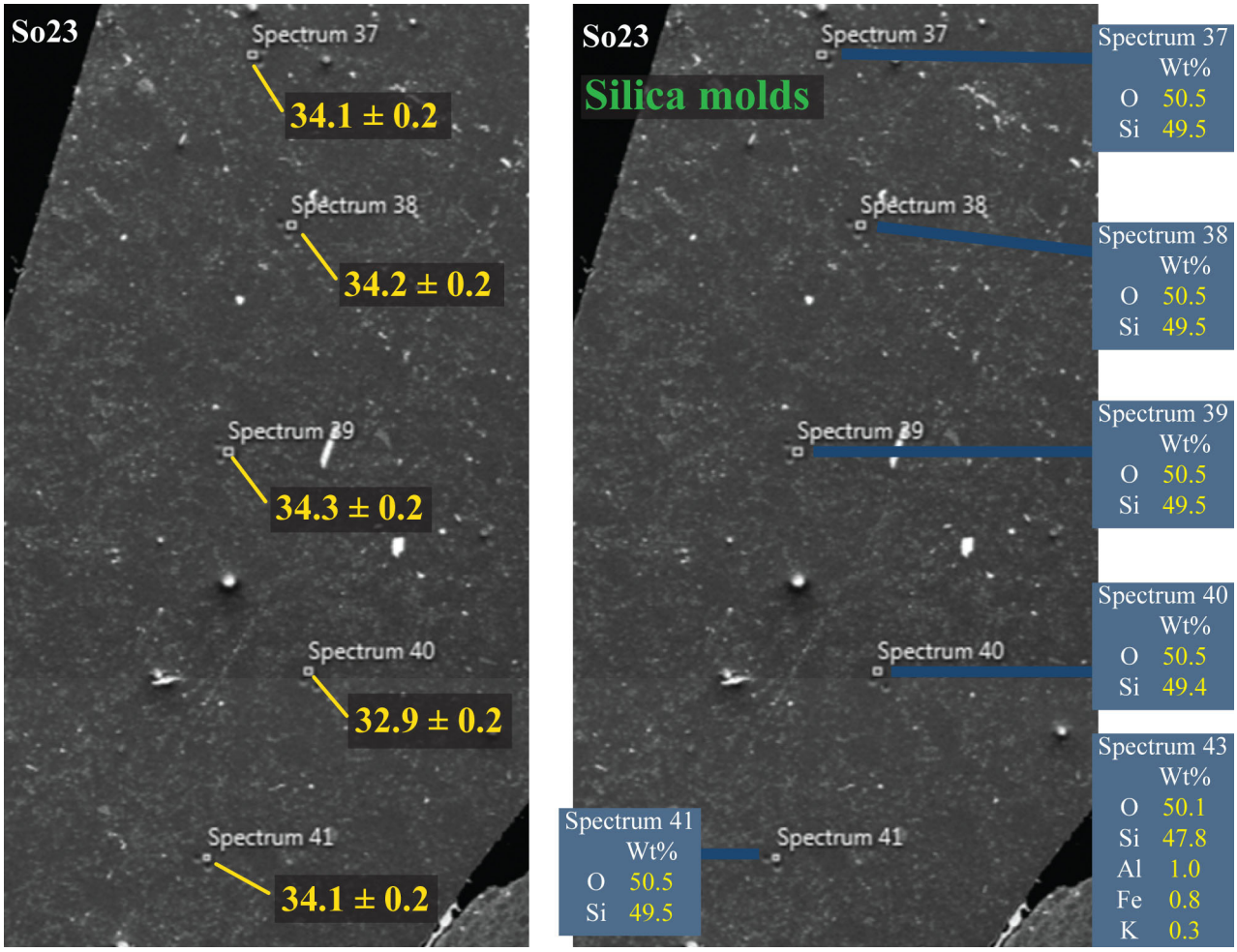

Fig. 6 Comparison between $\delta^{18}O_{VSMOW}$ and the chemical composition estimated by SEM-EDX spectrum in sample So23.

composition), because it affects the instrumental fractionation. If we correct the offset of 2.4 ± 1.2 ‰ between the NIST-610 glass standard and the UNIL-Q1 quartz standard using the initial chert samples (Pi01, Ki08C, and Ca01) as references, values of the UNIL-Q1 standards should be about 6.4 ‰ lighter than the NIST standard. This difference is in contradiction with absolute value of UNIL-Q1 standard (9.81 ± 0.14 ‰, VSMOW, 2SD) and of NIST-610 standard (10.79 ‰, VSMOW following GEOREM database from Jochum *et al.*, 2005), and might be explained by different instrumental fractionations between quartz and silica glass (amorphous material). Similar instrumental fractionations having already been inferred between microquartz, filling radiolarian molds, and quartz (Marin *et al.*, 2010), it is likely that the instrumental fractionation is different with silica glass. Higher uncalibrated $\delta^{18}O$ values for radiolarian molds (25.4 ± 1.8 ‰, 2SD) than for the matrix (23.6 ± 1.2 ‰, 2SD) in sample Ki08C might also be the result of a different instrumental fractionation between pure quartz in radiolarian molds and the mineral mixture in the matrix (matrix effect).

The $\delta^{18}O$-values relative to VSMOW calibrated by UNIL-Q1 are 34.55 ± 0.4 ‰ (32 points, 1SD) for Pi01, 30.75 ± 0.61 ‰ (86 points, 1SD) for Ki08C and 34.33 ± 0.23 ‰ (10 points, 1SD) for Ca01. These intra-sample and inter-sample $\delta^{18}O$-variability in radiolarite molds are larger than instrumental resolution (<0.3 ‰, 2SD), indicating that our measurements represent some signatures in addition to instrumental uncertainties.

Our $\delta^{18}O_{VSMOW}$ ranges from LS-means (19.8 ‰ to 35.3 ‰; Fig. 8) is also consistent with the 18 ‰ to 38 ‰ of bulk $\delta^{18}O_{VSMOW}$ of Phanerozoic cherts by Knauth (1973). This further supports the validity of our SIMS $\delta^{18}O$ measurements and our calibration routine.

5. 2 SIMS $\delta^{18}O$ from radiolarian molds and diagenetic effects

We here discuss some of the factors influencing the $\delta^{18}O_{radiolarians}$ based on our data and comparison with other dataset. Numbers of factors could have influenced on $\delta^{18}O_{radiolarians}$ in Mesozoic cherts, including such as: 1) temperature and $\delta^{18}O$ of seawater for oxygen in original radiolarian opal-A as referred for diatoms (e.g. Juillet-Leclerc and Labeyrie, 1987; Brandriss *et al.*, 1998), 2) Vital effects (Swann *et al.* 2007), 3) Dissolution and

Table 3 Comparison of our SIMS $\delta^{18}O$ least square means and standard deviations (in ‰; 2SD) for the samples Pi01, Ki08C and Ca01 between their NIST-610 and UNIL-Q1 sessions. Raw $\delta^{18}O_{VSMOW}$ of our samples are slightly shifted between the NIST-610 and UNIL-Q1 sessions due to changes of the analytical parameters but they conserve a similar pattern (~2.5 ‰). Least square standard deviations do not change between raw and drift corrected $\delta^{18}O_{VSMOW}$ indicating that there were no major instrumental drifts during our sessions.

	Sample	Points	Yield (CPS/nA)			Raw $\delta^{18}O_{VSMOW}$ (‰)		Drift corrected $\delta^{18}O_{VSMOW}$ (‰)		Calibrated $\delta^{18}O_{VSMOW}$ (‰)	
			Mean	Std	Yield % relative to NIST-610	LS-Mean	LS-Std	LS-Mean	LS-Std	LS-Mean	LS-Std
NIST Sessions	NIST-610	5	9.37E+08	4.55E+06		10.5	0.2	10.4	0.2		
	Pi01	10	9.65E+08	6.18E+06	102.9%	28.2	1.5	28.2	1.5		
	NIST	16	9.28E+08	3.43E+07		10.8	0.4	10.8	0.4		
	Pi01	27	9.49E+08	3.29E+07	102.2%	28.4	5.1	28.4	5.1		
	NIST-610	16	9.04E+08	7.96E+06		10.5	0.4	10.5	0.4		
	Ki08C	27	9.17E+08	1.65E+07	101.5%	25.4	1.8	25.4	1.8		
	Matrix	3	8.96E+08	1.49E+07	99.1%	23.6	1.2	23.6	1.2		
	NIST-610	8	9.41E+08	1.65E+07		10.6	0.2	10.6	0.1		
	Ca01	11	9.52E+08	6.01E+06	101.1%	29.0	1.6	29.0	1.6		
UNIL-Q1 Session	UNIL-Q1	48				6.5	0.3	6.5	0.3	9.8	0.3
	Ki08C base	4				27.3	0.6	27.3	0.6	30.7	0.6
	Ki08C med	28				27.9	1.0	27.9	1.0	31.2	1.0
	Ki08C top	15				27.0	1.0	27.0	1.0	30.4	1.0
	Total Ki08C	86				27.4	1.2	27.4	1.2	30.8	1.2
	Pi01	32				31.2	0.7	31.2	0.7	34.6	0.8
	Ca01	10				30.9	0.4	30.9	0.4	34.3	0.5

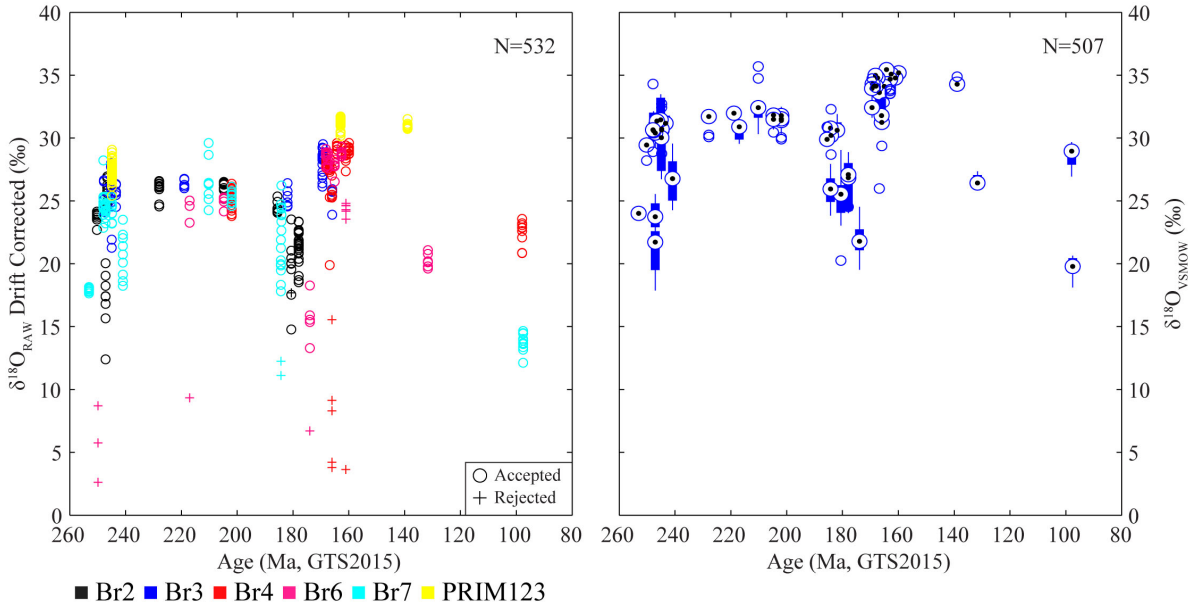

Fig. 7 $\delta^{18}O$-measurements in function of sample mounts on left and boxplot for each sample on the right. For the measurements, each color corresponds to a sample mount showing that samples of similar age tend to converge toward similar $\delta^{18}O$. Cross makers correspond to analyses with lower analytical yields, uncommon internal analytical errors or which did not pass the microscopic checking. Based on these parameters, these values are not considered as valid and excluded for the boxplot diagrams and the average values of samples. Br2 to 7 and PRIM123 are the session names.

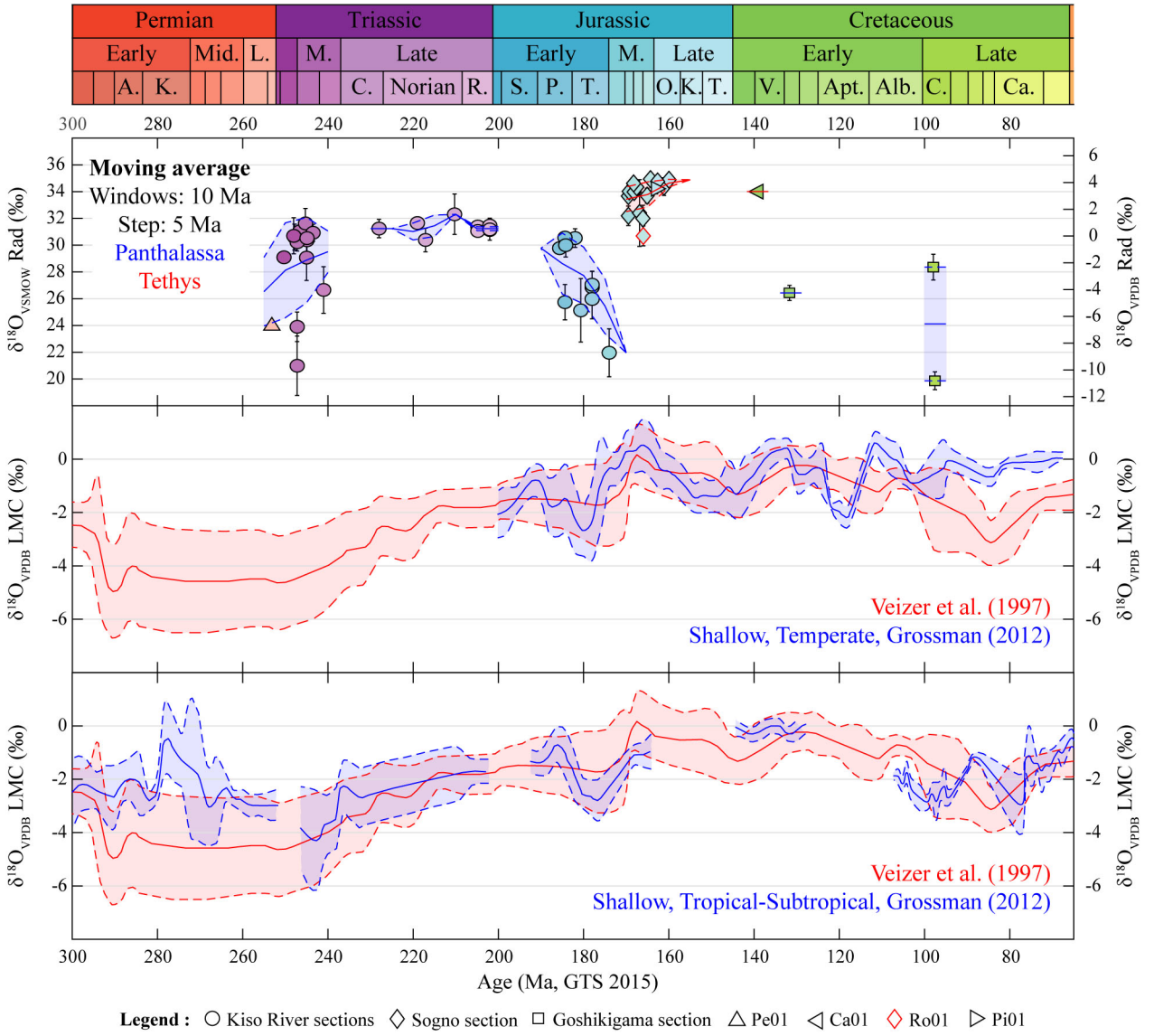

Fig. 8 Comparison between $\delta^{18}O$ from radiolarian silica ($\delta^{18}O$ Rad; this study) and digitalized curves for $\delta^{18}O$ from low magnesium calcite shells ($\delta^{18}O$ LMC; Veizer *et al.*, 1999 and Grossman, 2012), expressed either relative to the Vienna Standard Mean Ocean Water ($\delta^{18}O_{VSMOW}$) or to the Vienna Pee Dee Belemnite standard ($\delta^{18}O_{VPDB}$). The minimum values of $\delta^{18}O$ measured in radiolarian silica correspond to light values in the LMC curves during the Early Triassic, the Toarcian and eventually during the Early Cretaceous. In addition, the Middle Jurassic acme is also recorded with heavier $\delta^{18}O$ in the radiolarites. The geological timescale (GTS 2015) used for this figure is the timescale of the international commission of stratigraphy in 2015 based on Cohen *et al.* (2013). The color filling inside markers corresponds to the color of the geological stage. The boundaries of curves, when plotted, are equivalent to 1SD. The moving averages for radiolarian silica are realized separately for Panthalassa and Tethys using both a 10 Ma windows and 5 Ma steps. The $\delta^{18}O$ error bars correspond to the least square standard deviation of samples presented in Table 2.

dehydroxylation during settling and early diagenesis preferentially releasing light ^{16}O as for diatom frustules (see Schmidt *et al.* 2001; Moschen *et al.*, 2006; Swann and Leng, 2009), 4) Diagenetic temperature and isotopic composition of sediment pore water (e.g. Matheney and Knauth, 1993). In addition to these factors, we can not exclude that $\delta^{18}O$ is also influenced by 5) degree of diagenetic migration of opal-A during the phase transitions from opal-A to quartz via opal-CT, which is mainly controlled by the solubilities of the different phases (e.g. Gunnarsson *et al.*, 2000) and 6) partially by kinetic isotopic fractionation associated with silica tetrahedrons, which at least occur for $\delta^{30}Si$ during silica precipitation under 200 °C (see He and Liu, 2015; Pollington *et al.*, 2016). Factors influencing the kinetic of the phase transitions from opal-A to quartz via opal-CT, such as temperature

(Ernst and Calvert, 1969; Dralus *et al.*, 2011) and pH of pore water associated with the presence of accessory minerals (c.f. Kastner *et al.*, 1977; Isaacs, 1981; Hinman, 1998) might thus also have some influences.

In the Cenozoic unconsolidated sediments, $\delta^{18}O_{radiolarians}$ ranges from 21 ‰ to 35 ‰ in equatorial Pacific (Wu *et al.*, 1997) and from 42 ‰ to 45 ‰ in Southern Ocean (e.g. Abelmann *et al.*, 2015), possibly related with different oceanographic setting. The former $\delta^{18}O_{radiolarians}$ from equatorial Pacific are within the range of our measurements on low latitude Mesozoic deep-sea bedded cherts (19.8 ‰ to 35.3 ‰). Contrary to ~6 ‰ changes in Cenozoic $\delta^{18}O_{benthic\ foraminifera}$ (Zachos *et al.*, 2008), different dwelling depth of radiolarians might be attributed to ~7 ‰ (Katz *et al.*, 2010; Xu *et al.*, 2012; Völpel *et al.*, 2017). Other factor is partial silica dissolution and isotopic enrichment of up to 6.8 ‰ for diatom (Moschen *et al.*, 2006). Because dissolution rate mainly depends on Si undersaturation and pH, fluctuation of $\delta^{18}O$ values amplified the temperature effect. Although contamination of siliciclastics with light $\delta^{18}O$ values, ranging from 10 to 20 ‰ (Eiler, 2001), cannot be rejected, similar ~10 ‰ large fluctuations in pelagic equatorial (paleo-) Pacific $\delta^{18}O_{radiolarians}$ during the Cenozoic and Mesozoic might imply that diagenetic $\delta^{18}O$ shift is insignificant relative to unconsolidated biosiliceous sediments, and that $\delta^{18}O$ from radiolarian molds still preserve an environmental signature after diagenesis.

The cause of spatial variations of $\delta^{18}O_{radiolarians}$ needs to be examined. Our equatorial paleo-Pacific $\delta^{18}O_{radiolarians}$ from Triassic-Early Jurassic Inuyama and Cretaceous Goshikigahama sections (~20 to 32 ‰) is slightly lighter than the low-middle latitude $\delta^{18}O_{radiolarians}$ from the Middle Jurassic Tethys regions (~30 to 35 ‰), although our data cannot reject the possibility of age difference (Fig. 8). In the Tethys region, oppositely, a higher latitude $\delta^{18}O_{radiolarians}$ from Romania is slightly lighter than other data from Italy (Fig. 8). Further spatio-temporal comparison will be needed to understand the nature of $\delta^{18}O_{radiolarians}$ in the past.

The intra-chert variability of $\delta^{18}O$ (0.16 to 2.49 ‰) larger than analytical errors could be related with different degree of diagenesis and/or original variations. Such $\delta^{18}O$ microvariations in cherts have also described from Precambrian chert (Marin *et al.*, 2010). During the transformation from opal-A to opal-CT, the diagenetic migration of opal-A from layers with low-Si content to layers with high-Si content could have homogenized $\delta^{18}O$ within a chert (Isaacs, 1981; Tada, 1991). Subsequent transformation from opal-CT to quartz could have also homogenized through similar mechanism. Nevertheless, significant $\delta^{18}O$-variability in each chert suggests that such diagenetic segregation could not have perfectly homogenized $\delta^{18}O$ within each chert bed, and original variability might be larger.

If original, the intra-sample variations within cherts (0.16 to 2.49 ‰) corresponds to temperature differences of 2.3 to 40.9 ˚C, using equation from Brandriss *et al.* (1998) with an initial seawater $\delta^{18}O$ of about 0 ‰. A temperature difference of 40.9 ˚C is certainly too high to reflect original $\delta^{18}O$ from radiolarian skeletons, suggesting possible changes in degree of diagenesis and/or paleoceanographic condition, such as global ice volume, precipitation/evaporation, and/or upwelling of deep-water. Because most of the Mesozoic is ice-free in polar region (e.g. Frakes *et al.*, 1992) and because Triassic-Jurassic Inuyama samples were deposited under equatorial pelagic Panthalassa, changes in upwelling of deep-water, dwelling depth of radiolarians, partial silica dissolution, and diagenesis might be likely cause of the intra-sample variations. The sedimentary rhythms of bedded chert are hypothesized to be linked with periodic changes in upwelling intensity and associated radiolarian productivity based on the systematic changes in cosmic spherule content between chert and mudstone (e.g. Hori *et al.*, 1993). The average duration of a chert-shale couplet is ~20 kyr based on radiolarian and conodont biostratigraphic age model in the early Mesozoic bedded chert sequence in the Inuyama area, Japan, which is consistent with a dominant periodicity of a precession cycle (Hori *et al.*, 1993; Ikeda *et al.*, 2010; Ikeda and Tada, 2014). Therefore, <20 kyr-scale oscillation in radiolarian $\delta^{18}O$ might be preserved in bedded chert to some extent after diagenesis. Further detailed works are necessary to understand this issue.

5. 3 Mesozoic $\delta^{18}O$ trends of radiolarian silica and other proxies

$\delta^{18}O$ of low magnesium carbonate shells (LMC shells) are widely used for paleo-$\delta^{18}O$ of seawater during the Paleozoic and Mesozoic because of their less diagenetic overprint (e.g. Veizer *et al.* 1999; Grossman, 2012). The Mesozoic $\delta^{18}O$ of LMC shells from Tethys ocean shows a ~2 ‰ positive excursion during the Early-Middle Triassic, a relatively stable plateau during the Late Triassic, a large variation with <10-Myr variations during the Early Jurassic, a slight positive excursion during the Middle Jurassic (Fig. 8; Veizer *et al.* 1999; Grossman, 2012).

Although our SIMS measurement of $\delta^{18}O_{radiolarians}$ is low-resolution, our LS-mean data also shows a positive excursion during the Early-Middle Triassic, and relatively stable plateau during the Late Triassic, but up to ~8 ‰ negative excursion is not present in $\delta^{18}O$ curves of LMC shells (Fig. 8). Subsequent ~2 ‰ positive excursion during the Middle Jurassic seems to be also similar (Fig. 8). Although <10 Myr scale variability in our data is also large, similar repetitive measurements on sample Pi01 (uncalibrated LS-means of 28.2 ± 1.5 ‰ and 28.4 ± 5.1 ‰ from 10 and 27 measurements, respectively (2SD)) and Ki08C (27.3 ± 0.6 ‰, 27.9 ± 1.0 ‰, and 27.0 ± 1.0 ‰ from 4, 28, and 15 measurements (2SD)) imply that heterogeneities are well distributed in each chert and that chert could be relatively homogenous at bigger scale. Similar $\delta^{18}O$ trends of LMC shells and radiolarians might imply similar factors controlling these $\delta^{18}O$ records during

the Triassic and the Middle Jurassic (Fig. 8).

The cause of the ~8 ‰ negative excursion of radiolarian $\delta^{18}O$ during the Early Jurassic is unclear. Because our data is radiolarian silica of equatorial Panthalassa, various factors can be related, such as differences in paleoceanographic setting, temperature and pH of water column and sediment pore water for early dissolution, diagenetic processes. Considering large scattering of LMC shells records (e.g. Veizer *et al.* 1999; Grossman, 2012), further high-resolution and multi-proxy works are needed to examine this issue.

The $\delta^{18}O$ of conodont apatite ($\delta^{18}O_{conodont}$) is recently used for paleoceanographic analysis, and also shows similar positive excursion during the Early-Middle Triassic, and relatively stable plateau during the Late Triassic (e.g. Trotter *et al.*, 2015). Unfortunately, $\delta^{18}O_{conodont}$ cannot be applied for post-Triassic successions due to the complete extinction of conodont at the end-Triassic extinction (e.g. Clark, 1983). The $\delta^{18}O_{conodont}$ could be useful to compare with $\delta^{18}O_{radiolarians}$ with high-resolution because conodonts co-occur with radiolarians in chert and other siliceous sediments. Further crosscheck with other $\delta^{18}O$-signatures, such as conodont, have to be done to validate radiolarian silica as a paleoceanographic proxy.

6. Concluding remarks

Here we report the in situ $\delta^{18}O_{VPDB}$ -values from Mesozoic radiolarian molds show range between 19.8 to 35.8 ‰, which is consistent with that of modern and Cenozoic radiolarian tests from deep-sea core of equatorial Pacific (Wu *et al.*, 1997). Relatively large variability of $\delta^{18}O$ in intra-chert bed could support $\delta^{18}O$ of the Mesozoic radiolarian tests are not perfectly homogenized in a chert bed during the diagenetic segregation and through time.

The temporal changes in the $\delta^{18}O_{VSMOW}$ values from Mesozoic radiolarian molds show an Early-Middle Triassic slight positive excursion, a Late Triassic high plateau, an Early Jurassic negative excursion with up to 8 ‰, a Middle Jurassic slight positive excursion, and few light values for the Cretaceous. Although the Early Jurassic negative excursion is not consistent with the $\delta^{18}O$ trend of less-diagenetic low-Mg calcite shells in shallow marine Tethys, similar $\delta^{18}O$ trends among radiolarians, LMC shells, and conodonts during the Triassic and the Middle Jurassic imply potential preservation of an environmental component even after diagenesis of biogenic silica. Further crosscheck with other $\delta^{18}O$-signatures have to be done to validate radiolarian silica as a paleoceanographic proxy.

Acknowledgements:We thank the Swiss National Science Foundation (Project Numbers 200021_185067 and 200020_162670) and the University of Lausanne for their financial support. This research was partly supported by grants from the JSPS 2680026 awarded to MI and JSPS Postdoctoral Fellowship for Foreign Researchers awarded to BM.

References

Abelmann, A., Gersonde, R., Knorr, G., Zhang, X., Chapligin, B., Maier, E., Esper, O., Friedrichsen, H., Lohmann, G., Meyer, H. and Tiedemann, R. (2015) The seasonal sea-ice zone in the glacial Southern Ocean as a carbon sink. *Nature Communications*, **6**, 1–13.

Baumgartner, P. O. (1984) A Middle Jurassic—Early Cretaceous low latitude radiolarian zonation based on Unitary Associations and age of Tethyan radiolarites. *Eclogae Geologicae Helvetiae*, **77**, 729–841.

Baumgartner, P. O. (2013) Mesozoic radiolarites–accumulation as a function of sea surface fertility on Tethyan margins and in ocean basins. *Sedimentology*, **60**, 292–318.

Baumgartner, P. O., De Wever, P. and Kocher, R. (1980) Correlation of Tethyan Late Jurassic—Early Cretaceous radiolarian events. *Cahiers de Micropaléontologie*, **2**, 23–86.

Baumgartner, P. O., Matire, L., Goričan, Š., O'Dogherty, L., Erba, E. and Pillevuit, A. (1995) New Middle and Upper Jurassic radiolarian assemblage co-occurring with ammonites and nannofossils from the Southern Alps (Nothern Italy). *In* Baumgartner, P. O., O'Dogherty, L. *et al.*, eds., *Middle Jurassic to Lower Cretaceous radiolaria of Tethys: Occurences, systematics, biochronology. Mémoires Géologie (Lausanne)*, **23**, 737–750.

Bindeman, I. (2008) Oxygen Isotopes in Mantle and Crustal Magmas as Revealed by Single Crystal Analysis. *Reviews in Mineralogy and Geochemistry*, **69**, 445–478.

Bôle, M., Ikeda, M., Baumgartner, P. O., Hori, R. S. and Bouvier A.-S. (2020) SIMS analysis of Si isotope for radiolarian test in Mesozoic bedded chert, Inuyama, central Japan, *Bulletin of Geological Survey of Japan*, **71**, 331–353.

Brandriss, M. E., O'Neil, J. R., Edlund, M. B. and Stoermer, E. F. (1998) Oxygen isotope fractionation between diatomaceous silica and water. *Geochimica et Cosmochima Acta*, **62**, 1119–1125.

Carter, E. S. and Hori, R. S. (2005) Global correlation of the radiolarian faunal change across the Triassic Jurassic boundary. *Canadian Journal of Earth Sciences*, **42**, 777–790.

Channell, J. E. T., Bralower, T. J. and Grandesso, P. (1987) Biostratigraphic correlation of Mesozoic polarity chrons CM1 to CM23 at Capriolo and Xausa (Southern Alps, Italy). *Earth and Planetary Science Letters*, **85**, 203–221.

Clark, D. L. (1983) Extinction of conodonts. *Journal of Paleontology*, **57**, 652–661.

Cohen, K. M., Finney, S. C., Gibbard, P. L. and Fan, J.-X. (2013; updated) The ICS International Chronostratigraphic Chart. *Episodes*, **36**, 199–204.

Davis, E. F. (1918) The radiolarian cherts of the Franciscan

Group. *University of California Publications Bulletin of the Department of Geology*, **11**, 252–432.

Dralus, D., Peters, K. E., Lewan, M. D., Schenk, O., Herron, M. and Tsuchida, K. (2011) Kinetics of the Opal-CT to Quartz Phase Transition Control Diagenetic Traps in Siliceous Shale Source Rock from the San Joaquin Basin and Hokkaido. *AAPG Search and Discovery*, Article # 40771.

Dumitrica, P. (1995) Biostratigraphy of the radiolarites at Pojorîta (Rarău syncline, East Carpathians). *In* Baumgartner, P. O., O'Dogherty, L. *et al.*, eds., *Middle Jurassic to Lower Cretaceous Radiolaria of Tethys: Occurences, systematics, biochronology. Mémoires de Géologie (Lausanne)*, **23**, 907–914.

Eiler, J. M. (2001) Oxygen isotope variations of basaltic lavas and upper mantle rocks. *Reviews in mineralogy and geochemistry*, **43**, 319–364.

Emiliani, C. (1955) Pleistocene temperatures. *The Journal of Geology*, **63**, 538–578.

Ernst, W. G. and Calvert, S. E. (1969) An experimental study of the recrystallization of porcelanite and its bearing on the origin of some bedded cherts. *American Journal of Science*, **267**, 114–133.

Föllmi, K. B., Bôle, M., Jammet, N., Froidevaux, P., Godet, A., Bodin, S., Adatte, T., Matera, V., Fleitmann, D. and Spangenberg, J. E. (2012) Bridging the Faraoni and Selli oceanic anoxic events: late Hauterivian to early Aptian dysaerobic to anaerobic phases in the Tethys. *Climate of the Past*, **8**, 171–189.

Fontorbe, G., Frings, P. J., De La Rocha, C. L., Hendry, J. R. and Conley, D. J. (2016) A silicon depleted North Atlantic since the Palaeogene: Evidence from sponge and radiolarian silicon isotopes. *Earth and Planetary Science Letters*, **453**, 67–77.

Frakes, L. A., Francis, J. E. and Syktus, J. L. (1992) *Climate Modes of the Phanerozoic: the history of the earth's climate over the past 600 million years,* Cambridge Univ Press, 274pp.

Gaetani, M. and Poliani, G. (1978) Il Toarciano ed il Giurassico medio in Albenza (Bergamo). *Rivista Italalina di Paleontologia e Stratigrafia*, **84**, 349–382.

Grossman, E. L. (2012) Oxygen isotope stratigraphy. *In* Gradstein, F.M., Ogg, J.G., Schmitz, M. and Ogg, G., eds., *The Geologic Time Scale 2012*, Elsevier B.V., 181–206.

Gunnarsson, I., Arnorsson, S. and Arnórsson, S. (2000) Amorphous silica solubility and the thermodynamic properties of H_4SiO_4 in the range of 0° to 350 °C at Psat. *Geochimica et Cosmochima Acta*, **64**, 2295–2307.

He, H. and Liu, Y. (2015) Silicon isotope fractionation during the precipitation of quartz and the adsorption of H_4SiO_4(aq) on Fe(III)-oxyhydroxide surfaces. *Chinese Journal of Geochemistry*, **34**, 459–468.

Hein, J. R. and Parrish, J. T. (1987) Distribution of Siliceous Deposits in Space and Time. *In* Hein, J. R., ed., *Siliceous Sediment Rock-Hosted Ores and Petroleum*, Van Nostrand Reinhold Compagny, Inc., New York, 10–57.

Hinman, N. W. (1998) Sequences of silica phase transitions: effects of Na, Mg, K, Al, and Fe ions. *Marine Geology*, **147**, 13–24.

Hori, R. (1988) Some characteristic radiolarians from Lower Jurassic bedded cherts of the Inuyama area, Southwest Japan. *Transactions and proceedings of the Paleontological Society of Japan, New series*, **151**, 543–563.

Hori, R. S., Cho, C. and Umeda, H. (1993) Origin of cyclicity in Triassic-Jurassic radiolarian bedded cherts of the Mino accretionary complex from Japan. *Island Arc*, **2**, 170–180.

Ikeda, M. and Tada, R. (2014) A 70 million year astronomical time scale for the deep-sea bedded chert sequence (Inuyama, Japan): Implications for Triassic–Jurassic geochronology. *Earth and Planetary Science Letters*, **399**, 30–43.

Ikeda, M., Tada, R. and Sakuma, H. (2010) Astronomical cycle origin of bedded chert: A middle Triassic bedded chert sequence. *Earth and Planetary Science Letters*, **297**, 369–378.

Ikeda, M., Bôle, M. and Baumgartner, P. O. (2016) Orbital-scale changes in redox condition and biogenic silica/detrital fluxes of the Middle Jurassic Radiolarite in Tethys (Sogno, Lombardy, N-Italy): Possible link with glaciation? *Palaeogeography, Palaeoclimatology, Palaeoecology*, **457**, 247–257.

Isaacs, C. M. (1981) Porosity reduction during diagenesis of the Monterey Formation, Santa Barbara coastal area, California. *In* Garrison, R. E. and Douglas, R. G., eds., *The Monterey Formation and related siliceous rocks of California: Los Angeles*. Pacific Section, SEPM, 257–271.

Jaffrés, J. B. D., Shields, G. A. and Wallmann, K. (2007) The oxygen isotope evolution of seawater: A critical review of a long-standing controversy and an improved geological water cycle model for the past 3.4 billion years. *Earth-Science Reviews*, **83**, 83–122.

Jochum, K. P., Nohl, U., Herwig, K., Lammel, E., Stoll, B. and Hoffman, A. W. (2005) GeoReM: A New Geochemical Database for Reference Materials and Isotopic Standards. *Geostandards and Geoanalytical Research*, **29**, 333–338.

Juillet-Leclerc, A. and Labeyrie, L. (1987) Temperature dependence of the oxygen isotopic fractionation between diatom silica and water. *Earth and Planetary Science Letters*, **84**, 69–74.

Kastner, M., Keene, J. B. and Gieskes, J. M. (1977) Diagenesis of siliceous oozes—I. Chemical controls on the rate of opal-A to opal-CT transformation—an experimental study. *Geochimica et Cosmochimica Acta*, **41**, 1041–1059.

Katz, M. E., Cramer, B. S., Franzese, A., Hönisch, B., Miller, K. G., Rosenthal, Y. and Wright, J. D. (2010) Traditional and emerging geochemical proxies in

foraminifera. *The Journal of Foraminiferal Research*, **40**, 165–192.

Kidder, D. L. and Erwin, D. H. (2001) Secular Distribution of Biogenic Silica through the Phanerozoic: Comparison of Silica-Replaced Fossils and Bedded Cherts at the Series Level. *The Journal of Geology*, **109**, 509–522.

Kim, S. T., Coplen, T. B. and Horita, J. (2015) Normalization of stable isotope data for carbonate minerals: Implementation of IUPAC guidelines. *Geochimica et Cosmochima Acta*, **158**, 276–289.

Kimura, K. and Hori, R. (1993) Offscraping accretionary process of Jurassic chert-clastic complexes in the Mino-Tamba belt, central Japan. *Journal of Structural Geology*, **15**, 145–161.

Knauth, L. P. (1973) Oxygen and hydrogen isotope ratios in cherts and related rocks. *Doctoral dissertation, California Institute of Technology*, 378p.

Knauth, L. P. and Epstein, S. (1976) Hydrogen and oxygen isotope ratios in nodular and bedded cherts. *Geochimica et Cosmochimic Acta*, **40**, 1095–1108.

Kocher, R. N. (1981) Biochronostratigraphische Untersuchungen oberjurassischer radiolarian führender Gesteine, insbesondere der Südalpen. *Mitteilungen aus dem Geologischen Institut der Eidgenössischen Technische Hochschule und der Univerität Zürich*, **234**, 184p.

Kodama, K., Taira, A., Okamura, M. and Saito, Y. (1983) Paleomagnetism of the Shimanto Belt in Shikoku, Southwest Japan. *In* Hashimoto, M. and Uyeda, H., eds., *Accretion Tectonics in the Circum-Pacific Region*, Terra Scientific Publishing Company, Tokyo, 231–241.

Labeyrie, L. D. (1974) New approach to surface seawater palaeotemperatures using $^{18}O/^{16}O$ ratios in silica of diatom frustules. *Nature*, **248**, 40–42.

Lini, A., Weissert, H. and Erba, E. (1992) The Valanginian carbon isotope event: a first episode of greenhouse climate conditions during the Cretaceous. *Terra Nova*, **4**, 374–384.

Maier, E., Chapligin, B., Abelmann, A., Gersonde, R., Esper, O., Ren, J., Friedrichsen, H., Meyer, H. and Tiedemann, R. (2013) Combined oxygen and silicon isotope analysis of diatom silica from a deglacial subarctic Pacific record. *Journal of Quaternary Science*, **28**, 571–581.

Marin, J., Chaussidon, M. and Robert, F. (2010) Microscale oxygen isotope variations in 1.9 Ga Gunflint cherts: Assessments of diagenesis effects and implications for oceanic paleotemperature reconstructions. *Geochimica et Cosmochimica Acta*, **74**, 116–130.

Matheney, R. K. and Knauth, L. P. (1993) New isotopic temperature estimates for early silica diagenesis cherts. *Geology*, **21**, 519–522.

Mikkelsen, N., Labeyrie, Jr L. and Berger, W. H. (1978) Silica oxygen isotopes in diatoms: A 20,000 yr record in deep-sea sediments. *Nature*, **271**, 536–538.

Mizutani, S. and Koike, T. (1982) Radiolarians in the Jurassic siliceous shale and in the Triassic bedded chert of Unuma, Kagamigahara City, Gifu Prefecture, central Japan. *News of Osaka Micropaleontologists Special Volume*, no. 5, 117–134. (in Japanese with English abstract)

Moschen, R., Lücke, A., Parplies, J., Radtke, U. and Schleser, G. H. (2006) Transfer and early diagenesis of biogenic silica oxygen isotope signals during settling and sedimentation of diatoms in a temperate freshwater lake (Lake Holzmaar, Germany). *Geochimica et Cosmochimica Acta*, **70**, 4367–4379.

Nakaseko, K. and Nishimura, A. (1979) Upper Triassic radiolaria from Southwest Japan. *Science Reports, College of General Education, Osaka University*, **28**, 61–109.

Okamura, M. and Uto, H. (1982) Notes on stratigraphic distributions of radiolarians from the Lower Cretaceous sequence of chert in the Yokonami Melange of Shimanto Belt, Kochi Prefecture, Shikoku. *Research Reports of Kochi University Natural Science*, **31**, 87–94. (in Japanese with English abstract)

Pollington, A. D., Kozdon, R., Anovitz, L. M., Georg, R. B., Spicuzza, M. J. and Valley, J. W. (2016) Experimental calibration of silicon and oxygen isotope fractionations between quartz and water at 250 °C by in situ microanalysis of experimental products and application to zoned low $\delta^{30}Si$ quartz overgrowths. *Chemical Geology*, **421**, 127–142.

Racki, G. and Cordey, F. (2000) Radiolarian palaeoecology and radiolarites: Is the present the key to the past? *Earth-Science Reviews*, **52**, 83–120.

Schmidt, M., Botz, R., Stoffers, P., Anders, T. and Bohrmann, G. (1997) Oxygen isotopes in marine diatoms: a comparative study of analytical techniques and new results on the isotope composition of recent marine diatoms. *Geochimica et Cosmochimica Acta*, **61**, 2275–2280.

Schmidt, M., Botz, R., Rickert, D., Bohrmann, G., Hall, S. R. and Mann, S. (2001) Oxygen isotopes of marine diatoms and relations to opal-A maturation. *Geochimica et Cosmochimica Acta*, **65**, 201–211.

Seitz, S., Baumgartner, L. P., Bouvier, A. S., Putlitz, B. and Vennemann, T. (2016) Quartz Reference Materials for Oxygen Isotope Analysis by SIMS. *Geostandards and Geoanalytical Research*, **41**, 69–75.

Shackleton, N. J. and Kennett, J. P. (1975) Paleotemperature history of the Cenozoic and the initiation of Antarctic glaciation: oxygen and carbon isotope analyses in DSDP Sites 277, 279, and 281. *In* Kennett, J. O., Houtz, R. E. *et al.*, eds., *Initial Reports of the Deep Sea Drilling Project*, **29**, 743–755.

Shemesh, A., Charles, C. D. and Fairbanks, R. G. (1992) Oxygen isotopes in biogenic silica: global changes in ocean temperature and isotopic composition. *Science*, **256**, 1434–1436.

Shemesh, A., Rietti-Shati, M., Rioual, P., Battarbee, R., de

Beaulieu, J.-L., Reille, M., Andrieu, V. and Svobodova, H. (2001) An oxygen isotope record of lacustrine opal from a European Maar indicates climatic stability during the last interglacial. *Geophysical Research Letters*, **28**, 2305–2308.

Stampfli, G. M. and Borel G. D. (2002) A plate tectonic model for Paleozoic and Mesozoic constrained by dynamic plate boundaries and restored synthetic oceanic isochrons. *Earth and Planetary Science Letters*, **196**, 17–33.

Sugiyama, K. (1997) Triassic and Lower Jurassic radiolarian biostratigraphy in the siliceous claystone and bedded chert units of the southeastern Mino Terrane, Central Japan. *Bulletin of the Mizunami Fossil Museum*, **24**, 79–193.

Swann, G. E. A. and Leng, M. J. (2009) A review of diatom $\delta^{18}O$ in palaeoceanography. *Quaternary Science Reviews*, **28**, 384–398.

Swann, G. E. A., Leng, M. J., Sloane, H. J., Maslin, M. A. and Onodera, J. (2007) Diatom oxygen isotopes: evidence of a species effect in the sediment record. *Geochemistry, Geophysics, Geosystems*, **8**, 1–10.

Swann, G. E. A., Leng, M. J., Sloane, H. J. and Maslin, M. A. (2008) Isotope offsets in marine diatom $\delta^{18}O$ over the last 200 ka. *Journal of Quaternary Science*, **23**, 389–400.

Tada, R. (1991) Origin of rhythmical bedding in middle Miocene siliceous rocks of the Onnagawa Formation, northern Japan. *Journal of Sedimentary Research*, **61**, 1123–1145.

Trotter, J. A., Williams, I. S., Nicora, A., Mazza, M. and Rigo, M. (2015) Long-term cycles of Triassic climate change: a new $\delta^{18}O$ record from conodont apatite. *Earth and Planetary Science Letters*, **415**, 165–174.

Veizer, J., Ala, D., Azmy, K., Bruckschen, P., Buhl, D., Bruhn, F., Carden, G. A. F., Diener, A., Ebneth, S. and Godderis, Y. (1999) $^{87}Sr/^{86}Sr$, $\delta^{13}C$ and $\delta^{18}O$ evolution of Phanerozoic seawater. *Chemical Geology*, **161**, 59–88.

Viswanathan, S. and Mahabaleswar, B. (2014) Silicate oxygen isotope geochemistry: History, principles, techniques, and application to petrological problems. *Journal of the Geological Society of India*, **83**, 47–53.

Völpel, R., Paul, A., Krandick, A., Mulitza, S. and Schulz, M. (2017) Stable water isotopes in the MITgcm. Geoscientific Model Development, 10, 3125-3144.

Weissert, H., McKenzie, J. and Hochuli, P. (1979) Cyclic anoxic events in the Early Cretaceous Tethys Ocean. *Geology*, **7**, 147–151.

Wu, S., Ding, T., Meng, X. and Bai, L. (1997) Determination and geological implication of 0-Si isotope of the sediment core in the CC area, the Pacific Ocean. *Chinese Science Bulletin*, **42**, 1462–1465.

Xu, X., Werner, M., Butzin, M. and Lohmann, G. (2012) Water isotope variations in the global ocean model MPI-OM. *Geoscience Model Development*, **5**, 809–818.

Yao, A., Matsuda, T. and Isozaki, Y. (1980) Triassic and Jurassic radiolarians from the Inuyama area, central Japan. *Journal of Geosciences Osaka City University*, **23**, 135–154.

Yao, A. and Kuwahara, K. (1997) Radiolarian faunal change from Late Permian to Middle Triassic times. *News of Osaka Micropaleontolists, Special Volume*, no. 10, 87–96.

Zachos, J. C., Dickens, G. R. and Zeebe, R. E. (2008) An early Cenozoic perspective on greenhouse warming and carbon-cycle dynamics. *Nature*, **451**, 279–283.

Recieved January 7, 2019
Accepted October 20, 2020

Appendix

Table A1 Least square drift corrected and calibrated $\delta^{18}O$ measurements for each sample and for each accepted analyses. All $\delta^{18}O$ are relative to VPDB and all standard deviations are given as 2SD.

Sample		Pe01	Ki09	Ki12s	Ki01	Ki02	Ki03s	Ki03s	Ki03	Ki04	Ki06	Ki07
age		253.15	250.30	249.9	248	247.80	247.20	247.20	247.20	246.60	245.25	245.00
LS-mean ($\delta^{18}O_{VSMOW}$) and LS-Standard deviation (2SD) (‰)		**23.99 ± 0.33**	**29.27 ± 0.88**		**30.93 ± 2.81**	**30.83 ± 2.01**	**20.92 ± 4.61**	**23.92 ± 2.29**	**30.44 ± 1.38**	**31.27 ± 1.8**	**31.88 ± 2.32**	**29.25 ± 3.55**
Number of measurements		10	9	6	10	6	4	5	10	9	6	6
Accepted measurements		10	9	0	10	6	4	5	10	9	6	6
Rejected measurements				6								
$\delta^{18}O_{VSMOW}$ and analytical standard deviation (2SD) of all accepted measurements (‰)	1	24.04 ± 0.18	29.2 ± 0.31		28.91 ± 0.2	29.59 ± 0.21	22.31 ± 0.32	24.55 ± 0.25	30.24 ± 0.2	30.04 ± 0.12	31.42 ± 0.13	30.39 ± 0.25
	2	23.86 ± 0.22	29.45 ± 0.19		30.53 ± 0.18	32.13 ± 0.19	22.9 ± 0.22	22.92 ± 0.19	30.87 ± 0.19	30.19 ± 0.19	30.81 ± 0.19	31.03 ± 0.24
	3	23.97 ± 0.2	29.48 ± 0.16		30.59 ± 0.13	30.58 ± 0.16	21.15 ± 0.2	22.9 ± 0.22	30.5 ± 0.13	30.5 ± 0.27	31.49 ± 0.23	27.39 ± 0.25
	4	23.99 ± 0.22	29.35 ± 0.18		31.29 ± 0.13	30.18 ± 0.15	17.87 ± 0.14	23.75 ± 0.24	31.37 ± 0.2	31.36 ± 0.17	33.2 ± 0.19	29.99 ± 0.24
	5	23.67 ± 0.25	29.54 ± 0.19		31.38 ± 0.26	30.57 ± 0.2		25.55 ± 0.21	30.09 ± 0.33	32.5 ± 0.21	30.93 ± 0.17	26.73 ± 0.21
	6	24.15 ± 0.19	29.68 ± 0.18		30.97 ± 0.25	32.02 ± 0.22			30.31 ± 0.18	31.15 ± 0.18	33.48 ± 0.17	30.08 ± 0.23
	7	23.79 ± 0.21	29.47 ± 0.19		34.3 ± 0.17				31.4 ± 0.26	31.6 ± 0.25		
	8	24.15 ± 0.24	28.21 ± 0.2		30.45 ± 0.23				29.7 ± 0.23	31.8 ± 0.18		
	9	24.07 ± 0.21	29.05 ± 0.17		29.96 ± 0.2				30.78 ± 0.17	32.36 ± 0.16		
	10	24.18 ± 0.23			30.72 ± 0.2				29.26 ± 0.13			
	11											
	12											
	13											
	14											
	15											
	16											
	17											
	18											
	19											
	20											
Session		Br7	Br2	Br6	Br7	Br3	Br2	Br2	Br7	Br2	Br3	Br3
Sample order during the session		8	6	7	11	8	1	2	5	8	6	3

Sample		Ki08	Ki08					Ki58C	Ki57	Ki15	Ki51	Ki48
age		244.9	244.9					243.48	241.00	228.00	219.00	217.09
LS-mean ($\delta^{18}O_{VSMOW}$) and LS-Standard deviation (2SD) (‰)		**30.58 ± 2.05**	**30.75 ± 1.21**					**31.16 ± 1.32**	**26.76 ± 3.62**	**31.49 ± 1.43**	**31.91 ± 0.68**	**30.61 ± 1.83**
Number of measurements		10	86					6	10	10	6	6
Accepted measurements		10	86					6	9	10	6	3
Rejected measurements									1			3
$\delta^{18}O_{VSMOW}$ and analytical standard deviation (2SD) of all accepted measurements (‰)	1	30.05 ± 0.23	30.9 ± 0.2	32.43 ± 0.17	30.12 ± 0.1	30.81 ± 0.18	30.34 ± 0.12	31.78 ± 0.2	24.27 ± 0.25	31.74 ± 0.18	31.76 ± 0.22	29.55 ± 0.21
	2	30.58 ± 0.18	30.64 ± 0.18	31.25 ± 0.23	29.77 ± 0.17	30.4 ± 0.16	30.01 ± 0.12	31.22 ± 0.24	26.78 ± 0.24	31.47 ± 0.2	32.23 ± 0.25	31.33 ± 0.19
	3	32.72 ± 0.22	30.89 ± 0.15	30.79 ± 0.22	30.11 ± 0.2	30.78 ± 0.1	30 ± 0.17	30 ± 0.24	27.45 ± 0.18	30.25 ± 0.2	31.49 ± 0.16	30.9 ± 0.18
	4	29.25 ± 0.23	30.25 ± 0.17	30.68 ± 0.17	30.3 ± 0.15	30.91 ± 0.11	30.9 ± 0.21	31.84 ± 0.22	26.13 ± 0.22	32.13 ± 0.26	32.2 ± 0.24	
	5	30.92 ± 0.31	31.73 ± 0.14	30.68 ± 0.16	30.09 ± 0.27	30.36 ± 0.12	30.54 ± 0.14	31.13 ± 0.17	29.56 ± 0.18	31.92 ± 0.16	31.63 ± 0.2	
	6	29.3 ± 0.2	31.02 ± 0.14	31.04 ± 0.16	30.35 ± 0.17	30.94 ± 0.15	30.26 ± 0.16	30.95 ± 0.21	28.09 ± 0.19	31.69 ± 0.25	32.25 ± 0.17	
	7	30.7 ± 0.19	30.31 ± 0.16	30.91 ± 0.2	29.84 ± 0.17	30.63 ± 0.14			24.64 ± 0.23	32.07 ± 0.25		
	8	31.35 ± 0.21	31.01 ± 0.2	30.95 ± 0.18	30.25 ± 0.1	30.08 ± 0.17			28.36 ± 0.26	31.88 ± 0.2		
	9	30.9 ± 0.21	30.96 ± 0.19	31.24 ± 0.12	30.49 ± 0.1	30.15 ± 0.12			25.16 ± 0.19	30.09 ± 0.26		
	10	30.08 ± 0.26	31.3 ± 0.22	30.52 ± 0.18	31.19 ± 0.18	30.23 ± 0.16				31.61 ± 0.24		
	11		31.22 ± 0.21	30.66 ± 0.17	30.64 ± 0.2	31 ± 0.18						
	12		31.16 ± 0.16	32.22 ± 0.14	30.32 ± 0.15	30.64 ± 0.14						
	13		30.83 ± 0.14	30.51 ± 0.17	30.54 ± 0.21	30.8 ± 0.14						
	14		31.48 ± 0.11	31.11 ± 0.23	30.34 ± 0.15	28.77 ± 0.16						
	15		31.25 ± 0.14	31.44 ± 0.19	29.51 ± 0.13	30.61 ± 0.16						
	16		31.31 ± 0.16	31.17 ± 0.14	31.93 ± 0.15	30.64 ± 0.14						
	17		31.74 ± 0.19	30.4 ± 0.18	30.88 ± 0.2	31 ± 0.12						
	18		31.7 ± 0.18	29.8 ± 0.17	31.79 ± 0.19	30.63 ± 0.17						
	19		31.81 ± 0.21	30.9 ± 0.18	30.42 ± 0.18	31.22 ± 0.16						
	20		31.77 ± 0.15	30.24 ± 0.16	30.58 ± 0.19	30.76 ± 0.15						
Session		Br7	PRIM123					Br3	Br7	Br2	Br3	Br6
Sample order during the session		3	1					7	6	7	4	2

Table A1 Continued.

Sample	Ki46	Ki43s	Ki44	Ki39	Ki40	Ki41	Ki42	Ki35	Ki34s	Ki34s	Ki32
age	210.27	204.82	204.82	201.50	201.50	201.50	201.5	185.62	184.37	184.37	184.20
LS-mean ($\delta^{18}O_{VSMOW}$) and LS-Standard deviation (2SD) (‰)	**32.59 ± 3.13**	**31.3 ± 0.89**	**31.65 ± 0.86**	**31.41 ± 1.05**	**31.72 ± 1.17**	**31.38 ± 1.57**	**31.42 ± 0.94**	**29.98 ± 0.81**	**25.82 ± 2.74**	**30.79 ± 0.3**	**30.21 ± 1.83**
Number of measurements	10	6	9	9	10	10	10	9	9	1	10
Accepted measurements	10	6	9	9	10	10	10	9	8	1	10
Rejected measurements									1		
1	31.63 ± 0.22	31.47 ± 0.25	31.44 ± 0.19	30.79 ± 0.15	31.88 ± 0.17	31.46 ± 0.25	32.2 ± 0.19	29.95 ± 0.25	23.83 ± 0.12	30.79 ± 0.3	29.98 ± 0.17
2	30.32 ± 0.19	31.57 ± 0.14	31.95 ± 0.2	31.51 ± 0.12	31.46 ± 0.24	32.49 ± 0.16	31.2 ± 0.18	30.47 ± 0.28	27.29 ± 0.21		30.43 ± 0.22
3	32.43 ± 0.21	31.25 ± 0.22	32 ± 0.22	32.08 ± 0.24	32.28 ± 0.16	31.33 ± 0.18	30.66 ± 0.25	29.88 ± 0.17	25.5 ± 0.28		29.41 ± 0.16
4	32.51 ± 0.15	31.52 ± 0.22	32.06 ± 0.24	32.16 ± 0.19	31.79 ± 0.23	31.84 ± 0.15	30.94 ± 0.18	29.72 ± 0.2	26 ± 0.21		30.55 ± 0.2
5	34.75 ± 0.22	30.46 ± 0.18	30.69 ± 0.22	30.52 ± 0.17	32.12 ± 0.21	29.91 ± 0.19	30.88 ± 0.2	29.59 ± 0.26	27.94 ± 0.29		28.69 ± 0.25
6	32.41 ± 0.14	31.56 ± 0.19	31.91 ± 0.19	31.39 ± 0.14	31.71 ± 0.26	30.34 ± 0.18	31.85 ± 0.19	29.65 ± 0.14	24.35 ± 0.26		29.96 ± 0.18
7	32.47 ± 0.18		31.83 ± 0.19	31.69 ± 0.28	31.79 ± 0.2	31.28 ± 0.2	31.51 ± 0.19	29.92 ± 0.22	26.31 ± 0.19		30.44 ± 0.24
8	31.2 ± 0.24		31.57 ± 0.19	31.35 ± 0.15	31.94 ± 0.14	31.9 ± 0.19	31.57 ± 0.15	29.9 ± 0.18	25.9 ± 0.2		32.3 ± 0.21
9	32.38 ± 0.2		31.4 ± 0.18	31.55 ± 0.14	30.06 ± 0.24	31.14 ± 0.2	31.73 ± 0.22	30.89 ± 0.29			29.92 ± 0.21
10	35.7 ± 0.18				31.76 ± 0.16	31.96 ± 0.19	31.56 ± 0.16				30.45 ± 0.24
11											
12											
13											
14											
15											
16											
17											
18											
19											
20											
Session	Br7	Br6	Br2	Br4	Br4	Br4	Br7	Br2	Br7	Br7	Br7
Sample order during the session	10	4	9	3	6	8	4	11	2	2	9

$\delta^{18}O_{VSMOW}$ and analytical standard deviation (2SD) of all accepted measurements (‰)

Sample	Ki24	Ki25	Ki22c2	Ki22c1	Ki21	Ki20	So07	So08	So09	So12	So13
age	182.00	180.66	178.00	178.00	178.00	174.00	169.50	169.50	169.30	168.27	168.13
LS-mean ($\delta^{18}O_{VSMOW}$) and LS-Standard deviation (2SD) (‰)	**30.76 ± 1.45**	**25.19 ± 4.92**	**26.07 ± 3.07**	**26.97 ± 2.44**	**27.16 ± 2.11**	**21.92 ± 3.73**	**32.47 ± 1.52**	**33.99 ± 0.82**	**34.35 ± 0.83**	**34.96 ± 0.9**	**34.31 ± 0.83**
Number of measurements	6	9	6	9	10	6	6	7	6	6	9
Accepted measurements	6	8	6	9	10	5	6	7	6	6	9
Rejected measurements		1				1					
1	31.9 ± 0.23	23.04 ± 0.28	24.03 ± 0.25	26.42 ± 0.22	26.33 ± 0.21	19.52 ± 0.21	32.8 ± 0.29	34.01 ± 0.14	34.21 ± 0.22	34.93 ± 0.16	33.99 ± 0.26
2	30.88 ± 0.22	25.56 ± 0.18	26.76 ± 0.31	27.1 ± 0.22	28.02 ± 0.19	21.61 ± 0.26	32.34 ± 0.14	34.74 ± 0.16	33.99 ± 0.15	35.19 ± 0.22	34.36 ± 0.19
3	30.36 ± 0.2	25.96 ± 0.24	24.21 ± 0.22	28.86 ± 0.25	27.14 ± 0.14	21.79 ± 0.28	33.81 ± 0.22	33.89 ± 0.21	34.68 ± 0.31	34.01 ± 0.28	33.74 ± 0.24
4	30.03 ± 0.26	26.56 ± 0.17	26.93 ± 0.2	26.33 ± 0.2	26.64 ± 0.2	22.14 ± 0.24	32.52 ± 0.18	33.95 ± 0.18	34.38 ± 0.14	35.05 ± 0.15	34.83 ± 0.18
5	30.11 ± 0.17	20.26 ± 0.3	27.4 ± 0.26	24.53 ± 0.19	27.95 ± 0.19	24.53 ± 0.21	31.62 ± 0.18	34.15 ± 0.18	33.96 ± 0.14	35.44 ± 0.15	34.04 ± 0.13
6	31.25 ± 0.19	29.06 ± 0.28	27.12 ± 0.21	27.36 ± 0.19	27.04 ± 0.22		31.89 ± 0.21	33.4 ± 0.17	35.02 ± 0.2	34.9 ± 0.19	34.13 ± 0.27
7		25.07 ± 0.17		28.21 ± 0.24	28.88 ± 0.2			33.76 ± 0.22			33.96 ± 0.2
8		25.51 ± 0.13		26.91 ± 0.26	25.91 ± 0.17						34.9 ± 0.12
9				27.22 ± 0.13	28.12 ± 0.21						34.53 ± 0.21
10					25.67 ± 0.2						
11											
12											
13											
14											
15											
16											
17											
18											
19											
20											
Session	Br3	Br2	Br2	Br2	Br2	Br6	Br3	Br3	Br3	Br6	Br4
Sample order during the session	5	10	4	3	5	5	2	1	10	9	4

$\delta^{18}O_{VSMOW}$ and analytical standard deviation (2SD) of all accepted measurements (‰)

Table A1 Continued.

Sample	So15	So17	So21	Ro01	So23	So25	P01		So26	So28	So29
age	167.54	166.89	166.09	166.00	165.10	164.31	163.00		162.65	161.14	161.06
LS-mean ($\delta^{18}O_{VSMOW}$) and LS-Standard deviation (2SD) (‰)	**34.68 ± 1.05**	**32.69 ± 5.18**	**32.27 ± 2.04**	**30.92 ± 1.54**	**34.02 ± 1.18**	**35.3 ± 0.65**	**34.55 ± 0.8**		**35.12 ± 0.55**	**34.71 ± 1.37**	
Number of measurements	6	9	11	6	6	9	32		6	9	6
Accepted measurements	6	9	6	6	6	9	32		6	8	0
Rejected measurements			5							1	6
1	34.58 ± 0.18	33.73 ± 0.15	31.96 ± 0.25	31.2 ± 0.16	34.61 ± 0.2	35.74 ± 0.21	34.74 ± 0.15	34.69 ± 0.17	35.03 ± 0.2	35.38 ± 0.22	
2	34.99 ± 0.19	33.93 ± 0.28	31.49 ± 0.17	30.85 ± 0.13	34.06 ± 0.16	35.5 ± 0.25	33.54 ± 0.15	34.92 ± 0.1	34.85 ± 0.18	34.52 ± 0.2	
3	35.18 ± 0.2	33.44 ± 0.23	33.75 ± 0.16	29.38 ± 0.21	32.85 ± 0.2	35.23 ± 0.2	33.53 ± 0.2	34.56 ± 0.18	34.89 ± 0.2	34.81 ± 0.24	
4	33.92 ± 0.26	25.99 ± 0.21	31.39 ± 0.26	31.29 ± 0.22	34.32 ± 0.17	34.88 ± 0.19	34.73 ± 0.1	33.75 ± 0.14	35.62 ± 0.22	35.15 ± 0.17	
5	34.12 ± 0.21	31.42 ± 0.2	31.62 ± 0.2	31.42 ± 0.24	34.15 ± 0.16	34.91 ± 0.27	34.75 ± 0.16	34.55 ± 0.17	35.15 ± 0.22	34.75 ± 0.17	
6	35.15 ± 0.22	33.59 ± 0.13	33.15 ± 0.24	31.39 ± 0.21	34.07 ± 0.17	35.45 ± 0.17	34.59 ± 0.14	34.74 ± 0.1	35.22 ± 0.18	34.33 ± 0.19	
7		34.01 ± 0.17				34.89 ± 0.18	34.66 ± 0.12	34.48 ± 0.1		33.49 ± 0.13	
8		34.26 ± 0.24				35.5 ± 0.18	34.88 ± 0.13	35 ± 0.17		35.56 ± 0.2	
9		33.62 ± 0.17				35.55 ± 0.2	34.71 ± 0.2	34.33 ± 0.14			
10							34.77 ± 0.15	34.62 ± 0.17			
11							35.09 ± 0.22	34.84 ± 0.2			
12							34.92 ± 0.15	34.73 ± 0.11			
13							34.47 ± 0.16				
14							34.62 ± 0.1				
15							33.87 ± 0.13				
16							33.89 ± 0.2				
17							34.68 ± 0.13				
18							34.72 ± 0.17				
19							34.8 ± 0.16				
20							34.43 ± 0.16				
Session	Br6	Br4	Br4	Br3	Br6	Br4	PRIM123		Br6	Br4	Br6
Sample order during the session	1	2	10	9	3	7	2		8	1	6

Sample	So31	Ca01	Go68	Go73	Go74
age	159.97	139.00	131.70	97.95	97.59
LS-mean ($\delta^{18}O_{VSMOW}$) and LS-Standard deviation (2SD) (‰)	**35.25 ± 0.57**	**34.33 ± 0.45**	**26.53 ± 1.16**	**28.52 ± 1.99**	**19.76 ± 1.4**
Number of measurements	9		6	9	10
Accepted measurements	9		6	9	10
Rejected measurements					
1	35.42 ± 0.22	34.27 ± 0.14	27.06 ± 0.26	29.68 ± 0.2	18.12 ± 0.29
2	35.09 ± 0.19	34.3 ± 0.12	25.89 ± 0.19	26.95 ± 0.18	19.61 ± 0.22
3	35.76 ± 0.15	34.89 ± 0.17	26.39 ± 0.17	28.71 ± 0.14	20.49 ± 0.23
4	34.87 ± 0.22	34.18 ± 0.17	26.47 ± 0.26	28.2 ± 0.15	19.36 ± 0.13
5	34.9 ± 0.24	34.1 ± 0.13	26.06 ± 0.18	28.96 ± 0.18	19.16 ± 0.15
6	35.1 ± 0.19	34.13 ± 0.13	27.36 ± 0.17	26.96 ± 0.17	20.03 ± 0.14
7	35.19 ± 0.18	34.36 ± 0.19		29.33 ± 0.19	20.45 ± 0.19
8	35.42 ± 0.16	34.28 ± 0.17		29 ± 0.22	19.89 ± 0.11
9	35.32 ± 0.24	34.51 ± 0.2		29.19 ± 0.23	20.65 ± 0.22
10		34.4 ± 0.19			19.7 ± 0.17
11					
12					
13					
14					
15					
16					
17					
18					
19					
20					
Session	Br4	PRIM123	Br6	Br4	Br7
Sample order during the session	9	3	10	5	1

$\delta^{18}O_{VSMOW}$ and analytical standard deviation (2SD) of all accepted measurements (‰)

Table A2 All the analytical dataset of the samples and standards. This data set include raw information such as the beam intensity (nA) during the analyses, counts per second on the L'2 and H'2 FC for ^{16}O and ^{18}O, respectively, time at which was realized (HH:MM). The raw isotopic ratios (H'2/L'2 ($^{18}O/^{16}O$)) is computed from the counts per second on the L'2 and H'2 FC and transformed into raw $\delta^{18}O$ using the regular formula ($\delta^{18}O=[(^{18}O / ^{16}O)spl / (^{18}O / ^{16}O)ref]- 1$) with VSMOW as reference. For each standard and sample cluster, we calculated mean and standard deviation for raw $\delta^{18}O$. Raw $\delta^{18}O$ were drifted corrected and calibrated using the procedure described in methods. The analytical yield (cps/nA) is calculated from the counts per second on the L'2 FC and the beam intensity.

SIMS ANALYSES						Mount: Pi01			Standard: UNIL-Q1 (Paine)	Analyse: $\delta^{18}O$			Value= 9.81±0.14 (VSMOW, 2σ)			Date: 06.12.2013	
	Beam	H'2/L'2 ($^{18}O/^{16}O$)		L'2 (^{18}O/Coeff)		H'2 (^{16}O/Coeff)		Time	Yield	Measurements (‰)		mean	Drift correction (‰)		Calibration (‰)		
	nA	*CPS*	*2SD*	*CPS*	*2SD*	*CPS*	*2SD*		CPS/nA	$\delta^{18}O$	*2SD int*	*2SD*	$\delta^{18}O$	*2SD*	$\delta^{18}O_{VSMOW}$	*2SD*	*Comment*
d18O_NIST_051213	1.76	2.03E-03	6.74E-03	1.65E+09	1.69E-01	3.34E+06	1.71E-01	18:40	937036723.6	10.53	0.07		10.50	0.07			Standard
d18O_NIST_051213@00	1.75	2.03E-03	9.37E-03	1.62E+09	2.22E-01	3.29E+06	2.24E-01	18:46	929754014.2	10.44	0.09		10.42	0.09			Standard
d18O_NIST_051213@01	1.76	2.03E-03	8.94E-03	1.66E+09	2.19E-01	3.36E+06	2.21E-01	18:52	940293982.6	10.55	0.09		10.52	0.09			Standard
d18O_NIST_051213@02	1.75	2.03E-03	8.15E-03	1.65E+09	1.78E-01	3.34E+06	1.77E-01	18:57	940747052.5	10.26	0.08		10.25	0.08			Standard
d18O_CSDT_051213_Rad@1	1.73	2.06E-03	8.40E-03	1.69E+09	1.88E-01	3.48E+06	1.87E-01	19:03	975833586.0	28.25	0.08		28.24	0.08			Pi01
d18O_CSDT_051213_Rad@2	1.74	2.06E-03	8.93E-03	1.69E+09	1.88E-01	3.49E+06	1.86E-01	19:09	970639709.1	28.52	0.09		28.51	0.09			Pi01 matrix
d18O_CSDT_051213_Rad@3	1.74	2.06E-03	7.66E-03	1.68E+09	1.39E-01	3.46E+06	1.39E-01	19:14	965642159.9	28.34	0.07		28.33	0.07			Pi01
d18O_CSDT_051213_Rad@4	1.73	2.06E-03	9.30E-03	1.66E+09	1.75E-01	3.43E+06	1.72E-01	19:20	962178241.0	28.39	0.09		28.39	0.09			Pi01
d18O_CSDT_051213_Rad@5	1.74	2.06E-03	6.68E-03	1.66E+09	1.47E-01	3.43E+06	1.46E-01	19:25	958772118.2	28.61	0.06		28.62	0.06			Pi01
d18O_CSDT_051213_Rad@6	1.72	2.06E-03	8.69E-03	1.66E+09	1.76E-01	3.42E+06	1.74E-01	19:31	964038027.7	26.02	0.08		26.03	0.08			Pi01
d18O_CSDT_051213_Rad@7	1.73	2.06E-03	7.49E-03	1.66E+09	1.85E-01	3.41E+06	1.84E-01	19:37	956921826.6	28.62	0.07		28.64	0.07			Pi01 matrix
d18O_CSDT_051213_Rad@8	1.73	2.06E-03	7.25E-03	1.68E+09	1.75E-01	3.46E+06	1.75E-01	19:43	971843241.2	27.63	0.07		27.65	0.07			Pi01 matrix
d18O_CSDT_051213_Rad@9	1.73	2.06E-03	7.20E-03	1.66E+09	1.67E-01	3.43E+06	1.65E-01	19:48	961408328.6	28.58	0.07		28.60	0.07			Pi01
d18O_CSDT_051213_Rad@10	1.73	2.06E-03	7.88E-03	1.66E+09	1.76E-01	3.42E+06	1.78E-01	19:54	960327526.0	28.13	0.08		28.16	0.08			Pi01
d18O_NIST_051213@03	1.74	2.03E-03	9.51E-03	1.64E+09	1.88E-01	3.32E+06	1.89E-01	19:59	939541026.8	10.44	0.09		10.48	0.09			Standard
d18O_NIST_051213@04	1.74	-5.54E-02	6.84E-03	8.08E+08	2.00E+01	1.61E+06	2.07E+01	20:04	465282628.7	-28621.71	0.00						Standard Rejected
d18O_NIST_CSDT1_061213_test	1.97	2.03E-03	9.82E-03	1.91E+09	2.92E-01	3.86E+06	2.95E-01	10:08	966977620.6	10.66	0.10						Standard
d18O_NIST_CSDT1_061213_test@0	1.99	2.03E-03	4.46E-03	1.90E+09	2.65E-01	3.86E+06	2.65E-01	10:13	958449755.8	10.62	0.04						Standard
d18O_NIST_CSDT1_061213_test@1	1.99	2.03E-03	6.66E-03	1.91E+09	2.76E-01	3.86E+06	2.77E-01	10:19	958940040.1	10.90	0.07						Standard
d18O_NIST_CSDT1_061213_test@2	1.99	2.03E-03	4.97E-03	1.89E+09	2.14E-01	3.83E+06	2.17E-01	10:24	946796831.9	10.95	0.05						Standard
d18O_NIST_CSDT1_061213	1.99	2.03E-03	8.31E-03	1.89E+09	2.01E-01	3.82E+06	2.01E-01	10:30	945772952.2	10.94	0.08		10.93	0.08			Standard
d18O_NIST_CSDT1_061213@1	1.99	2.03E-03	1.01E-02	1.88E+09	1.95E-01	3.81E+06	1.98E-01	10:35	942748647.2	11.09	0.10		11.07	0.10			Standard
d18O_NIST_CSDT1_061213@2	1.99	2.03E-03	6.50E-03	1.88E+09	2.05E-01	3.82E+06	2.06E-01	10:41	944925425.5	11.04	0.06		11.02	0.06			Standard
d18O_NIST_CSDT1_061213@3	1.99	2.03E-03	8.73E-03	2.08E+09	3.33E-01	4.21E+06	3.28E-01	10:46	1044254888.4	10.13	0.09		10.12	0.09			Standard
d18O_CSDT_051213_Rad@2b	1.99	2.06E-03	5.88E-03	1.92E+09	1.03E-01	3.96E+06	1.02E-01	10:52	962957678.9	28.96	0.06		28.95	0.06			Pi01 matrix
d18O_CSDT_051213_Rad@2c	1.99	2.06E-03	8.72E-03	1.90E+09	1.29E-01	3.93E+06	1.30E-01	10:57	957509062.5	28.87	0.08		28.85	0.08			Pi01 matrix
d18O_CSDT_051213_Rad@6b	1.98	2.06E-03	7.34E-03	1.91E+09	1.51E-01	3.94E+06	1.52E-01	11:03	964028824.2	28.66	0.07		28.65	0.07			Pi01
d18O_CSDT_051213_Rad@7b	1.98	2.06E-03	6.87E-03	1.89E+09	1.17E-01	3.90E+06	1.19E-01	11:09	956315169.9	28.74	0.07		28.73	0.07			Pi01 matrix
d18O_CSDT_051213_Rad@7c	1.97	2.06E-03	7.44E-03	1.90E+09	1.51E-01	3.93E+06	1.54E-01	11:14	964120635.3	28.51	0.07		28.50	0.07			Pi01 matrix
d18O_CSDT_051213_Rad@7d	1.97	2.06E-03	8.10E-03	1.87E+09	1.10E-01	3.86E+06	1.09E-01	11:20	948241294.4	28.67	0.08		28.66	0.08			Pi01 matrix
d18O_CSDT_051213_Rad@8b	1.97	2.06E-03	4.89E-03	1.89E+09	1.25E-01	3.90E+06	1.25E-01	11:25	957616444.5	28.53	0.05		28.52	0.05			Pi01 matrix
d18O_NIST_CSDT1_061213@4	1.97	2.03E-03	8.08E-03	1.82E+09	1.67E-01	3.68E+06	1.67E-01	11:31	923048549.4	10.79	0.08		10.78	0.08			Standard
d18O_NIST_CSDT1_061213@5	1.96	2.03E-03	6.45E-03	1.81E+09	1.18E-01	3.67E+06	1.18E-01	11:36	920637037.3	10.77	0.06		10.77	0.06			Standard
d18O_NIST_CSDT1_061213@6	1.96	2.03E-03	1.03E-02	1.81E+09	1.59E-01	3.67E+06	1.58E-01	11:42	925487784.3	10.81	0.10		10.80	0.10			Standard
d18O_NIST_CSDT1_061213@7	1.95	2.03E-03	6.81E-03	1.82E+09	1.42E-01	3.68E+06	1.43E-01	11:47	929622947.4	10.85	0.07		10.84	0.07			Standard
d18O_CSDT_051213_Rad@11	1.95	2.06E-03	4.48E-03	1.84E+09	1.64E-01	3.80E+06	1.62E-01	11:53	943272631.9	28.80	0.04		28.80	0.04			Pi01
d18O_CSDT_051213_Rad@12	1.95	2.06E-03	6.32E-03	1.81E+09	6.63E-02	3.72E+06	6.70E-02	11:58	925184905.1	28.54	0.06		28.54	0.06			Pi01
d18O_CSDT_051213_Rad@13	1.95	2.06E-03	7.19E-03	1.78E+09	6.82E-02	3.66E+06	7.24E-02	12:04	911993098.8	27.48	0.07		27.47	0.07			Pi01
d18O_CSDT_051213_Rad@14	1.94	2.06E-03	7.07E-03	1.80E+09	8.37E-02	3.71E+06	8.49E-02	12:09	930176591.5	28.85	0.07		28.85	0.07			Pi01
d18O_CSDT_051213_Rad@15	1.94	2.06E-03	8.55E-03	1.79E+09	7.33E-02	3.69E+06	7.08E-02	12:15	922862978.0	27.99	0.08		27.99	0.08			Pi01
d18O_CSDT_051213_Rad@16	1.93	2.06E-03	5.83E-03	1.87E+09	9.65E-02	3.85E+06	8.70E-02	12:21	969055053.1	25.64	0.06		25.64	0.06			Pi01
d18O_CSDT_051213_Rad@17	1.93	2.06E-03	5.99E-03	1.88E+09	1.39E-01	3.86E+06	1.39E-01	12:26	973256076.8	25.40	0.06		25.40	0.06			Pi01
d18O_CSDT_051213_Rad@18	1.93	2.05E-03	1.32E-02	2.03E+09	3.54E-01	4.16E+06	3.44E-01	12:32	1052497605.5	22.41	0.13		22.41	0.13			Pi01
d18O_CSDT_051213_Rad@19	1.92	2.06E-03	8.04E-03	1.89E+09	3.20E-02	3.88E+06	3.50E-02	12:37	985122842.5	25.51	0.08		25.51	0.08			Pi01
d18O_CSDT_051213_Rad@20	1.92	2.06E-03	7.13E-03	1.81E+09	7.41E-02	3.71E+06	7.50E-02	12:43	942994176.3	24.94	0.07		24.95	0.07			Pi01
d18O_NIST_CSDT1_061213@8	1.92	2.03E-03	7.31E-03	1.73E+09	1.17E-01	3.50E+06	1.10E-01	12:48	901636040.5	11.01	0.07		11.01	0.07			Standard
d18O_NIST_CSDT1_061213@9	1.92	2.03E-03	7.52E-03	1.75E+09	1.22E-01	3.56E+06	1.21E-01	12:54	916158385.4	10.78	0.07		10.78	0.07			Standard
d18O_NIST_CSDT1_061213@10	1.90	2.03E-03	6.85E-03	1.75E+09	1.42E-01	3.54E+06	1.45E-01	12:59	916750362.4	10.90	0.07		10.91	0.07			Standard
d18O_NIST_CSDT1_061213@11	1.90	2.03E-03	7.97E-03	1.71E+09	1.15E-01	3.47E+06	1.17E-01	13:05	900903011.1	10.74	0.08		10.75	0.08			Standard
d18O_CSDT_051213_Rad@22	1.90	2.07E-03	6.08E-03	1.76E+09	7.42E-02	3.65E+06	7.48E-02	13:11	929756446.0	31.64	0.06		31.64	0.06			Pi01
d18O_CSDT_051213_Rad@23	1.88	2.07E-03	6.79E-03	1.70E+09	8.30E-02	3.53E+06	8.85E-02	13:16	903009555.7	34.29	0.07		34.30	0.07			Pi01
d18O_CSDT_051213_Rad@24	1.89	2.07E-03	6.94E-03	1.71E+09	6.15E-02	3.55E+06	5.80E-02	13:22	907660798.1	33.70	0.07		33.71	0.07			Pi01
d18O_CSDT_051213_Rad@25	1.87	2.07E-03	7.01E-03	1.72E+09	8.74E-02	3.56E+06	9.03E-02	13:27	917764595.2	32.04	0.07		32.05	0.07			Pi01
d18O_CSDT_051213_Rad@26	1.88	2.07E-03	8.10E-03	1.72E+09	9.19E-02	3.56E+06	9.30E-02	13:33	919271595.5	30.29	0.08		30.30	0.08			Pi01
d18O_CSDT_051213_Rad@27	1.87	2.06E-03	8.31E-03	1.74E+09	9.35E-02	3.58E+06	9.55E-02	13:38	925963968.3	29.62	0.08		29.63	0.08			Pi01
d18O_CSDT_051213_Rad@28	1.86	2.06E-03	8.30E-03	1.74E+09	8.43E-02	3.58E+06	8.64E-02	13:44	932452157.7	28.93	0.08		28.95	0.08			Pi01 matrix
d18O_CSDT_051213_Rad@29	1.87	2.06E-03	5.50E-03	1.72E+09	8.35E-02	3.54E+06	9.09E-02	13:49	923602679.3	25.03	0.05		25.04	0.05			Pi01 matrix
d18O_CSDT_051213_Rad@30	1.87	2.06E-03	7.72E-03	1.85E+09	4.00E-02	3.81E+06	4.19E-02	13:55	989775408.6	26.11	0.08		26.12	0.08			Pi01
d18O_CSDT_051213_Rad@31	1.86	2.06E-03	7.54E-03	1.85E+09	1.91E-01	3.81E+06	1.88E-01	14:00	995048477.8	25.93	0.07		25.95	0.07			Pi01
d18O_NIST_CSDT1_061213@12	1.84	2.03E-03	7.14E-03	1.68E+09	1.22E-01	3.40E+06	1.26E-01	14:06	909700126.4	10.85	0.07		10.87	0.07			Standard
d18O_NIST_CSDT1_061213@13	1.85	2.03E-03	5.27E-03	1.69E+09	1.06E-01	3.42E+06	1.06E-01	14:12	913009652.7	10.66	0.05		10.68	0.05			Standard
d18O_NIST_CSDT1_061213@14	1.84	2.03E-03	9.58E-03	1.68E+09	1.14E-01	3.40E+06	1.16E-01	14:17	910940934.0	11.17	0.09		11.18	0.09			Standard
d18O_NIST_CSDT1_061213@15	1.84	2.03E-03	6.22E-03	1.66E+09	1.14E-01	3.36E+06	1.15E-01	14:23	902535113.2	10.77	0.06		10.79	0.06			Standard

Table A2 Continued.

SIMS ANALYSES						Mount: Ca01			Standard: UNIL-Q1 (Paine)		Analyse: $\delta^{18}O$			Value= 9.81±0.14 (VSMOW, 2σ)			Date: 06.12.2013
	Beam	H'2/L'2 ($^{18}O/^{16}O$)		L'2 (^{18}O/Coeff)		H'2 (^{16}O/Coeff)		Time	Yield	Measurements (‰)		mean	Drift correction (‰)		Calibration (‰)		Comment
	nA	CPS	2SD	CPS	2SD	CPS	2SD		CPS/nA	$\delta^{18}O$	2SD int	2SD	$\delta^{18}O$	2SD	$\delta^{18}O_{V\text{-}SMOW}$	2SD	
d18O_NIST_CSDT3_061213@1	1.82	2.0264E-03	6.2543E-03	1.7811E+09	1.6631E-01	3.6091E+06	1.6931E-01	14:43	977287741.6	10.55	0.06		10.60	0.06			Standard
d18O_NIST_CSDT3_061213@2	1.86	2.0262E-03	6.6390E-03	1.7215E+09	1.3108E-01	3.4878E+06	1.3042E-01	14:49	923326071.4	10.46	0.07		10.50	0.07			Standard
d18O_NIST_CSDT3_061213@3	1.83	2.0264E-03	8.2308E-03	1.7213E+09	1.3329E-01	3.4882E+06	1.3440E-01	14:54	940427324.4	10.59	0.08		10.63	0.08			Standard
d18O_NIST_CSDT3_061213@4	1.83	2.0265E-03	6.9264E-03	1.7292E+09	1.6352E-01	3.5041E+06	1.6538E-01	15:00	944087859	10.60	0.07		10.64	0.07			Standard
d18O_CSDT3_061213@1	1.83	2.0633E-03	8.1094E-03	1.7540E+09	1.7668E-01	3.6189E+06	1.7420E-01	15:06	959941221.2	28.95	0.08		28.98	0.08			Ca01
d18O_CSDT3_061213@02	1.82	2.0637E-03	6.5090E-03	1.7317E+09	1.5226E-01	3.5737E+06	1.5606E-01	15:11	953843306.6	29.17	0.06		29.19	0.06			Ca01
d18O_CSDT3_061213@03	1.82	2.0628E-03	9.2159E-03	1.7281E+09	1.9555E-01	3.5647E+06	1.9694E-01	15:17	949098048.9	28.71	0.09		28.73	0.09			Ca01
d18O_CSDT3_061213@04	1.82	2.0631E-03	7.4815E-03	1.7261E+09	1.6595E-01	3.5612E+06	1.6541E-01	15:22	947365734.6	28.87	0.07		28.89	0.07			Ca01
d18O_CSDT3_061213@05	1.81	2.0640E-03	7.1060E-03	1.7193E+09	1.1586E-01	3.5489E+06	1.1650E-01	15:28	949698680.4	29.35	0.07		29.35	0.07			Ca01
d18O_CSDT3_061213@06	1.80	2.0639E-03	7.6013E-03	1.7005E+09	1.8841E-01	3.5096E+06	1.8826E-01	15:33	943666450.4	29.28	0.07		29.28	0.07			Ca01
d18O_CSDT3_061213@07	1.80	2.0629E-03	9.5068E-03	1.7158E+09	1.7008E-01	3.5395E+06	1.7215E-01	15:39	952188802.9	28.78	0.09		28.77	0.09			Ca01
d18O_CSDT3_061213@08	1.81	2.0641E-03	6.0840E-03	1.7249E+09	1.2808E-01	3.5603E+06	1.2892E-01	15:44	955612863.9	29.40	0.06		29.38	0.06			Ca01
d18O_CSDT3_061213@09	1.81	2.0587E-03	7.5731E-03	1.7426E+09	1.7302E-01	3.5874E+06	1.7638E-01	15:50	961179866.4	26.67	0.07		26.65	0.07			Ca01
d18O_CSDT3_061213@10	1.81	2.0641E-03	6.2662E-03	1.7066E+09	1.4075E-01	3.5226E+06	1.4065E-01	15:56	942681882.7	29.38	0.06		29.35	0.06			Ca01
d18O_CSDT3_061213@11	1.81	2.0646E-03	5.8261E-03	1.7274E+09	1.1620E-01	3.5661E+06	1.1581E-01	16:01	954562560.4	29.60	0.06		29.57	0.06			Ca01
d18O_NIST_CSDT3_061213@5	1.80	2.0265E-03	7.0211E-03	1.7018E+09	1.7275E-01	3.4489E+06	1.7323E-01	16:07	942963434.6	10.62	0.07		10.58	0.07			Standard
d18O_NIST_CSDT3_061213@6	1.81	2.0264E-03	6.0760E-03	1.7091E+09	1.5355E-01	3.4632E+06	1.5199E-01	16:12	942730682.2	10.55	0.06		10.50	0.06			Standard
d18O_NIST_CSDT3_061213@7	1.81	2.0267E-03	8.1140E-03	1.6881E+09	1.3467E-01	3.4211E+06	1.3457E-01	16:18	930517467.1	10.73	0.08		10.68	0.08			Standard
d18O_NIST_CSDT3_061213@8	1.81	2.0266E-03	7.1672E-03	1.6836E+09	1.2255E-01	3.4117E+06	1.2340E-01	16:23	929121369.4	10.67	0.07		10.62	0.07			Standard

SIMS ANALYSES						Mount: Ki08			Standard: UNIL-Q1 (Paine)		Analyse: $\delta^{18}O$			Value= 9.81±0.14 (VSMOW, 2σ)			Date: 06.12.2013
	Beam	H'2/L'2 ($^{18}O/^{16}O$)		L'2 (^{18}O/Coeff)		H'2 (^{16}O/Coeff)		Time	Yield	Measurements (‰)		mean	Drift correction (‰)		Calibration (‰)		Comment
	nA	CPS	2SD	CPS	2SD	CPS	2SD		CPS/nA	$\delta^{18}O$	2SD int	2SD	$\delta^{18}O$	2SD	$\delta^{18}O_{V\text{-}SMOW}$	2SD	
d18O_NIST_K108_061213@1	1.78	2.03E-03	5.80E-03	1.63E+09	1.56E-01	3.29E+06	1.58E-01	17:07	913329556.4	10.31	0.06		10.32	0.06			Standard
d18O_NIST_K108_061213@2	1.78	2.03E-03	8.59E-03	1.62E+09	1.17E-01	3.28E+06	1.10E-01	17:12	907935802.6	10.61	0.08		10.63	0.08			Standard
d18O_NIST_K108_061213@3	1.79	2.03E-03	1.03E-02	1.60E+09	1.01E-01	3.24E+06	1.01E-01	17:18	895583374.2	10.45	0.10		10.46	0.10			Standard
d18O_NIST_K108_061213@4	1.78	2.03E-03	8.80E-03	1.59E+09	1.22E-01	3.22E+06	1.24E-01	17:24	893204020.0	10.58	0.09		10.59	0.09			Standard
d18O_K108_061213_Rad@1	1.78	2.06E-03	8.25E-03	1.67E+09	9.66E-02	3.43E+06	9.83E-02	17:29	935865704.8	25.57	0.08		25.59	0.08			Ki08
d18O_K108_061213_Rad@2	1.78	2.05E-03	9.49E-03	1.67E+09	1.19E-01	3.43E+06	1.20E-01	17:35	935067212.9	24.15	0.09		24.16	0.09			Ki08
d18O_K108_061213_Rad@3	1.78	2.05E-03	7.41E-03	1.66E+09	1.18E-01	3.41E+06	1.14E-01	17:40	930860841.3	24.30	0.07		24.31	0.07			Ki08
d18O_K108_061213_Rad@4a	1.78	2.06E-03	8.00E-03	1.68E+09	3.41E-01	3.46E+06	3.42E-01	17:46	946623505.0	26.90	0.08		26.91	0.08			Ki08
d18O_K108_061213_Rad@4b1	1.80	2.06E-03	8.19E-03	1.69E+09	1.34E-01	3.48E+06	1.33E-01	17:51	941500427.1	25.60	0.08		25.61	0.08			Ki08
d18O_K108_061213_Rad@4c	1.78	2.05E-03	9.94E-03	1.67E+09	9.72E-02	3.43E+06	9.17E-02	17:57	936396816.4	24.28	0.10		24.29	0.10			Ki08
d18O_K108_061213_Rad@5a	1.77	2.06E-03	8.09E-03	1.65E+09	7.29E-02	3.40E+06	7.15E-02	18:02	936503855.7	26.70	0.08		26.70	0.08			Ki08
d18O_K108_061213_Rad@5b	1.77	2.06E-03	8.51E-03	1.65E+09	9.43E-02	3.40E+06	9.60E-02	18:08	936336153.4	26.46	0.08		26.47	0.08			Ki08
d18O_K108_061213_Rad@6	1.75	2.06E-03	7.56E-03	1.64E+09	7.53E-02	3.37E+06	7.84E-02	18:13	935726935.9	25.14	0.07		25.14	0.07			Ki08
d18O_K108_061213_Rad@7	1.75	2.05E-03	7.95E-03	1.61E+09	6.58E-02	3.30E+06	6.67E-02	18:19	920237746.2	24.16	0.08		24.17	0.08			Ki08
d18O_NIST_K108_061213@5	1.74	2.03E-03	1.04E-02	1.57E+09	1.14E-01	3.17E+06	1.12E-01	18:25	899689925.4	10.35	0.10		10.36	0.10			Standard
d18O_NIST_K108_061213@6	1.74	2.03E-03	9.43E-03	1.57E+09	5.84E-02	3.17E+06	5.71E-02	18:30	901186676.2	10.71	0.09		10.72	0.09			Standard
d18O_NIST_K108_061213@7	1.73	2.03E-03	8.34E-03	1.58E+09	1.25E-01	3.19E+06	1.27E-01	18:36	909775738.3	10.36	0.08		10.36	0.08			Standard
d18O_NIST_K108_061213@8	1.73	2.03E-03	8.06E-03	1.56E+09	1.24E-01	3.17E+06	1.23E-01	18:41	905524233.3	10.51	0.08		10.52	0.08			Standard
d18O_K108_061213_Rad@8	1.72	2.06E-03	8.50E-03	1.60E+09	5.16E-02	3.29E+06	4.85E-02	18:47	929426857.6	26.77	0.08		26.77	0.08			Ki08
d18O_K108_061213_Rad@9	1.73	2.06E-03	8.72E-03	1.55E+09	6.61E-02	3.19E+06	6.47E-02	18:52	898925923.2	25.53	0.08		25.53	0.08			Ki08
d18O_K108_061213_Rad@10	1.72	2.06E-03	5.80E-03	1.55E+09	6.32E-02	3.19E+06	6.22E-02	18:58	902282757.9	25.43	0.06		25.44	0.06			Ki08
d18O_K108_061213_Rad@11a	1.71	2.06E-03	7.01E-03	1.56E+09	4.67E-02	3.20E+06	4.86E-02	19:03	908354883.7	25.38	0.07		25.38	0.07			Ki08
d18O_K108_061213_Rad@11b	1.72	2.05E-03	8.52E-03	1.56E+09	6.65E-02	3.20E+06	6.94E-02	19:09	904497693.1	24.79	0.08		24.79	0.08			Ki08
d18O_K108_061213_Rad@11c	1.72	2.06E-03	8.61E-03	1.53E+09	2.83E-02	3.16E+06	2.51E-02	19:15	893300584.6	25.48	0.08		25.48	0.08			Ki08
d18O_K108_061213_Rad@12	1.71	2.06E-03	9.33E-03	1.54E+09	7.27E-02	3.18E+06	7.04E-02	19:20	903770057.3	26.61	0.09		26.61	0.09			Ki08
d18O_K108_061213_argile@1	1.71	2.05E-03	1.02E-02	1.55E+09	8.98E-02	3.18E+06	9.21E-02	19:26	907442845.9	23.48	0.10		23.48	0.10			Ki08 Clay
d18O_K108_061213_argile@2	1.71	2.05E-03	9.01E-03	1.54E+09	1.94E-02	3.16E+06	1.91E-02	19:31	900282302.0	23.12	0.09		23.12	0.09			Ki08 Clay
d18O_K108_061213_argile@3	1.71	2.05E-03	9.48E-03	1.50E+09	4.46E-02	3.09E+06	4.49E-02	19:37	8788889186.9	24.26	0.09		24.26	0.09			Ki08 Clay
d18O_NIST_K108_061213@9	1.70	2.03E-03	8.56E-03	1.52E+09	1.07E-01	3.07E+06	1.06E-01	19:42	890615758.4	10.60	0.08		10.60	0.08			Standard
d18O_NIST_K108_061213@10	1.70	2.03E-03	7.13E-03	1.53E+09	1.02E-01	3.10E+06	1.03E-01	19:48	897582878.4	10.86	0.07		10.86	0.07			Standard
d18O_NIST_K108_061213@11	1.71	2.03E-03	7.53E-03	1.53E+09	1.04E-01	3.10E+06	1.06E-01	19:53	895962799.3	10.48	0.07		10.48	0.07			Standard
d18O_NIST_K108_061213@12	1.69	2.03E-03	1.04E-02	1.53E+09	4.86E-02	3.11E+06	5.73E-02	19:59	904223006.1	10.54	0.10		10.53	0.10			Standard
d18O_K108_061213_Rad@13a	1.69	2.06E-03	9.67E-03	1.53E+09	7.23E-02	3.14E+06	7.02E-02	20:05	900774762.8	26.39	0.09		26.38	0.09			Ki08
d18O_K108_061213_Rad@13b	1.69	2.06E-03	6.86E-03	1.53E+09	2.76E-02	3.14E+06	3.03E-02	20:10	901944427.4	26.49	0.07		26.48	0.07			Ki08
d18O_K108_061213_Rad@13c	1.68	2.06E-03	7.22E-03	1.52E+09	5.27E-02	3.14E+06	5.03E-02	20:16	905901309.0	26.70	0.07		26.69	0.07			Ki08
d18O_K108_061213_Rad@14	1.67	2.06E-03	8.18E-03	1.52E+09	8.04E-02	3.13E+06	8.10E-02	20:21	908367952.4	24.89	0.08		24.88	0.08			Ki08
d18O_K108_061213_Rad@15	1.68	2.06E-03	7.50E-03	1.53E+09	6.83E-02	3.15E+06	6.89E-02	20:27	911867589.2	24.96	0.07		24.95	0.07			Ki08
d18O_K108_061213_Rad@16	1.68	2.05E-03	9.10E-03	1.52E+09	1.15E-01	3.12E+06	1.14E-01	20:32	907143100.2	24.57	0.09		24.56	0.09			Ki08
d18O_K108_061213_Rad@17	1.66	2.05E-03	9.76E-03	1.49E+09	1.01E-01	3.06E+06	1.05E-01	20:38	895445071.7	24.00	0.10		23.99	0.10			Ki08
d18O_K108_061213_Rad@18	1.66	2.06E-03	6.93E-03	1.51E+09	9.39E-02	3.10E+06	9.18E-02	20:43	906469387.6	25.25	0.07		25.24	0.07			Ki08
d18O_K108_061213_Rad@19	1.66	2.05E-03	7.26E-03	1.50E+09	1.33E-01	3.08E+06	1.37E-01	20:49	904443728.6	24.69	0.07		24.68	0.07			Ki08
d18O_K108_061213_Rad@20	1.66	2.05E-03	1.05E-02	1.53E+09	1.28E-01	3.14E+06	1.28E-01	20:55	922089710.8	24.57	0.10		24.56	0.10			Ki08
d18O_NIST_K108_061213@13	1.66	2.03E-03	6.81E-03	1.52E+09	1.31E-01	3.08E+06	1.32E-01	21:00	919143671.6	10.36	0.07		10.34	0.07			Standard
d18O_NIST_K108_061213@14	1.66	2.03E-03	8.65E-03	1.51E+09	1.39E-01	3.06E+06	1.41E-01	21:06	909604945.1	10.17	0.09		10.15	0.09			Standard
d18O_NIST_K108_061213@15	1.66	2.03E-03	9.03E-03	1.50E+09	8.08E-02	3.05E+06	8.06E-02	21:11	909045049.1	10.44	0.09		10.43	0.09			Standard
d18O_NIST_K108_061213@16	1.65	2.03E-03	8.55E-03	1.50E+09	1.23E-01	3.05E+06	1.25E-01	21:17	909199694.1	10.71	0.08		10.69	0.08			Standard

Table A2 Continued.

SIMS ANALYSES						Mount: PRIM123		Standard: UNIL-Q1 (Paine)	Analyse: $\delta^{18}O$			Value= 9.81±0.14 (VSMOW, 2σ)				Date: 26.06.2014
	Beam	H'2/L'2 ($^{18}O/^{16}O$)		L'2 (^{16}O/Coeff)		H'2 (^{16}O/Coeff)		Time	Yield	Measurements (‰)		mean	Drift correction (‰)		Calibration (‰)		*Comment*
	nA	*CPS*	*2SD*	*CPS*	*2SD*	*CPS*	*2SD*		CPS/nA	$\delta^{18}O$	*2SD int*	*2SD*	$\delta^{18}O$	*2SD*	$\delta^{18}O_{VSMOW}$	*2SD*	
d18O_prim123_paine@48								17:54		6.69	0.17	6.59	6.66	0.17	9.94	0.20	Standard
d18O_prim123_paine@49								18:07		6.73	0.18	0.23	6.70	0.18	9.98	0.20	Standard
d18O_prim123_paine@50								18:12		6.76	0.18		6.73	0.18	10.02	0.20	Standard
d18O_prim123_paine@51								18:17		6.49	0.12		6.46	0.12	9.75	0.19	Standard
d18O_prim123_paine@52								18:21		6.54	0.21		6.51	0.21	9.80	0.21	Standard
d18O_prim123_paine@53								18:26		6.62	0.14		6.59	0.14	9.88	0.19	Standard
d18O_prim123_paine@54								18:31		6.55	0.16		6.52	0.16	9.81	0.20	Standard
d18O_prim123_paine@55								18:35		6.65	0.13		6.62	0.13	9.91	0.19	Standard
d18O_prim123_paine@56								18:40		6.54	0.16		6.51	0.16	9.79	0.20	Standard
d18O_prim123_paine@57								18:45		6.69	0.17		6.66	0.17	9.95	0.20	Standard
d18O_prim123_paine@58								18:50		6.43	0.17		6.40	0.17	9.68	0.20	Standard
d18O_prim123_paine@59								18:54		6.41	0.20		6.38	0.20	9.66	0.21	Standard
d18O_prim123_paine@60								18:59		6.52	0.17		6.50	0.17	9.78	0.20	Standard
d18O_prim123_r4c1@1								19:04		27.57	0.20	27.49	27.54	0.20	30.90	0.21	base Ki08C
d18O_prim123_r4c1@2								19:09		27.31	0.18	1.00	27.28	0.18	30.64	0.20	base Ki08C
d18O_prim123_r4c1@3								19:13		27.56	0.15		27.54	0.15	30.89	0.20	base Ki08C
d18O_prim123_r4c1@4								19:18		26.92	0.17		26.90	0.17	30.25	0.20	base Ki08C
d18O_prim123_r1c2@1								19:23		28.40	0.14		28.37	0.14	31.73	0.20	middle Ki08C
d18O_prim123_r1c2@2								19:27		27.69	0.14		27.67	0.14	31.02	0.20	middle Ki08C
d18O_prim123_r1c2@3								19:32		26.99	0.16		26.96	0.16	30.31	0.20	middle Ki08C
d18O_prim123_paine@61								19:37		6.47	0.17	6.53	6.44	0.17	9.73	0.20	Standard
d18O_prim123_paine@62								19:42		6.42	0.19	0.23	6.40	0.19	9.68	0.20	Standard
d18O_prim123_paine@63								19:46		6.53	0.14		6.51	0.14	9.79	0.19	Standard
d18O_prim123_paine@64								19:51		6.68	0.23		6.66	0.23	9.95	0.21	Standard
d18O_prim123_r1c2@4								19:56		27.68	0.20	28.08	27.66	0.20	31.01	0.21	middle Ki08C
d18O_prim123_r2c2@1								20:01		27.63	0.19	0.82	27.61	0.19	30.96	0.21	middle Ki08C
d18O_prim123_r2c2@2								20:05		27.97	0.22		27.94	0.22	31.30	0.21	middle Ki08C
d18O_prim123_r2c2@3								20:10		27.89	0.21		27.86	0.21	31.22	0.21	middle Ki08C
d18O_prim123_r2c2@4								20:15		27.83	0.16		27.81	0.16	31.16	0.20	middle Ki08C
d18O_prim123_r2c2@5								20:20		27.49	0.14		27.47	0.14	30.83	0.20	middle Ki08C
d18O_prim123_r2c2@6								20:24		28.14	0.11		28.12	0.11	31.48	0.19	middle Ki08C
d18O_prim123_r3c2@1								20:29		27.92	0.14		27.90	0.14	31.25	0.20	middle Ki08C
d18O_prim123_r3c2@2								20:34		27.98	0.16		27.96	0.16	31.31	0.20	middle Ki08C
d18O_prim123_r3c2@3								20:38		28.40	0.19		28.38	0.19	31.74	0.21	middle Ki08C
d18O_prim123_r3c2@4								20:43		28.36	0.18		28.34	0.18	31.70	0.20	middle Ki08C
d18O_prim123_r4c2@1								20:48		28.47	0.21		28.45	0.21	31.81	0.21	middle Ki08C
d18O_prim123_r4c2@2								20:53		28.43	0.15		28.41	0.15	31.77	0.20	middle Ki08C
d18O_prim123_r4c2@3								20:57		29.09	0.17		29.07	0.17	32.43	0.20	middle Ki08C
d18O_prim123_r4c2@4								21:02		27.92	0.23		27.90	0.23	31.25	0.22	middle Ki08C
d18O_prim123_paine@65								21:07		6.36	0.12	6.54	6.35	0.12	9.63	0.19	Standard
d18O_prim123_paine@66								21:12		6.67	0.14	0.56	6.65	0.14	9.94	0.19	Standard
d18O_prim123_paine@67								21:16		6.27	0.12		6.25	0.12	9.54	0.19	Standard
d18O_prim123_paine@68								21:21		6.87	0.17		6.86	0.17	10.14	0.20	Standard
d18O_prim123_r4c2@5								21:26		27.45	0.22	27.62	27.44	0.22	30.79	0.21	middle Ki08C
d18O_prim123_r4c2@6								21:31		27.34	0.17	0.92	27.32	0.17	30.68	0.20	middle Ki08C
d18O_prim123_r4c2@7								21:35		27.34	0.16		27.33	0.16	30.68	0.20	middle Ki08C
d18O_prim123_r4c2@8								21:40		27.70	0.16		27.69	0.16	31.04	0.20	middle Ki08C
d18O_prim123_r5c1@1								21:45		27.57	0.20		27.55	0.20	30.91	0.21	middle Ki08C
d18O_prim123_r5c1@2								21:49		27.61	0.18		27.60	0.18	30.95	0.20	middle Ki08C
d18O_prim123_r5c1@3								21:54		27.90	0.12		27.88	0.12	31.24	0.19	middle Ki08C
d18O_prim123_r5c1@4								21:59		27.18	0.18		27.17	0.18	30.52	0.21	middle Ki08C
d18O_prim123_r5c1@5								22:03		27.32	0.17		27.31	0.17	30.66	0.20	middle Ki08C
d18O_prim123_r5c1@6								22:08		28.88	0.14		28.87	0.14	32.22	0.20	middle Ki08C
d18O_prim123_r1c3@1								22:13		27.17	0.17		27.16	0.17	30.51	0.20	top Ki08C
d18O_prim123_r2c3@1								22:18		27.77	0.23		27.76	0.23	31.11	0.22	top Ki08C
d18O_prim123_r2c3@2								22:22		28.10	0.19		28.08	0.19	31.44	0.21	top Ki08C
d18O_prim123_r2c3@3								22:27		27.83	0.14		27.82	0.14	31.17	0.20	top Ki08C
d18O_prim123_r2c3@4								22:32		27.06	0.18		27.05	0.18	30.40	0.20	top Ki08C
d18O_prim123_paine@69								22:37		6.73	0.12	6.45	6.72	0.12	10.00	0.19	Standard
d18O_prim123_paine@70								22:41		6.53	0.20	0.60	6.52	0.20	9.81	0.20	Standard
d18O_prim123_paine@71								22:46		6.50	0.14		6.49	0.14	9.78	0.19	Standard
d18O_prim123_paine@72								22:51		6.02	0.19		6.01	0.19	9.30	0.20	Standard
d18O_prim123_r3c3@1								22:56		26.46	0.17	26.95	26.45	0.17	29.80	0.20	top Ki08C
d18O_prim123_r3c3@2								23:00		27.56	0.18	0.78	27.55	0.18	30.90	0.20	top Ki08C
d18O_prim123_r3c3@3								23:05		26.90	0.16		26.89	0.16	30.24	0.20	top Ki08C
d18O_prim123_r4c3@1								23:10		26.77	0.10		26.76	0.10	30.12	0.19	top Ki08C
d18O_prim123_r4c3@2								23:15		26.43	0.17		26.42	0.17	29.77	0.20	top Ki08C
d18O_prim123_r4c3@3								23:19		26.77	0.20		26.76	0.20	30.11	0.21	top Ki08C
d18O_prim123_r4c3@4								23:24		26.95	0.15		26.94	0.15	30.30	0.20	top Ki08C
d18O_prim123_r5c3@1								23:29		26.74	0.27		26.74	0.27	30.09	0.23	top Ki08C
d18O_prim123_r5c3@2								23:34		27.00	0.17		27.00	0.17	30.35	0.20	top Ki08C

Table A2 Continued.

SIMS ANALYSES						Mount: PRIM123	Standard: UNIL-Q1 (Paine)	Analyse: $\delta^{18}O$			Value= 9.81±0.14 (VSMOW, 2σ)				Date: 26.06.2014
	Beam	H'2/L'2 ($^{18}O/^{16}O$)		L'2 (^{18}O/Coeff)		H'2 (^{16}O/Coeff)		Measurements (‰)		mean	Drift correction (‰)		Calibration (‰)		
	nA	*CPS*	*2SD*	*CPS*	*2SD*	*CPS*	*2SD*	Time	Yield CPS/nA	$\delta^{18}O$	*2SD int*	*2SD*	$\delta^{18}O$	*2SD*	$\delta^{18}O_{(VSMOW)}$	*2SD*	*Comment*
d18O_prim123_r5c3@3								23:38		26.50	0.17		26.49	0.17	29.84	0.20	top Ki08C
d18O_prim123_r1c4@1								23:43		26.91	0.10		26.90	0.10	30.25	0.19	Ki08C
d18O_prim123_r1c4@2								23:48		27.14	0.10		27.14	0.10	30.49	0.19	Ki08C
d18O_prim123_r1c4@3								23:53		27.84	0.18		27.84	0.18	31.19	0.21	Ki08C
d18O_prim123_r1c4@4								23:57		27.29	0.20		27.29	0.20	30.64	0.21	Ki08C
d18O_prim123_r1c4@5								0:02		26.97	0.15		26.97	0.15	30.32	0.20	Ki08C
d18O_prim123_paine@74								0:07		6.44	0.11	6.43	6.44	0.11	9.72	0.19	Standard
d18O_prim123_paine@75								0:12		6.43	0.13	0.03	6.43	0.13	9.71	0.19	Standard
d18O_prim123_paine@76								0:16		6.44	0.13		6.44	0.13	9.73	0.19	Standard
d18O_prim123_paine@77								0:21		6.41	0.10		6.40	0.10	9.69	0.19	Standard
d18O_prim123_r2c4@1								0:26		27.19	0.21	27.37	27.19	0.21	30.54	0.21	Ki08C
d18O_prim123_r2c4@2								0:31		26.99	0.15	1.16	26.99	0.15	30.34	0.20	Ki08C
d18O_prim123_r2c4@3								0:35		26.16	0.13		26.16	0.13	29.51	0.19	Ki08C
d18O_prim123_r3c4@1								0:40		28.58	0.15		28.58	0.15	31.93	0.20	Ki08C
d18O_prim123_r3c4@2								0:45		27.52	0.20		27.52	0.20	30.88	0.21	Ki08C
d18O_prim123_r3c4@3								0:50		28.44	0.19		28.44	0.19	31.79	0.21	Ki08C
d18O_prim123_r3c4@4								0:54		27.07	0.18		27.07	0.18	30.42	0.20	Ki08C
d18O_prim123_r3c4@5								0:59		27.23	0.19		27.23	0.19	30.58	0.21	Ki08C
d18O_prim123_r4c4@1								1:04		27.46	0.18		27.46	0.18	30.81	0.20	Ki08C
d18O_prim123_r4c4@2								1:08		27.05	0.16		27.05	0.16	30.40	0.20	Ki08C
d18O_prim123_r4c4@3								1:13		27.42	0.10		27.42	0.10	30.78	0.19	Ki08C
d18O_prim123_r4c4@4								1:18		27.56	0.11		27.56	0.11	30.91	0.19	Ki08C
d18O_prim123_r5c4@1								1:23		27.00	0.12		27.01	0.12	30.36	0.19	Ki08C
d18O_prim123_r5c4@2								1:27		27.59	0.15		27.59	0.15	30.94	0.20	Ki08C
d18O_prim123_r5c4@3								1:32		27.27	0.14		27.27	0.14	30.63	0.20	Ki08C
d18O_prim123_paine@78								1:37		6.77	0.15	6.64	6.77	0.15	10.06	0.19	Standard
d18O_prim123_paine@79								1:42		6.79	0.16	0.43	6.80	0.16	10.08	0.20	Standard
d18O_prim123_paine@80								1:46		6.33	0.24		6.33	0.24	9.61	0.22	Standard
d18O_prim123_paine@81								1:51		6.66	0.11		6.66	0.11	9.95	0.19	Standard
d18O_prim123_r1c5@1								1:56		26.73	0.17	27.10	26.73	0.17	30.08	0.20	Ki08C
d18O_prim123_r1c5@2								2:01		26.79	0.12	1.17	26.79	0.12	30.15	0.19	Ki08C
d18O_prim123_r1c5@3								2:05		26.88	0.16		26.88	0.16	30.23	0.20	Ki08C
d18O_prim123_r2c5@1								2:10		27.64	0.18		27.65	0.18	31.00	0.20	Ki08C
d18O_prim123_r2c5@2								2:15		27.28	0.14		27.29	0.14	30.64	0.20	Ki08C
d18O_prim123_r2c5@3								2:19		27.44	0.14		27.45	0.14	30.80	0.20	Ki08C
d18O_prim123_r3c5@1								2:24		25.41	0.16		25.42	0.16	28.77	0.20	Ki08C
d18O_prim123_r3c5@2								2:29		27.25	0.16		27.26	0.16	30.61	0.20	Ki08C
d18O_prim123_r3c5@3								2:34		27.28	0.14		27.28	0.14	30.64	0.20	Ki08C
d18O_prim123_r3c5@4								2:38		27.64	0.12		27.64	0.12	31.00	0.19	Ki08C
d18O_prim123_r3c5@5								2:43		27.27	0.17		27.28	0.17	30.63	0.20	Ki08C
d18O_prim123_r4c5@1								2:48		27.85	0.16		27.86	0.16	31.22	0.20	Ki08C
d18O_prim123_r4c5@2								2:53		27.40	0.15		27.41	0.15	30.76	0.20	Ki08C
d18O_prim123_r4c5@3								2:57		26.98	0.12		26.99	0.12	30.34	0.19	Ki08C
d18O_prim123_r4c5@4								3:02		26.65	0.12		26.66	0.12	30.01	0.19	Ki08C
d18O_prim123_paine@82								3:07		6.66	0.18	6.49	6.67	0.18	9.96	0.20	Standard
d18O_prim123_paine@83								3:12		6.09	0.18	0.54	6.10	0.18	9.39	0.20	Standard
d18O_prim123_paine@84								3:16		6.64	0.13		6.65	0.13	9.94	0.19	Standard
d18O_prim123_paine@85								3:21		6.57	0.14		6.58	0.14	9.87	0.19	Standard
d18O_prim123_r4c5@5								3:26		26.63	0.17	27.06	26.65	0.17	30.00	0.20	Ki08C
d18O_prim123_r4c5@6								3:31		27.53	0.21	0.77	27.55	0.21	30.90	0.21	Ki08C
d18O_prim123_r5c5@1								3:35		27.17	0.14		27.18	0.14	30.54	0.20	Ki08C
d18O_prim123_r5c5@2								3:40		26.89	0.16		26.90	0.16	30.26	0.20	Ki08C
d18O_prim123_r1c6@1								3:45		31.36	0.15	31.16	31.37	0.15	34.74	0.20	Pi01
d18O_prim123_r1c6@2								3:50		30.17	0.15	1.03	30.18	0.15	33.54	0.20	Pi01
d18O_prim123_r1c6@3								3:54		30.15	0.20		30.16	0.20	33.53	0.21	Pi01
d18O_prim123_r2c6@1								3:59		31.35	0.10		31.36	0.10	34.73	0.19	Pi01
d18O_prim123_r2c6@2								4:04		31.37	0.16		31.39	0.16	34.75	0.20	Pi01
d18O_prim123_r2c6@3								4:09		31.21	0.14		31.23	0.14	34.59	0.20	Pi01
d18O_prim123_r2c6@4								4:13		31.28	0.12		31.29	0.12	34.66	0.19	Pi01
d18O_prim123_r2c6@5								4:18		31.49	0.13		31.51	0.13	34.88	0.19	Pi01
d18O_prim123_r2c6@6								4:23		31.32	0.20		31.34	0.20	34.71	0.21	Pi01
d18O_prim123_r2c6@7								4:27		31.38	0.15		31.40	0.15	34.77	0.20	Pi01
d18O_prim123_r2c6@8								4:32		31.71	0.22		31.72	0.22	35.09	0.21	Pi01

Table A2 Continued.

SIMS ANALYSES						Mount: PRIM123	Standard: UNIL-Q1 (Paine)	Analyse: $\delta^{18}O$			Value= 9.81±0.14 (VSMOW, 2σ)			Date: 26.06.2014
	Beam	H'2/L'2 ($^{18}O/^{16}O$)		L'2 (^{18}O/Coeff)		H'2 (^{16}O/Coeff)		Measurements (‰)		mean	Drift correction (‰)		Calibration (‰)	
	nA	*CPS*	*2SD*	*CPS*	*2SD*	*CPS*	*2SD*	Time	Yield CPS/nA	$\delta^{18}O$	*2SD int*	*2SD*	$\delta^{18}O$	*2SD*	$\delta^{18}O_{VSMOW}$	*2SD*	*Comment*
d18O_prim123_paine@86								4:37		6.37	0.22	6.55	6.39	0.22	9.67	0.21	Standard
d18O_prim123_paine@87								4:42		6.64	0.12	0.28	6.66	0.12	9.95	0.19	Standard
d18O_prim123_paine@88								4:46		6.52	0.21		6.54	0.21	9.83	0.21	Standard
d18O_prim123_paine@89								4:51		6.67	0.19		6.69	0.19	9.98	0.20	Standard
d18O_prim123_r4c6@1								4:56		31.54	0.15	31.12	31.56	0.15	34.92	0.20	Pi01
d18O_prim123_r4c6@2								5:01		31.09	0.16	0.75	31.11	0.16	34.47	0.20	Pi01
d18O_prim123_r4c6@3								5:05		31.24	0.10		31.26	0.10	34.62	0.19	Pi01
d18O_prim123_r5c6@1								5:10		30.49	0.13		30.50	0.13	33.87	0.19	Pi01
d18O_prim123_r5c6@2								5:15		30.50	0.20		30.52	0.20	33.89	0.21	Pi01
d18O_prim123_r5c6@3								5:20		31.29	0.13		31.31	0.13	34.68	0.20	Pi01
d18O_prim123_r1c7@1								5:25		31.34	0.17		31.36	0.17	34.72	0.20	Pi01
d18O_prim123_r1c7@2								5:29		31.41	0.16		31.43	0.16	34.80	0.20	Pi01
d18O_prim123_r1c7@3								5:34		31.04	0.16		31.07	0.16	34.43	0.20	Pi01
d18O_prim123_r1c7@4								5:39		31.31	0.17		31.33	0.17	34.69	0.20	Pi01
d18O_prim123_r2c7@1								5:44		31.53	0.10		31.55	0.10	34.92	0.19	Pi01
d18O_prim123_r2c7@2								5:48		31.17	0.18		31.19	0.18	34.56	0.20	Pi01
d18O_prim123_r3c7@1								5:53		30.36	0.14		30.38	0.14	33.75	0.20	Pi01
d18O_prim123_r3c7@2								5:58		31.16	0.17		31.18	0.17	34.55	0.20	Pi01
d18O_prim123_r4c7@1								6:03		31.35	0.10		31.38	0.10	34.74	0.19	Pi01
d18O_prim123_paine@90								6:08		6.78	0.24	6.50	6.81	0.24	10.09	0.22	Standard
d18O_prim123_paine@91								6:12		6.21	0.15	0.51	6.23	0.15	9.52	0.20	Standard
d18O_prim123_paine@92								6:17		6.62	0.14		6.64	0.14	9.93	0.19	Standard
d18O_prim123_paine@93								6:22		6.38	0.14		6.41	0.14	9.69	0.19	Standard
d18O_prim123_r4c7@2								6:27		31.09	0.10	31.07	31.12	0.10	34.48	0.19	Pi01
d18O_prim123_r5c7@1								6:31		31.61	0.17	0.56	31.64	0.17	35.00	0.20	Pi01
d18O_prim123_r5c7@2								6:36		30.94	0.14		30.96	0.14	34.33	0.20	Pi01
d18O_prim123_r5c7@3								6:41		31.23	0.17		31.26	0.17	34.62	0.20	Pi01
d18O_prim123_r5c7@4								6:46		31.45	0.20		31.48	0.20	34.84	0.21	Pi01
d18O_prim123_r5c7@5								6:50		31.34	0.11		31.37	0.11	34.73	0.19	Pi01
d18O_prim123_r1c8@1								6:55		30.88	0.14		30.91	0.14	34.27	0.20	Ca01
d18O_prim123_r1c8@2								7:00		30.91	0.12		30.93	0.12	34.30	0.19	Ca01
d18O_prim123_r2c8@1								7:05		31.49	0.17		31.52	0.17	34.89	0.20	Ca01
d18O_prim123_r2c8@2								7:09		30.79	0.17		30.82	0.17	34.18	0.20	Ca01
d18O_prim123_r3c8@1								7:14		30.71	0.13		30.73	0.13	34.10	0.20	Ca01
d18O_prim123_r3c8@2								7:19		30.74	0.13		30.77	0.13	34.13	0.20	Ca01
d18O_prim123_r4c8@1								7:24		30.96	0.19		30.99	0.19	34.36	0.21	Ca01
d18O_prim123_r4c8@2								7:28		30.88	0.17		30.91	0.17	34.28	0.20	Ca01
d18O_prim123_r5c8@1								7:33		31.11	0.20		31.14	0.20	34.51	0.21	Ca01
d18O_prim123_r5c8@2								7:38		31.00	0.19		31.03	0.19	34.40	0.21	Ca01
d18O_prim123_paine@94								7:43		6.55	0.17	6.48	6.59	0.17	9.87	0.20	Standard
d18O_prim123_paine@95								7:48		6.45	0.19	0.12	6.48	0.19	9.77	0.20	Standard
d18O_prim123_paine@96								7:52		6.45	0.13		6.48	0.13	9.76	0.19	Standard

Table A2 Continued.

Appendix Table A2. Continued

SIMS ANALYSES							Mount: BR2		Standard: UNIL-Q1 (Paine)		Analyse: $\delta^{18}O$			Value= 9.81±0.14 (VSMOW, 2σ)				Date: 14.04.2015
	Beam	H'2/L'2 ($^{18}O/^{16}O$)		L'2 (^{18}O/Coeff)		H'2 (^{16}O/Coeff)		Time	Yield		Measurements (‰)		mean	Drift correction (‰)		Calibration (‰)		
	nA	CPS	2SD	CPS	2SD	CPS	2SD		CPS/nA		$\delta^{18}O$	2SD int	2SD	$\delta^{18}O$	2SD	$\delta^{18}O_{VSMOW}$	2SD	Comment
140515_br2_testpaine@1	1.97	2.0145E-03	1.2679E-02	1.4717E+09	5.2494E-02	2.9656E+06	4.3500E-02	17:20	7.4783E+08	7.4607E+08	4.66	0.25	4.65					Standard
140515_br2_testpaine@2	1.98	2.0140E-03	8.9695E-03	1.4819E+09	2.8681E-02	2.9847E+06	2.9597E-02	17:25	7.4953E+08	1.0993E+07	4.41	0.18	0.37					Standard
140515_br2_testpaine@3	1.98	2.0142E-03	1.1183E-02	1.4795E+09	3.8761E-02	2.9802E+06	4.2002E-02	17:29	7.4894E+08		4.47	0.22						Standard
140515_br2_testpaine@4	1.98	2.0149E-03	1.0001E-02	1.4609E+09	1.6068E-02	2.9437E+06	1.6269E-02	17:34	7.3853E+08		4.85	0.20						Standard
140515_br2_testpaine@5	1.98	2.0142E-03	1.4034E-02	1.4944E+09	2.1438E-01	3.0143E+06	2.3441E-01	17:39	7.5507E+08		4.46	0.28						Standard
140515_br2_testpaine@6	1.98	2.0147E-03	7.8538E-03	1.4653E+09	5.4533E-02	2.9519E+06	5.7382E-02	17:43	7.3950E+08		4.73	0.16						Standard
140515_br2_testpaine@7	1.98	2.0147E-03	1.1185E-02	1.4715E+09	4.6543E-02	2.9635E+06	5.4643E-02	17:48	7.4342E+08		4.74	0.22						Standard
140515_br2_testpaine@8	1.98	2.0150E-03	1.0887E-02	1.4758E+09	1.1557E-01	2.9738E+06	1.1759E-01	17:52	7.4569E+08		4.90	0.22						Standard
140515_br2_paine@1	1.97	2.0143E-03	8.9543E-03	1.4216E+09	7.9991E-02	2.8634E+06	7.8642E-02	19:00	7.2035E+08	7.2178E+08	4.54	0.18	4.45	4.54	0.18	9.96	0.27	Standard
140515_br2_paine@2	1.99	2.0142E-03	1.3856E-02	1.4200E+09	9.9809E-02	2.8583E+06	1.1641E-01	19:05	7.1375E+08	1.5227E+07	4.50	0.28	0.25	4.51	0.28	9.93	0.29	Standard
140515_br2_paine@3	1.99	2.0138E-03	6.9811E-03	1.4283E+09	3.9485E-02	2.8766E+06	3.8631E-02	19:09	7.1795E+08		4.31	0.14		4.31	0.14	9.73	0.27	Standard
140515_br2_paine@4	1.99	2.0137E-03	9.1124E-03	1.4290E+09	6.5486E-02	2.8777E+06	6.3412E-02	19:14	7.1803E+08		4.23	0.18		4.23	0.18	9.65	0.27	Standard
140515_br2_paine@5	1.99	2.0143E-03	8.7964E-03	1.4328E+09	3.4024E-02	2.8861E+06	3.8082E-02	19:18	7.2073E+08		4.53	0.18		4.54	0.18	9.95	0.27	Standard
140515_br2_paine@6	1.99	2.0144E-03	1.2133E-02	1.4436E+09	5.8303E-02	2.9079E+06	6.1019E-02	19:23	7.2413E+08		4.58	0.24		4.58	0.24	10.00	0.29	Standard
140515_br2_paine@7	2.00	2.0142E-03	1.0712E-02	1.4393E+09	2.7755E-02	2.8989E+06	3.1101E-02	19:28	7.2016E+08		4.51	0.21		4.51	0.21	9.93	0.28	Standard
140515_br2_paine@8	2.00	2.0141E-03	9.6234E-03	1.4760E+09	3.2841E-02	2.9728E+06	2.8371E-02	19:32	7.3914E+08		4.43	0.19		4.44	0.19	9.85	0.28	Standard
d18O_radio140515_Br2_gr1@1	2.00	2.0389E-03	1.5807E-02	1.4017E+09	6.0009E-02	2.8570E+06	4.0383E-02	19:37	7.0251E+08	7.0047E+08	16.82	0.32	15.58	16.82	0.32	22.31	0.31	Ki03s
d18O_radio140515_Br2_gr1@2	1.99	2.0401E-03	1.1066E-02	1.3951E+09	2.6177E-02	2.8463E+06	2.8260E-02	19:42	6.9982E+08	3.9415E+06	17.41	0.22	4.46	17.41	0.22	22.90	0.28	Ki03s
d18O_radio140515_Br2_gr1@3	1.99	2.0366E-03	9.9212E-03	1.3969E+09	3.0066E-02	2.8446E+06	3.4419E-02	19:46	7.0152E+08		15.67	0.20		15.67	0.20	21.15	0.28	Ki03s
d18O_radio140515_Br2_gr1@4	1.99	2.0301E-03	6.7530E-03	1.3913E+09	6.0588E-02	2.8247E+06	5.8691E-02	19:51	6.9802E+08		12.41	0.14		12.41	0.14	17.87	0.27	Ki03s
d18O_radio140515_Br2_gr2@1	2.00	2.0434E-03	1.2515E-02	1.3939E+09	3.5156E-02	2.8481E+06	3.2805E-02	19:55	6.9705E+08	6.9814E+08	19.06	0.25	18.44	19.06	0.25	24.55	0.29	Ki03s
d18O_radio140515_Br2_gr2@2	2.00	2.0401E-03	9.5465E-03	1.4051E+09	4.5668E-02	2.8666E+06	4.5191E-02	20:00	7.0281E+08	6.6714E+06	17.43	0.19	2.26	17.43	0.19	22.92	0.28	Ki03s
d18O_radio140515_Br2_gr2@3	2.00	2.0401E-03	1.0915E-02	1.3876E+09	3.4774E-02	2.8301E+06	2.9395E-02	20:05	6.9383E+08		17.41	0.22		17.41	0.22	22.90	0.28	Ki03s
d18O_radio140515_Br2_gr2@4	1.99	2.0418E-03	1.2076E-02	1.3929E+09	3.8936E-02	2.8446E+06	3.2173E-02	20:09	6.9964E+08		18.25	0.24		18.26	0.24	23.75	0.29	Ki03s
d18O_radio140515_Br2_gr2@5	1.99	2.0454E-03	1.0534E-02	1.3886E+09	3.1597E-02	2.8400E+06	3.1218E-02	20:14	6.9735E+08		20.05	0.21		20.05	0.21	25.55	0.28	Ki03s
140515_br2_paine@9	1.99	2.0142E-03	1.0504E-02	1.4825E+09	2.1759E-02	2.9862E+06	2.6957E-02	20:19	7.4444E+08	7.3844E+08	4.50	0.21	4.66	4.50	0.21	9.92	0.28	Standard
140515_br2_paine@10	2.00	2.0148E-03	1.4517E-02	1.4641E+09	4.3177E-02	2.9500E+06	4.1462E-02	20:23	7.3292E+08	1.2316E+07	4.80	0.29	0.30	4.80	0.29	10.22	0.30	Standard
140515_br2_paine@11	2.00	2.0143E-03	9.8040E-03	1.4658E+09	6.1377E-02	2.9528E+06	6.8370E-02	20:28	7.3335E+08		4.56	0.20		4.56	0.20	9.98	0.28	Standard
140515_br2_paine@12	1.99	2.0148E-03	1.2234E-02	1.4790E+09	3.6988E-02	2.9800E+06	4.3894E-02	20:32	7.4306E+08		4.77	0.24		4.78	0.24	10.19	0.29	Standard
d18O_radio140515_Br2_gr3@1	1.98	2.0471E-03	1.0873E-02	1.4265E+09	5.3185E-02	2.9205E+06	5.5674E-02	20:37	7.1934E+08	7.3124E+08	20.91	0.22	21.48	20.91	0.22	26.42	0.28	Ki22C1
d18O_radio140515_Br2_gr3@2	1.99	2.0485E-03	1.0795E-02	1.4613E+09	9.1119E-02	2.9933E+06	9.0378E-02	20:42	7.3557E+08	2.5396E+07	21.59	0.22	2.43	21.59	0.22	27.10	0.28	Ki22C1
d18O_radio140515_Br2_gr3@3	1.99	2.0520E-03	1.2653E-02	1.4484E+09	3.5080E-02	2.9722E+06	3.8923E-02	20:46	7.2778E+08		23.34	0.25		23.34	0.25	28.86	0.29	Ki22C1
d18O_radio140515_Br2_gr3@4	1.99	2.0470E-03	1.0114E-02	1.4856E+09	3.6346E-02	3.0400E+06	4.4932E-02	20:51	7.4644E+08		20.82	0.20		20.83	0.20	26.33	0.28	Ki22C1
d18O_radio140515_Br2_gr3@5	1.99	2.0434E-03	9.6476E-03	1.4038E+09	2.6716E-02	2.8682E+06	3.2176E-02	20:56	7.0582E+08		19.03	0.19		19.04	0.19	24.53	0.28	Ki22C1
d18O_radio140515_Br2_gr3@6	1.98	2.0490E-03	9.3152E-03	1.4458E+09	5.4291E-02	2.9627E+06	5.7843E-02	21:00	7.2875E+08		21.85	0.19		21.85	0.19	27.36	0.28	Ki22C1
d18O_radio140515_Br2_gr3@7	1.99	2.0507E-03	1.2197E-02	1.4703E+09	4.2753E-02	3.0152E+06	4.7936E-02	21:05	7.3772E+08		22.69	0.24		22.69	0.24	28.21	0.29	Ki22C1
d18O_radio140515_Br2_gr3@8	1.99	2.0481E-03	1.3244E-02	1.4837E+09	3.9313E-02	3.0387E+06	3.8180E-02	21:09	7.4454E+08		21.40	0.26		21.40	0.26	26.91	0.29	Ki22C1
d18O_radio140515_Br2_gr3@9	2.00	2.0487E-03	6.6624E-03	1.4671E+09	4.0567E-02	3.0057E+06	3.7622E-02	21:14	7.3516E+08		21.71	0.13		21.71	0.13	27.22	0.27	Ki22C1
140515_br2_paine@13	1.99	2.0142E-03	1.0027E-02	1.4674E+09	3.9020E-02	2.9559E+06	3.6676E-02	21:19	7.3604E+08	7.3321E+08	4.48	0.20	4.40	4.48	0.20	9.90	0.28	Standard
140515_br2_paine@14	1.99	2.0141E-03	9.3583E-03	1.4559E+09	5.8341E-02	2.9323E+06	6.0529E-02	21:23	7.3174E+08	3.9080E+06	4.46	0.19	0.18	4.46	0.19	9.88	0.27	Standard
140515_br2_paine@15	1.99	2.0139E-03	9.4521E-03	1.4584E+09	2.4628E-02	2.9378E+06	1.9779E-02	21:28	7.3295E+08		4.35	0.19		4.35	0.19	9.76	0.27	Standard
140515_br2_paine@16	1.99	2.0138E-03	1.3860E-02	1.4599E+09	2.7210E-02	2.9398E+06	3.2193E-02	21:33	7.3211E+08		4.30	0.28		4.30	0.28	9.72	0.29	Standard
d18O_radio140515_Br2_gr4@1	1.99	2.0424E-03	1.2517E-02	1.4415E+09	5.7240E-02	2.9441E+06	6.2154E-02	21:37	7.2258E+08	7.4529E+08	18.54	0.25	21.25	18.54	0.25	24.03	0.29	Ki22C2
d18O_radio140515_Br2_gr4@2	1.99	2.0478E-03	1.5479E-02	1.4899E+09	3.3808E-02	3.0516E+06	3.4507E-02	21:42	7.4771E+08	2.7189E+07	21.25	0.31	2.63	21.25	0.31	26.76	0.31	Ki22C2
d18O_radio140515_Br2_gr4@3	1.98	2.0427E-03	1.1041E-02	1.4480E+09	3.5966E-02	2.9575E+06	3.9393E-02	21:47	7.3067E+08		18.72	0.22		18.72	0.22	24.21	0.28	Ki22C2
d18O_radio140515_Br2_gr4@4	1.99	2.0482E-03	9.8935E-03	1.4368E+09	5.3914E-02	2.9430E+06	5.8898E-02	21:51	7.2217E+08		21.42	0.20		21.42	0.20	26.93	0.28	Ki22C2
d18O_radio140515_Br2_gr4@5	1.99	2.0491E-03	1.2985E-02	1.4888E+09	3.1612E-02	3.0508E+06	3.0725E-02	21:56	7.4641E+08		21.89	0.26		21.89	0.26	27.40	0.29	Ki22C2
d18O_radio140515_Br2_gr4@6	1.99	2.0485E-03	1.0735E-02	1.4898E+09	3.2229E-02	3.0522E+06	4.0204E-02	22:00	7.4800E+08		21.61	0.21		21.61	0.21	27.12	0.28	Ki22C2
d18O_radio140515_Br2_gr5@1	1.99	2.0470E-03	1.0590E-02	1.4803E+09	2.7127E-02	3.0301E+06	2.8287E-02	22:05	7.4394E+08		20.83	0.21		20.83	0.21	26.33	0.28	Ki21
d18O_radio140515_Br2_gr5@2	1.99	2.0503E-03	9.6154E-03	1.4873E+09	2.6907E-02	3.0497E+06	2.4176E-02	22:10	7.4825E+08		22.50	0.19		22.51	0.19	28.02	0.28	Ki21
d18O_radio140515_Br2_gr5@3	1.99	2.0486E-03	6.8234E-03	1.4823E+09	2.9963E-02	3.0364E+06	2.7771E-02	22:14	7.4346E+08		21.63	0.14		21.63	0.14	27.14	0.27	Ki21
d18O_radio140515_Br2_gr5@4	2.00	2.0476E-03	1.0200E-02	1.5054E+09	2.6344E-02	3.0815E+06	2.4642E-02	22:19	7.5447E+08		21.13	0.20		21.13	0.20	26.64	0.28	Ki21
d18O_radio140515_Br2_gr5@5	2.00	2.0502E-03	9.6912E-03	1.5205E+09	4.4074E-02	3.1181E+06	3.9582E-02	22:24	7.5917E+08		22.44	0.19		22.44	0.19	27.95	0.28	Ki21
d18O_radio140515_Br2_gr5@6	2.00	2.0484E-03	1.0873E-02	1.4908E+09	4.3648E-02	3.0540E+06	4.4622E-02	22:28	7.4683E+08		21.53	0.22		21.54	0.22	27.04	0.28	Ki21
d18O_radio140515_Br2_gr5@7	1.99	2.0520E-03	1.0148E-02	1.4613E+09	2.4649E-02	2.9989E+06	2.3251E-02	22:33	7.3343E+08		23.36	0.20		23.36	0.20	28.88	0.28	Ki21
d18O_radio140515_Br2_gr5@8	1.99	2.0461E-03	8.3618E-03	1.5487E+09	5.0461E-02	3.1687E+06	4.8005E-02	22:38	7.7670E+08		20.40	0.17		20.41	0.17	25.91	0.28	Ki21
d18O_radio140515_Br2_gr5@9	2.00	2.0505E-03	1.0648E-02	1.4919E+09	3.0944E-02	3.0594E+06	3.2686E-02	22:42	7.4714E+08		22.60	0.21		22.60	0.21	28.12	0.28	Ki21
d18O_radio140515_Br2_gr5@10	2.00	2.0456E-03	9.9916E-03	1.5073E+09	3.9431E-02	3.0832E+06	4.2336E-02	22:47	7.5363E+08		20.17	0.20		20.17	0.20	25.67	0.28	Ki21
140515_br2_paine@17	2.00	2.0142E-03	9.4454E-03	1.4595E+09	4.5298E-02	2.9399E+06	4.6275E-02	22:52	7.3113E+08	7.4063E+08	4.47	0.19	4.37	4.47	0.19	9.89	0.27	Standard
140515_br2_paine@18	2.00	2.0141E-03	9.0255E-03	1.4719E+09	5.6323E-02	2.9644E+06	5.5145E-02	22:56	7.3678E+08	1.6158E+07	4.42	0.18	0.17	4.42	0.18	9.84	0.27	Standard
140515_br2_paine@19	1.99	2.0138E-03	8.5434E-03	1.4885E+09	4.4780E-02	2.9977E+06	4.3428E-02	23:01	7.4647E+08		4.31	0.17		4.31	0.17	9.73	0.27	Standard
140515_br2_paine@20	2.00	2.0138E-03	1.2886E-02	1.4962E+09	2.2739E-02	3.0126E+06	2.7453E-02	23:05	7.4815E+08		4.29	0.26		4.29	0.26	9.71	0.29	Standard
d18O_radio140515_Br2_gr6@1	2.00	2.0578E-03	9.1688E-03	1.5231E+09	2.8598E-02	3.1342E+06	2.9968E-02	23:10	7.6110E+08		26.21	0.18	25.95	26.21	0.18	31.74	0.28	Ki15
d18O_radio140515_Br2_gr6@2	2.00	2.0572E-03	1.0059E-02	1.5107E+09	1.6305E-02	3.1076E+06	1.5332E-02	23:15	7.5710E+08		25.94	0.20	1.44	25.94	0.20	31.47	0.28	Ki15
d18O_radio140515_Br2_gr6@3	1.99	2.0548E-03	9.8617E-03	1.4837E+09	3.1167E-02	3.0499E+06	3.2894E-02	23:19	7.4520E+08		24.73	0.20		24.73	0.20	30.25	0.28	Ki15
d18O_radio140515_Br2_gr6@4	2.00	2.0585E-03	1.2934E-02	1.4987E+09	4.7440E-02	3.0842E+06	4.2849E-02	23:24	7.5051E+08		26.59	0.26		26.59	0.26	32.13	0.29	Ki15
d18O_radio140515_Br2_gr6@5	2.01	2.0581E-03	7.8919E-03	1.5086E+09	1.9408E-02	3.1051E+06	1.9347E-02	23:29	7.5195E+08		26.39	0.16		26.39	0.16	31.92	0.28	Ki15
d18O_radio140515_Br2_gr6@6	2.00	2.0577E-03	1.2480E-02	1.5266E+09	1.9646E-02	3.1414E+06	2.1926E-02	23:33	7.6190E+08		26.16	0.25		26.16	0.25	31.69	0.29	Ki15
d18O_radio140515_Br2_gr6@7	2.00	2.0584E-03	1.2653E-02	1.5127E+09	4.5715E-02	3.1138E+06	5.0727E-02	23:38	7.5671E+08		26.53	0.25		26.53	0.25	32.07	0.29	Ki15
d18O_radio140515_Br2_gr6@8	2.00	2.0580E-03	9.9670E-03	1.5252E+09	2.3034E-02	3.1389E+06	1.8790E-02	23:42	7.6176E+08		26.34	0.20		26.35	0.20	31.88	0.28	Ki15
d18O_radio140515_Br2_gr6@9	2.00	2.0545E-03	1.2870E-02	1.5223E+09	6.5557E-02	3.1276E+06	6.4638E-02	23:47	7.6111E+08		24.57	0.26		24.57	0.26	30.09	0.29	Ki15
d18O_radio140515_Br2_gr6@10	2.00	2.0575E-03	1.2083E-02	1.5043E+09	3.3333E-02	3.0952E+06	3.1344E-02	23:52	7.5226E+08		26.08	0.24		26.08	0.24	31.61	0.29	Ki15

Table A2 Continued.

SIMS ANALYSES						Mount: BR2			Standard: UNIL-Q1 (Paine)	Analyse: $\delta^{18}O$			Value= 9.81±0.14 (VSMOW, 2σ)				Date: 14.04.2015	
	Beam	H'2/L'2 ($^{18}O/^{16}O$)		L'2 (^{18}O/Coeff)		H'2 (^{18}O/Coeff)		Time	Yield	Measurements (‰)		mean	Drift correction (‰)		Calibration (‰)			
	nA	*CPS*	*2SD*	*CPS*	*2SD*	*CPS*	*2SD*		CPS/nA	$\delta^{18}O$	*2SD int*	*2SD*	$\delta^{18}O$	*2SD*	$\delta^{18}O_{(VSMOW)}$	*2SD*	*Comment*	
140515_br2_paine@25	2.00	2.0125E-03	8.2597E-03	1.5085E+09	1.0837E-02	3.0359E+06	1.3709E-02	23:56	7.5417E+08	3.65	0.17	4.18	3.65	0.17	9.06	0.27	Standard	
140515_br2_paine@26	2.00	2.0141E-03	1.3749E-02	1.4626E+09	4.3975E-02	2.9458E+06	5.4017E-02	0:01	7.3000E+08	4.42	0.27	0.76	4.42	0.27	9.84	0.29	Standard	
140515_br2_paine@27	2.00	2.0136E-03	9.5459E-03	1.4850E+09	2.2870E-02	2.9900E+06	2.2158E-02	0:06	7.4219E+08	4.17	0.19		4.17	0.19	9.58	0.28	Standard	
140515_br2_paine@28	2.00	2.0142E-03	1.1873E-02	1.4853E+09	3.8832E-02	2.9919E+06	3.9387E-02	0:10	7.4386E+08	4.49	0.24		4.49	0.24	9.91	0.28	Standard	
d18O_radio140515_Br2_gr7@1	2.00	2.0527E-03	1.5478E-02	1.5605E+09	6.3102E-02	3.2034E+06	6.7789E-02	0:15	7.8210E+08	23.68	0.31	23.75	23.68	0.31	29.20	0.31	Ki09	
d18O_radio140515_Br2_gr7@2	1.99	2.0532E-03	9.4119E-03	1.5769E+09	2.9077E-02	3.2385E+06	3.4585E-02	0:20	7.9252E+08	23.93	0.19	0.87	23.93	0.19	29.45	0.28	Ki09	
d18O_radio140515_Br2_gr7@3	1.99	2.0532E-03	7.8983E-03	1.5668E+09	2.2060E-02	3.2173E+06	2.2523E-02	0:24	7.8751E+08	23.95	0.16		23.95	0.16	29.48	0.27	Ki09	
d18O_radio140515_Br2_gr7@4	1.99	2.0530E-03	8.9644E-03	1.5539E+09	2.3064E-02	3.1902E+06	3.0209E-02	0:29	7.8061E+08	23.83	0.18		23.83	0.18	29.35	0.28	Ki09	
d18O_radio140515_Br2_gr7@5	2.00	2.0534E-03	9.2730E-03	1.5748E+09	1.7150E-02	3.2338E+06	1.7185E-02	0:34	7.8768E+08	24.02	0.19		24.02	0.19	29.54	0.28	Ki09	
d18O_radio140515_Br2_gr7@6	2.00	2.0536E-03	8.7920E-03	1.5326E+09	2.0553E-02	3.1470E+06	2.2563E-02	0:38	7.6632E+08	24.16	0.18		24.16	*0.18*	29.68	*0.28*	Ki09	
d18O_radio140515_Br2_gr7@7	2.00	2.0532E-03	9.2751E-03	1.5403E+09	1.3827E-02	3.1623E+06	1.5197E-02	0:43	7.7121E+08	23.95	0.19		23.95	0.19	29.47	0.28	Ki09	
d18O_radio140515_Br2_gr7@8	2.00	2.0507E-03	9.8689E-03	1.4999E+09	1.1862E-02	3.0759E+06	1.8338E-02	0:48	7.5146E+08	22.70	0.20		22.70	0.20	28.21	0.28	Ki09	
d18O_radio140515_Br2_gr7@9	2.00	2.0524E-03	8.3424E-03	1.5175E+09	2.3201E-02	3.1148E+06	2.6401E-02	0:52	7.6045E+08	23.53	0.17		23.53	0.17	29.05	0.28	Ki09	
140515_br2_paine@25	2.00	2.0125E-03	8.2597E-03	1.5085E+09	1.0837E-02	3.0359E+06	1.3709E-02	0:57	7.5417E+08	3.65	0.17	4.18	3.65	0.17	9.06	0.27	Standard	
140515_br2_paine@26	2.00	2.0141E-03	1.3749E-02	1.4626E+09	4.3975E-02	2.9458E+06	5.4017E-02	1:02	7.3000E+08	4.42	0.27	0.76	4.42	0.27	9.84	0.29	Standard	
140515_br2_paine@27	2.00	2.0136E-03	9.5459E-03	1.4850E+09	2.2870E-02	2.9900E+06	2.2158E-02	1:06	7.4219E+08	4.17	0.19		4.17	0.19	9.58	0.28	Standard	
140515_br2_paine@28	2.00	2.0142E-03	1.1873E-02	1.4853E+09	3.8832E-02	2.9919E+06	3.9387E-02	1:11	7.4386E+08	4.49	0.24		4.49	0.24	9.91	0.28	Standard	
d18O_radio140515_Br2_gr8@1	1.99	2.0544E-03	6.2092E-03	1.5709E+09	1.5287E-02	3.2268E+06	1.2770E-02	1:16	7.8745E+08	24.52	0.12	25.75	24.52	0.12	30.04	0.27	Ki4C	
d18O_radio140515_Br2_gr8@2	2.00	2.0547E-03	9.7278E-03	1.5733E+09	2.5268E-02	3.2329E+06	2.5208E-02	1:20	7.8586E+08	24.66	0.19	1.78	24.66	0.19	30.19	0.28	Ki4C	
d18O_radio140515_Br2_gr8@3	2.00	2.0553E-03	1.3332E-02	1.5736E+09	2.9982E-02	3.2349E+06	2.8401E-02	1:25	7.8719E+08	24.98	0.27		24.98	0.27	30.50	0.30	Ki4C	
d18O_radio140515_Br2_gr8@4	2.00	2.0570E-03	8.6687E-03	1.5576E+09	1.3254E-02	3.2038E+06	2.1054E-02	1:29	7.7850E+08	25.83	0.17		25.83	0.17	31.36	0.28	Ki4C	
d18O_radio140515_Br2_gr8@5	2.00	2.0593E-03	1.0546E-02	1.5500E+09	1.9507E-02	3.1927E+06	2.4540E-02	1:34	7.7653E+08	26.96	0.21		26.96	0.21	32.50	0.28	Ki4C	
d18O_radio140515_Br2_gr8@6	2.00	2.0566E-03	8.8795E-03	1.5845E+09	2.3793E-02	3.2583E+06	2.0756E-02	1:39	7.9390E+08	25.63	0.18		25.62	0.18	31.15	0.28	Ki4C	
d18O_radio140515_Br2_gr8@7	2.00	2.0575E-03	1.2316E-02	1.5632E+09	1.8248E-02	3.2163E+06	2.0853E-02	1:43	7.8180E+08	26.07	0.25		26.06	0.25	31.60	0.29	Ki4C	
d18O_radio140515_Br2_gr8@8	1.99	2.0579E-03	9.2151E-03	1.5582E+09	1.6052E-02	3.2062E+06	2.0276E-02	1:48	7.8111E+08	26.27	0.18		26.27	0.18	31.80	0.28	Ki4C	
d18O_radio140515_Br2_gr8@9	1.99	2.0590E-03	8.0311E-03	1.5713E+09	1.2521E-02	3.2353E+06	1.3137E-02	1:53	7.8934E+08	26.83	0.16		26.83	0.16	32.36	0.28	Ki4C	
140515_br2_paine@29	1.99	2.0136E-03	1.2263E-02	1.4803E+09	2.0893E-02	2.9809E+06	2.1863E-02	1:57	7.4350E+08	4.18	0.25	4.53	4.18	0.25	9.60	0.29	Standard	
140515_br2_paine@30	1.99	2.0141E-03	1.0785E-02	1.4852E+09	4.4082E-02	2.9915E+06	4.8745E-02	2:02	7.4540E+08	4.45	0.22	0.56	4.45	0.22	9.86	0.28	Standard	
140515_br2_paine@31	2.00	2.0145E-03	1.3614E-02	1.4826E+09	4.3489E-02	2.9873E+06	4.4552E-02	2:07	7.4126E+08	4.63	0.27		4.63	0.27	10.05	0.29	Standard	
140515_br2_paine@32	2.00	2.0149E-03	1.0551E-02	1.4837E+09	6.7282E-02	2.9893E+06	6.6640E-02	2:11	7.4147E+08	4.85	0.21		4.85	0.21	10.27	0.28	Standard	
d18O_radio140515_Br2_gr9@1	2.00	2.0571E-03	9.5420E-03	1.5571E+09	2.1809E-02	3.2037E+06	2.2612E-02	2:16	7.7975E+08	25.91	0.19	26.12	25.90	0.19	31.44	0.28	Ki44	
d18O_radio140515_Br2_gr9@2	2.00	2.0582E-03	1.0153E-02	1.5405E+09	2.4376E-02	3.1705E+06	2.6045E-02	2:21	7.7119E+08	26.42	0.20	0.87	26.41	0.20	31.95	0.28	Ki44	
d18O_radio140515_Br2_gr9@3	2.00	2.0583E-03	1.0939E-02	1.5424E+09	2.5690E-02	3.1745E+06	3.1688E-02	2:25	7.7176E+08	26.46	0.22		26.46	0.22	32.00	0.29	Ki44	
d18O_radio140515_Br2_gr9@4	2.01	2.0584E-03	1.1965E-02	1.5462E+09	2.0302E-02	3.1827E+06	2.3204E-02	2:30	7.6922E+08	26.53	0.24		26.52	0.24	32.06	0.29	Ki44	
d18O_radio140515_Br2_gr9@5	2.01	2.0557E-03	1.0936E-02	1.5377E+09	1.3379E-02	3.1608E+06	2.0601E-02	2:35	7.6648E+08	25.17	0.22		25.16	0.22	30.69	0.29	Ki44	
d18O_radio140515_Br2_gr9@6	2.00	2.0581E-03	9.5489E-03	1.5643E+09	2.2290E-02	3.2198E+06	2.0301E-02	2:39	7.8068E+08	26.38	0.19		26.38	0.19	31.91	0.28	Ki44	
d18O_radio140515_Br2_gr9@7	2.00	2.0579E-03	9.5134E-03	1.5516E+09	2.2132E-02	3.1932E+06	2.3971E-02	2:44	7.7517E+08	26.30	0.19		26.30	0.19	31.83	0.28	Ki44	
d18O_radio140515_Br2_gr9@8	2.01	2.0574E-03	9.4813E-03	1.5494E+09	2.5269E-02	3.1876E+06	2.1038E-02	2:48	7.7035E+08	26.04	0.19		26.03	0.19	31.57	0.28	Ki44	
d18O_radio140515_Br2_gr9@9	2.01	2.0571E-03	9.1190E-03	1.5578E+09	2.0742E-02	3.2046E+06	2.4767E-02	2:53	7.7403E+08	25.87	0.18		25.87	0.18	31.40	0.28	Ki44	
140515_br2_paine@33	2.01	2.0138E-03	1.0547E-02	1.4845E+09	3.9720E-02	2.9896E+06	4.3025E-02	2:58	7.3905E+08	4.29	0.21	4.48	4.29	0.21	9.70	0.28	Standard	
140515_br2_paine@34	2.00	2.0142E-03	8.1319E-03	1.4902E+09	5.5718E-02	3.0017E+06	5.7874E-02	3:02	7.4328E+08	4.49	0.16	0.27	4.49	0.16	9.91	0.27	Standard	
140515_br2_paine@35	2.01	2.0144E-03	1.0499E-02	1.4860E+09	5.5475E-02	2.9932E+06	5.9384E-02	3:07	7.4053E+08	4.60	0.21		4.59	0.21	10.01	0.28	Standard	
140515_br2_paine@36	2.01	2.0143E-03	1.2267E-02	1.4821E+09	2.6190E-02	2.9849E+06	3.3507E-02	3:12	7.3852E+08	4.56	0.25		4.55	0.25	9.97	0.29	Standard	
d18O_radio140515_Br2_gr10@1	2.01	2.0404E-03	1.4050E-02	1.5284E+09	2.5807E-02	3.1185E+06	2.3635E-02	3:16	7.6098E+08	17.55	0.28	19.42	17.55	0.28	23.04	0.30	Ki25up	
d18O_radio140515_Br2_gr10@2	2.01	2.0454E-03	9.1052E-03	1.5268E+09	3.1637E-02	3.1230E+06	3.3011E-02	3:21	7.5889E+08	20.06	0.18	4.97	20.06	0.18	25.56	0.28	Ki25up	
d18O_radio140515_Br2_gr10@3	2.01	2.0462E-03	1.2212E-02	1.5325E+09	1.6666E-02	3.1361E+06	1.5799E-02	3:26	7.6390E+08	20.46	0.24		20.46	0.24	25.96	0.29	Ki25up	
d18O_radio140515_Br2_gr10@4	2.01	2.0474E-03	8.5655E-03	1.5157E+09	1.9028E-02	3.1037E+06	1.9533E-02	3:30	7.5298E+08	21.06	0.17		21.05	0.17	26.56	0.28	Ki25up	
d18O_radio140515_Br2_gr10@5	2.02	2.0349E-03	1.5043E-02	1.4694E+09	2.8121E-02	2.9900E+06	3.7696E-02	3:35	7.2828E+08	14.79	0.30		14.79	0.30	20.26	0.30	Ki25up	
d18O_radio140515_Br2_gr10@6	2.02	2.0524E-03	1.3965E-02	1.5275E+09	1.9213E-02	3.1361E+06	3.1977E-02	3:40	7.5528E+08	23.54	0.28		23.54	0.28	29.06	0.30	Ki25up	
d18O_radio140515_Br2_gr10@7	2.02	2.0407E-03	1.5395E-02	1.5262E+09	3.1763E-02	3.1145E+06	3.4770E-02	3:44	7.5625E+08	17.70	0.31						Ki25up	Optical rejection
d18O_radio140515_Br2_gr10@8	2.01	2.0445E-03	8.4551E-03	1.4997E+09	2.8287E-02	3.0655E+06	2.4565E-02	3:49	7.4628E+08	19.58	0.17		19.57	0.17	25.07	0.28	Ki25up	
d18O_radio140515_Br2_gr10@9	2.01	2.0453E-03	6.3718E-03	1.4969E+09	3.8126E-02	3.0627E+06	3.6583E-02	3:54	7.4372E+08	20.02	0.13		20.01	0.13	25.51	0.27	Ki25up	
140515_br2_paine@37	2.01	2.0142E-03	1.3017E-02	1.4842E+09	6.8412E-02	2.9895E+06	7.3530E-02	3:58	7.3850E+08	4.50	0.26	4.42	4.50	0.26	9.91	0.29	Standard	
140515_br2_paine@38	2.01	2.0139E-03	1.3526E-02	1.4713E+09	3.8917E-02	2.9631E+06	3.8115E-02	4:03	7.3090E+08	4.34	0.27	0.14	4.34	0.27	9.75	0.29	Standard	
140515_br2_paine@39	2.01	2.0140E-03	1.2609E-02	1.4901E+09	3.6778E-02	3.0011E+06	4.0231E-02	4:08	7.4089E+08	4.38	0.25		4.38	0.25	9.80	0.29	Standard	
140515_br2_paine@40	2.01	2.0141E-03	1.1093E-02	1.4844E+09	4.7458E-02	2.9895E+06	4.5383E-02	4:12	7.4027E+08	4.46	0.22		4.46	0.22	9.87	0.28	Standard	
d18O_radio140515_Br2_gr11@1	2.01	2.0542E-03	1.2385E-02	1.5052E+09	2.8608E-02	3.0917E+06	3.9070E-02	4:17	7.4808E+08	24.43	0.25	24.48	24.42	0.25	29.95	0.29	Ki35	
d18O_radio140515_Br2_gr11@2	2.01	2.0552E-03	1.3942E-02	1.4681E+09	5.0650E-02	3.0169E+06	4.9550E-02	4:22	7.2920E+08	24.94	0.28	0.84	24.94	0.28	30.47	0.30	Ki35	
d18O_radio140515_Br2_gr11@3	2.01	2.0540E-03	8.7273E-03	1.4545E+09	3.2119E-02	2.9878E+06	3.8597E-02	4:26	7.2296E+08	24.36	0.17		24.35	0.17	29.88	0.28	Ki35	
d18O_radio140515_Br2_gr11@4	2.01	2.0537E-03	9.8142E-03	1.4601E+09	4.9966E-02	2.9984E+06	5.2033E-02	4:31	7.2712E+08	24.21	0.20		24.20	0.20	29.72	0.28	Ki35	
d18O_radio140515_Br2_gr11@5	2.01	2.0535E-03	1.2990E-02	1.4505E+09	2.4116E-02	2.9791E+06	3.0135E-02	4:35	7.2247E+08	24.07	0.26		24.07	0.26	29.59	0.29	Ki35	
d18O_radio140515_Br2_gr11@6	2.02	2.0536E-03	7.0180E-03	1.4737E+09	3.1820E-02	3.0263E+06	3.4386E-02	4:40	7.2889E+08	24.14	0.14		24.13	0.14	29.65	0.27	Ki35	
d18O_radio140515_Br2_gr11@7	2.02	2.0541E-03	1.1239E-02	1.4644E+09	4.7109E-02	3.0079E+06	4.8573E-02	4:45	7.2516E+08	24.40	0.22		24.39	0.22	29.92	0.29	Ki35	
d18O_radio140515_Br2_gr11@8	2.01	2.0541E-03	8.9686E-03	1.4812E+09	4.3694E-02	3.0423E+06	4.4731E-02	4:49	7.3543E+08	24.38	0.18		24.38	0.18	29.90	0.28	Ki35	
d18O_radio140515_Br2_gr11@9	2.01	2.0561E-03	1.4276E-02	1.4918E+09	2.6651E-02	3.0668E+06	2.8144E-02	4:54	7.4118E+08	25.37	0.29		25.36	0.29	30.89	0.30	Ki35	

Table A2 Continued.

	SIMS ANALYSES				Mount: BR2			Standard: UNIL-Qi (Paine)		Analyses $\delta^{18}O$			Value= 9.81±0.14 (VSMOW, 2σ)			Date: 14.04.2015
	Beam	$1^{-}2^{1}2$ ($^{18}O/^{16}O$)		$1^{-}2^{18}O$/Coeff)		$1^{-}2^{1}2$ (^{18}O/Coeff)		Time	Yield	Measurements (‰)		mean	Drift correction (‰)		Calibration (‰)	*Comment*
	nA	*CPS*	*2SD*	*CPS*	*2SD*	*CPS*	*2SD*		*CPS/nA*	$\delta^{18}O$	*2SD int*	*2SD*	$\delta^{18}O$	*2SD*	$\delta^{18}O_{VSMOW}$	*2SD*	
140515_br2_paine@41	2.01	2.0139E-03	1.2606E-02	1.4916E+09	4.4111E-02	3.0041E+06	4.8000E-02	4:59	7.4051E+08	4.36	0.25	4.49	4.36	0.25	9.77	0.29	Standard
140515_br2_paine@42	2.02	2.0143E-03	7.5291E-03	1.4967E+09	5.8138E-02	3.0150E+06	6.0334E-02	5:03	7.4260E+08	4.54	0.15	0.33	4.53	0.15	9.95	0.27	Standard
140515_br2_paine@43	2.01	2.0136E-03	9.7661E-03	1.4941E+09	4.9060E-02	3.0085E+06	5.0592E-02	5:08	7.4173E+08	4.19	0.20		4.19	0.20	9.60	0.28	Standard
140515_br2_paine@44	2.01	2.0143E-03	1.0264E-02	1.4966E+09	5.7832E-02	3.0146E+06	5.8963E-02	5:13	7.4592E+08	4.52	0.21		4.52	0.21	9.93	0.28	Standard
140515_br2_paine@45	2.00	2.0142E-03	7.4181E-03	1.4883E+09	4.0642E-02	2.9978E+06	3.7716E-02	5:17	7.4327E+08	4.47	0.15		4.47	0.15	9.88	0.27	Standard
140515_br2_paine@46	2.00	2.0146E-03	1.4133E-02	1.4684E+09	4.9321E-02	2.9581E+06	5.5404E-02	5:22	7.3316E+08	4.68	0.28		4.68	0.28	10.10	0.29	Standard
140515_br2_paine@47	2.01	2.0145E-03	1.0599E-02	1.4818E+09	3.0936E-02	2.9847E+06	3.8462E-02	5:27	7.3779E+08	4.62	0.21		4.62	0.21	10.03	0.28	Standard

Table A2 Continued.

SIMS ANALYSES						Mount: BR3			Standard: UNIL-QI (Paine)	Analyse: $\delta^{18}O$			Value= 9.81±0.14 (VSMOW, 2σ)				Date: 14.04.2015
	Beam	H'2/L'2 ($^{18}O/^{16}O$)		L'2 (^{18}O/Coeff)		H'2 (^{16}O/Coeff)		Time	Yield	Measurements (‰)		mean	Drift correction (‰)		Calibration (‰)		Comment
	nA	CPS	2SD	CPS	2SD	CPS	2SD		CPS/nA	$\delta^{18}O$	2SD int	2SD	$\delta^{18}O$	2SD	$\delta^{18}O_{VSMOW}$	2SD	
140515_paine@1	1.97	2.0144E-03	7.5961E-03	1.5674E+09	4.5188E-02	3.1576E+06	4.7680E-02	8:26	7.9525E+08	4.57	0.15	4.56					Standard
140515_paine@2	1.98	2.0144E-03	1.1085E-02	1.5684E+09	4.4887E-02	3.1594E+06	4.3534E-02	8:30	7.9230E+08	4.61	0.22	0.22					Standard
140515_paine@3	1.98	2.0143E-03	1.7491E-02	1.5658E+09	3.6993E-02	3.1536E+06	3.3730E-02	8:34	7.9111E+08	4.52	0.35						Standard
140515_paine@4	1.97	2.0144E-03	1.3015E-02	1.5672E+09	3.0677E-02	3.1570E+06	2.9677E-02	8:38	7.9393E+08	4.60	0.26						Standard
140515_paine@5	1.98	2.0146E-03	8.9310E-03	1.5757E+09	5.6550E-02	3.1744E+06	5.1997E-02	8:43	7.9705E+08	4.69	0.18						Standard
140515_paine@6	1.98	2.0145E-03	9.6261E-03	1.5755E+09	4.8705E-02	3.1737E+06	5.2459E-02	8:47	7.9685E+08	4.66	0.19						Standard
140515_paine@7	1.99	2.0143E-03	8.8205E-03	1.5768E+09	4.9378E-02	3.1769E+06	4.1567E-02	8:51	7.9319E+08	4.52	0.18						Standard
140515_paine@8	1.98	2.0143E-03	9.9692E-03	1.5862E+09	3.7202E-02	3.1966E+06	3.5316E-02	8:56	8.0007E+08	4.54	0.20						Standard
140515_paine@9	1.98	2.0144E-03	9.9843E-03	1.5842E+09	3.7976E-02	3.1905E+06	3.2924E-02	9:00	8.0168E+08	4.59	0.20						Standard
140515_paine@10	1.98	2.0138E-03	1.3169E-02	1.5779E+09	4.8894E-02	3.1779E+06	4.9305E-02	9:04	7.9656E+08	4.30	0.26						Standard
d18O_radio140515_Br3_paine@1	1.97	2.0140E-03	1.1224E-02	1.5759E+09	5.9807E-02	3.1736E+06	6.2564E-02	9:53	8.0139E+08	4.40	0.22	4.53	4.24	0.22	9.60	0.22	Standard
d18O_radio140515_Br3_paine@2	1.98	2.0143E-03	1.0981E-02	1.5662E+09	3.3991E-02	3.1551E+06	3.6386E-02	9:57	7.9171E+08	4.52	0.22	0.38	4.36	0.22	9.73	0.22	Standard
d18O_radio140515_Br3_paine@3	1.98	2.0141E-03	7.7322E-03	1.5873E+09	5.4908E-02	3.1968E+06	5.3109E-02	10:02	8.0101E+08	4.45	0.15		4.30	0.15	9.66	0.20	Standard
d18O_radio140515_Br3_paine@4	1.98	2.0141E-03	1.2153E-02	1.5929E+09	3.1149E-02	3.2075E+06	3.2102E-02	10:07	8.0286E+08	4.45	0.24		4.30	0.24	9.66	0.23	Standard
d18O_radio140515_Br3_paine@5	1.98	2.0138E-03	8.9721E-03	1.5955E+09	3.4362E-02	3.2129E+06	3.2311E-02	10:11	8.0717E+08	4.27	0.18		4.12	0.18	9.48	0.21	Standard
d18O_radio140515_Br3_paine@6	1.98	2.0149E-03	9.7544E-03	1.6038E+09	5.1111E-02	3.2313E+06	5.2090E-02	10:16	8.1085E+08	4.84	0.20		4.69	0.20	10.06	0.21	Standard
d18O_radio140515_Br3_paine@7	1.98	2.0143E-03	9.7689E-03	1.6063E+09	5.7908E-02	3.2352E+06	5.6644E-02	10:20	8.1205E+08	4.53	0.20		4.39	0.20	9.75	0.21	Standard
d18O_radio140515_Br3_paine@8	1.98	2.0148E-03	9.1141E-03	1.5897E+09	4.7397E-02	3.2030E+06	5.1057E-02	10:25	8.0370E+08	4.79	0.18		4.65	0.18	10.02	0.21	Standard
d18O_radio140515_Br3_gr1@1	1.98	2.0627E-03	7.0126E-03	1.5795E+09	5.2311E-02	3.2590E+06	4.2582E-02	10:30	7.9896E+08	28.65	0.14	28.62	28.52	0.14	34.01	0.21	So08
d18O_radio140515_Br3_gr1@2	1.98	2.0641E-03	7.9866E-03	1.5653E+09	4.5819E-02	3.2303E+06	5.5423E-02	10:34	7.9042E+08	29.37	0.16	0.82	29.24	0.16	34.74	0.21	So08
d18O_radio140515_Br3_gr1@3	1.98	2.0624E-03	1.0332E-02	1.5809E+09	6.1447E-02	3.2606E+06	6.6979E-02	10:39	7.9943E+08	28.52	0.21		28.40	0.21	33.89	0.22	So08
d18O_radio140515_Br3_gr1@4	1.98	2.0625E-03	8.8849E-03	1.5863E+09	6.2522E-02	3.2716E+06	6.1141E-02	10:43	8.0237E+08	28.58	0.18		28.46	0.18	33.95	0.21	So08
d18O_radio140515_Br3_gr1@5	1.98	2.0629E-03	9.1006E-03	1.5762E+09	4.4274E-02	3.2515E+06	4.6674E-02	10:48	7.9672E+08	28.78	0.18		28.66	0.18	34.15	0.21	So08
d18O_radio140515_Br3_gr1@6	1.98	2.0614E-03	8.5968E-03	1.5802E+09	4.9633E-02	3.2582E+06	4.3214E-02	10:53	7.9820E+08	28.03	0.17		27.92	0.17	33.40	0.21	So08
d18O_radio140515_Br3_gr1@7	1.98	2.0621E-03	1.0961E-02	1.5830E+09	7.0530E-02	3.2646E+06	7.1747E-02	10:57	7.9943E+08	28.39	0.22		28.27	0.22	33.76	0.22	So08
d18O_radio140515_Br3_gr2@1	1.98	2.0602E-03	1.4264E-02	1.5541E+09	6.5466E-02	3.2018E+06	6.7887E-02	11:02	7.8398E+08	27.43	0.29	23.91	27.32	0.29	32.80	0.24	So07
d18O_radio140515_Br3_gr2@2	1.98	2.0593E-03	6.8244E-03	2.1206E+09	1.7804E-01	4.3670E+06	1.7613E-01	11:06	1.0697E+09	26.96	0.14	17.03	26.85	0.14	32.34	0.21	So07
d18O_radio140515_Br3_gr2@3	1.97	2.0622E-03	1.1080E-02	1.5730E+09	5.4932E-02	3.2439E+06	5.7170E-02	11:11	7.9736E+08	28.42	0.22		28.32	0.22	33.81	0.22	So07
d18O_radio140515_Br3_gr2@4	1.98	2.0596E-03	8.7962E-03	1.9483E+09	1.5611E-01	4.0124E+06	1.5205E-01	11:16	9.8607E+08	27.13	0.18		27.03	0.18	32.52	0.21	So07
d18O_radio140515_Br3_gr2@5	1.97	2.0578E-03	9.0787E-03	2.0793E+09	2.1865E-01	4.2788E+06	2.1698E-01	11:20	1.0528E+09	26.24	0.18		26.15	0.18	31.62	0.21	So07
d18O_radio140515_Br3_gr2@6	1.98	2.0583E-03	1.0504E-02	2.0309E+09	1.0032E-01	4.1805E+06	9.5310E-02	11:25	1.0254E+09	26.50	0.21		26.41	0.21	31.89	0.22	So07
d18O_radio140515_Br3_paine@9	1.99	2.0146E-03	9.1072E-03	1.6168E+09	3.4022E-01	3.2569E+06	3.4274E-01	11:29	8.1431E+08	4.67	0.18	4.62	4.58	0.18	9.94	0.21	Standard
d18O_radio140515_Br3_paine@10	1.98	2.0141E-03	8.3437E-03	1.5959E+09	3.7470E-02	3.2144E+06	3.5425E-02	11:34	8.0641E+08	4.45	0.17	0.31	4.37	0.17	9.73	0.21	Standard
d18O_radio140515_Br3_paine@11	1.98	2.0148E-03	7.4845E-03	1.6019E+09	1.7570E-01	3.2270E+06	1.7641E-01	11:39	8.0951E+08	4.81	0.15		4.73	0.15	10.09	0.20	Standard
d18O_radio140515_Br3_paine@12	1.98	2.0143E-03	9.3439E-03	1.6060E+09	5.5825E-02	3.2352E+06	5.7138E-02	11:43	8.1024E+08	4.56	0.19		4.49	0.19	9.85	0.21	Standard
d18O_radio140515_Br3_gr3@1	1.99	2.0553E-03	1.2495E-02	1.5931E+09	6.6427E-02	3.2742E+06	6.3870E-02	11:48	8.0224E+08	24.99	0.25	24.22	24.92	0.25	30.39	0.23	Ki07c
d18O_radio140515_Br3_gr3@2	1.98	2.0566E-03	1.1755E-02	1.5917E+09	5.0107E-02	3.2735E+06	5.1802E-02	11:52	8.0351E+08	25.63	0.24	3.71	25.56	0.24	31.03	0.23	Ki07c
d18O_radio140515_Br3_gr3@3	1.99	2.0493E-03	1.2591E-02	1.5870E+09	4.7491E-02	3.2522E+06	4.5062E-02	11:57	7.9928E+08	22.00	0.25		21.93	0.25	27.39	0.23	Ki07c
d18O_radio140515_Br3_gr3@4	1.98	2.0545E-03	1.2088E-02	1.5900E+09	6.7878E-02	3.2666E+06	6.7430E-02	12:02	8.0328E+08	24.59	0.24		24.52	0.24	29.99	0.23	Ki07c
d18O_radio140515_Br3_gr3@5	1.98	2.0480E-03	1.0745E-02	1.5753E+09	5.7108E-02	3.2265E+06	6.2246E-02	12:06	7.9607E+08	21.34	0.21		21.28	0.21	26.73	0.22	Ki07c
d18O_radio140515_Br3_gr3@6	1.98	2.0547E-03	1.1412E-02	1.5763E+09	6.5060E-02	3.2388E+06	6.3635E-02	12:11	7.9586E+08	24.66	0.23		24.61	0.23	30.08	0.23	Ki07c
d18O_radio140515_Br3_gr4@1	1.98	2.0580E-03	1.0909E-02	1.5857E+09	3.7810E-02	3.2646E+06	4.8430E-02	12:15	8.0051E+08	26.33	0.22	23.38	26.28	0.22	31.76	0.22	Ki51top
d18O_radio140515_Br3_gr4@2	1.99	2.0589E-03	1.2698E-02	1.5931E+09	4.1088E-02	3.2808E+06	4.6143E-02	12:20	7.9876E+08	26.79	0.25	16.46	26.74	0.25	32.23	0.23	Ki51top
d18O_radio140515_Br3_gr4@3	1.99	2.0574E-03	7.9695E-03	1.5862E+09	3.2610E-02	3.2631E+06	3.3827E-02	12:25	7.9745E+08	26.06	0.16	19.04	26.01	0.16	31.49	0.21	Ki51top
d18O_radio140515_Br3_gr4@4	1.99	2.0589E-03	1.2118E-02	1.5862E+09	3.9742E-02	3.2659E+06	4.5912E-02	12:29	7.9824E+08	26.76	0.24		26.72	0.24	32.20	0.23	Ki51top
d18O_radio140515_Br3_gr4@5	1.98	2.0577E-03	1.0026E-02	1.5980E+09	9.6213E-02	3.2885E+06	9.6650E-02	12:34	8.0593E+08	26.19	0.20		26.16	0.20	31.63	0.22	Ki51top
d18O_radio140515_Br3_gr4@6	1.99	2.0589E-03	8.5302E-03	1.5845E+09	4.9684E-02	3.2627E+06	4.6286E-02	12:38	7.9640E+08	26.80	0.17		26.77	0.17	32.25	0.21	Ki51top
d18O_radio140515_Br3_paine@13	1.98	2.0147E-03	9.8334E-03	1.6005E+09	3.9950E-02	3.2252E+06	4.5947E-02	12:43	8.0644E+08	4.74	0.20	4.63	4.71	0.20	10.07	0.21	Standard
d18O_radio140515_Br3_paine@14	1.98	2.0147E-03	9.1502E-03	1.5807E+09	2.6666E-02	3.1846E+06	2.5008E-02	12:48	7.9706E+08	4.76	0.18	0.27	4.73	0.18	10.10	0.21	Standard
d18O_radio140515_Br3_paine@15	1.98	2.0144E-03	6.5430E-03	1.6096E+09	3.1934E-02	3.2421E+06	3.4734E-02	12:52	8.1466E+08	4.56	0.13		4.54	0.13	9.90	0.20	Standard
d18O_radio140515_Br3_paine@16	1.98	2.0142E-03	1.4387E-02	1.5927E+09	3.1478E-02	3.2082E+06	3.7717E-02	12:57	8.0328E+08	4.47	0.29		4.45	0.29	9.82	0.24	Standard
d18O_radio140515_Br3_gr5@1	1.98	2.0582E-03	1.1254E-02	1.5784E+09	3.9344E-02	3.2485E+06	4.1283E-02	13:01	7.9635E+08	26.44	0.23	25.38	26.42	0.23	31.90	0.22	Ki24down
d18O_radio140515_Br3_gr5@2	1.99	2.0562E-03	1.0787E-02	1.5973E+09	4.9794E-02	3.2841E+06	4.9763E-02	13:06	8.0217E+08	25.42	0.22	1.42	25.41	0.22	30.88	0.22	Ki24down
d18O_radio140515_Br3_gr5@3	1.99	2.0551E-03	1.0210E-02	1.5998E+09	7.6048E-02	3.2881E+06	7.8757E-02	13:11	8.0521E+08	24.90	0.20		24.89	0.20	30.36	0.22	Ki24down
d18O_radio140515_Br3_gr5@4	1.98	2.0545E-03	1.3236E-02	1.6002E+09	5.8976E-02	3.2879E+06	5.6577E-02	13:15	8.0751E+08	24.57	0.26		24.57	0.26	30.03	0.24	Ki24down
d18O_radio140515_Br3_gr5@5	1.99	2.0546E-03	8.5196E-03	1.5929E+09	4.2350E-02	3.2734E+06	3.5596E-02	13:20	8.0103E+08	24.64	0.17		24.64	0.17	30.11	0.21	Ki24down
d18O_radio140515_Br3_gr5@6	1.99	2.0569E-03	9.6288E-03	1.5969E+09	2.4274E-02	3.2845E+06	3.3297E-02	13:24	8.0269E+08	25.77	0.19		25.78	0.19	31.25	0.22	Ki24down
d18O_radio140515_Br3_gr6@1	2.00	2.0572E-03	6.2610E-03	1.6021E+09	5.0197E-02	3.2959E+06	4.9153E-02	13:29	8.0216E+08	25.94	0.13	23.21	25.95	0.13	31.42	0.20	Ki06c
d18O_radio140515_Br3_gr6@2	1.99	2.0560E-03	9.6086E-03	1.6066E+09	6.4770E-02	3.3030E+06	6.6236E-02	13:33	8.0621E+08	25.33	0.19	16.98	25.34	0.19	30.81	0.22	Ki06c
d18O_radio140515_Br3_gr6@3	2.00	2.0573E-03	1.1267E-02	1.6098E+09	6.2885E-02	3.3115E+06	6.0649E-02	13:38	8.0554E+08	26.00	0.23		26.01	0.23	31.49	0.22	Ki06c
d18O_radio140515_Br3_gr6@4	2.00	2.0607E-03	9.5554E-03	1.6162E+09	4.4613E-02	3.3306E+06	4.1091E-02	13:43	8.0839E+08	27.70	0.19		27.72	0.19	33.20	0.22	Ki06c
d18O_radio140515_Br3_gr6@5	2.00	2.0562E-03	8.3557E-03	1.6083E+09	6.0586E-02	3.3070E+06	6.2021E-02	13:47	8.0441E+08	25.43	0.17		25.45	0.17	30.93	0.21	Ki06c
d18O_radio140515_Br3_gr6@6	2.00	2.0613E-03	8.5896E-03	1.5995E+09	4.4099E-02	3.2968E+06	4.4749E-02	13:52	7.9837E+08	27.97	0.17		27.99	0.17	33.48	0.21	Ki06c
d18O_radio140515_Br3_paine@17	2.00	2.0134E-03	1.8619E-02	1.6222E+09	4.2488E-02	3.2663E+06	4.9269E-02	13:57	8.1061E+08	4.11	0.37	4.24	4.13	0.37	9.49	0.27	Standard
d18O_radio140515_Br3_paine@18	2.00	2.0137E-03	1.0385E-02	1.6176E+09	4.8985E-02	3.2577E+06	5.4165E-02	14:01	8.0984E+08	4.23	0.21	0.29	4.26	0.21	9.63	0.22	Standard
d18O_radio140515_Br3_paine@19	1.99	2.0136E-03	6.2335E-03	1.6170E+09	5.5978E-02	3.2561E+06	5.7822E-02	14:06	8.1186E+08	4.17	0.12		4.20	0.12	9.56	0.20	Standard
d18O_radio140515_Br3_paine@920	2.00	2.0141E-03	1.3886E-02	1.6159E+09	3.8743E-02	3.2554E+06	4.0580E-02	14:10	8.0885E+08	4.44	0.28		4.47	0.28	9.84	0.23	Standard

Table A2 Continued.

SIMS ANALYSES						Mount: BR3			Standard: UNIL-Q1 (Paine)		Analyse: $\delta^{18}O$			Value= 9.81±0.14 (VSMOW, 2σ)			Date: 14.04.2015
	Beam	H'2/L'2 ($^{18}O/^{16}O$)		L'2 (^{18}O/Coeff)		H'2 (^{16}O/Coeff)		Time	Yield		Measurements (‰)		mean	Drift correction (‰)		Calibration (‰)		*Comment*
	nA	*CPS*	*2SD*	*CPS*	*2SD*	*CPS*	*2SD*		CPS/nA		$\delta^{18}O$	*2SD int*	*2SD*	$\delta^{18}O$	*2SD*	$\delta^{18}O_{(VSMOW)}$	*2SD*	
d18O_radio140515_Br3_gr7@1	1.99	2.0579E-03	9.8242E-03	1.5945E+09	4.1556E-02	3.2810E+06	4.7304E-02	14:15	8.0094E+08	8.0172E+08	26.26	0.20	25.41	26.30	0.20	31.78	0.22	Ki58
d18O_radio140515_Br3_gr7@2	1.99	2.0567E-03	1.1881E-02	1.5875E+09	3.6403E-02	3.2662E+06	3.4088E-02	14:19	7.9653E+08	7.1286E+06	25.71	0.24	1.70	25.75	0.24	31.22	0.23	Ki58
d18O_radio140515_Br3_gr7@3	1.99	2.0543E-03	1.1860E-02	1.6034E+09	3.8438E-02	3.2939E+06	4.3818E-02	14:24	8.0563E+08		24.48	0.24		24.53	0.24	30.00	0.23	Ki58
d18O_radio140515_Br3_gr7@4	2.00	2.0580E-03	1.0815E-02	1.5997E+09	3.3992E-02	3.2919E+06	3.5435E-02	14:29	8.0115E+08		26.31	0.22		26.36	0.22	31.84	0.22	Ki58
d18O_radio140515_Br3_gr7@5	2.00	2.0565E-03	8.6944E-03	1.6091E+09	4.7579E-02	3.3093E+06	4.7838E-02	14:33	8.0595E+08		25.60	0.17		25.66	0.17	31.13	0.21	Ki58
d18O_radio140515_Br3_gr7@6	2.00	2.0562E-03	1.0563E-02	1.5966E+09	5.5373E-02	3.2832E+06	6.2954E-02	14:38	8.0013E+08		25.42	0.21		25.47	0.21	30.95	0.22	Ki58
d18O_radio140515_Br3_gr8@1	1.99	2.0535E-03	1.0402E-02	1.6009E+09	5.4207E-02	3.2874E+06	5.5081E-02	14:42	8.0487E+08	8.0602E+08	24.07	0.21	22.30	24.13	0.21	29.59	0.22	Ki02c
d18O_radio140515_Br3_gr8@2	1.99	2.0585E-03	9.4521E-03	1.6209E+09	5.2628E-02	3.3369E+06	5.0725E-02	14:47	8.1461E+08	9.0089E+06	26.59	0.19	16.02	26.65	0.19	32.13	0.22	Ki02c
d18O_radio140515_Br3_gr8@3	2.00	2.0554E-03	8.1359E-03	1.6080E+09	5.9228E-02	3.3054E+06	6.0502E-02	14:52	8.0398E+08		25.04	0.16		25.11	0.16	30.58	0.21	Ki02c
d18O_radio140515_Br3_gr8@4	2.00	2.0546E-03	7.3647E-03	1.6120E+09	3.1208E-02	3.3113E+06	2.5613E-02	14:56	8.0713E+08		24.64	0.15		24.71	*0.15*	30.18	*0.21*	Ki02c
d18O_radio140515_Br3_gr8@5	2.00	2.0554E-03	9.8535E-03	1.6028E+09	4.9655E-02	3.2946E+06	5.1795E-02	15:01	8.0277E+08		25.03	0.20		25.10	0.20	30.57	0.22	Ki02c
d18O_radio140515_Br3_gr8@6	2.00	2.0583E-03	1.0983E-02	1.6032E+09	5.6943E-02	3.2998E+06	5.8913E-02	15:05	8.0279E+08		26.47	0.22		26.54	0.22	32.02	0.22	Ki02c
d18O_radio140515_Br3_paine@21	1.99	2.0137E-03	1.1746E-02	1.6216E+09	4.8692E-02	3.2667E+06	5.8164E-02	15:10	8.1317E+08	8.0763E+08	4.25	0.23	4.31	4.33	0.23	9.69	0.22	Standard
d18O_radio140515_Br3_paine@22	1.99	2.0136E-03	1.4682E-02	1.6079E+09	5.4959E-02	3.2377E+06	5.7112E-02	15:15	8.0674E+08	8.4847E+06	4.19	0.29	0.23	4.27	0.29	9.63	0.24	Standard
d18O_radio140515_Br3_paine@23	1.99	2.0139E-03	1.4136E-02	1.6090E+09	5.4740E-02	3.2405E+06	6.1151E-02	15:19	8.0771E+08		4.34	0.28		4.43	0.28	9.79	0.24	Standard
d18O_radio140515_Br3_paine@24	2.00	2.0141E-03	1.0659E-02	1.6022E+09	3.9530E-02	3.2268E+06	4.0008E-02	15:24	8.0288E+08		4.45	0.21		4.54	0.21	9.91	0.22	Standard
d18O_radio140515_Br3_gr9@1	2.00	2.0566E-03	7.8349E-03	1.6039E+09	3.6382E-02	3.2987E+06	3.8441E-02	15:28	8.0379E+08	8.0457E+08	25.63	0.16	25.81	25.73	0.16	31.20	0.21	Ro01
d18O_radio140515_Br3_gr9@2	2.00	2.0559E-03	6.5617E-03	1.6152E+09	5.5207E-02	3.3206E+06	5.7953E-02	15:33	8.0843E+08	4.3833E+06	25.27	0.13	2.85	25.37	0.13	30.85	0.20	Ro01
d18O_radio140515_Br3_gr9@3	1.99	2.0529E-03	1.0474E-02	1.5949E+09	4.4644E-02	3.2741E+06	4.8635E-02	15:38	8.0251E+08		23.81	0.21		23.91	0.21	29.38	0.22	Ro01
d18O_radio140515_Br3_gr9@4	2.00	2.0568E-03	1.1236E-02	1.6064E+09	5.4170E-02	3.3040E+06	5.5845E-02	15:42	8.0469E+08		25.71	0.22		25.82	0.22	31.29	0.22	Ro01
d18O_radio140515_Br3_gr9@5	2.00	2.0570E-03	1.1767E-02	1.6041E+09	2.9637E-02	3.2993E+06	2.9767E-02	15:47	8.0266E+08		25.84	0.24		25.95	0.24	31.42	0.23	Ro01
d18O_radio140515_Br3_gr9@6	2.00	2.0569E-03	1.0355E-02	1.6144E+09	5.5648E-02	3.3209E+06	5.8142E-02	15:51	8.0532E+08		25.80	0.21		25.91	0.21	31.39	0.22	Ro01
d18O_radio140515_Br3_gr10@1	2.00	2.0626E-03	1.0964E-02	1.6014E+09	6.1221E-02	3.3039E+06	6.9828E-02	15:56	8.0096E+08	8.0458E+08	28.60	0.22	25.27	28.72	0.22	34.21	0.22	So09
d18O_radio140515_Br3_gr10@2	1.99	2.0621E-03	7.3478E-03	1.6060E+09	3.8774E-02	3.3115E+06	3.9660E-02	16:01	8.0563E+08	8.1086E+06	28.38	0.15	18.44	28.50	0.15	33.99	0.21	So09
d18O_radio140515_Br3_gr10@3	1.99	2.0635E-03	1.5496E-02	1.6192E+09	6.4650E-02	3.3411E+06	6.6010E-02	16:05	8.1212E+08		29.06	0.31		29.18	0.31	34.68	0.25	So09
d18O_radio140515_Br3_gr10@4	2.00	2.0629E-03	6.7772E-03	1.6034E+09	6.3745E-02	3.3077E+06	6.5363E-02	16:10	8.0192E+08		28.76	0.14		28.89	0.14	34.38	0.21	So09
d18O_radio140515_Br3_gr10@5	2.00	2.0620E-03	7.1795E-03	1.6086E+09	4.5577E-02	3.3171E+06	4.4597E-02	16:14	8.0428E+08		28.34	0.14		28.47	0.14	33.96	0.21	So09
d18O_radio140515_Br3_gr10@6	2.01	2.0641E-03	9.8248E-03	1.6107E+09	5.9519E-02	3.3247E+06	5.7385E-02	16:19	8.0260E+08		29.39	0.20		29.52	0.20	35.02	0.22	So09
d18O_radio140515_Br3_paine@25	2.00	2.0140E-03	1.0113E-02	1.6226E+09	3.3302E-02	3.2678E+06	2.7709E-02	16:24	8.1061E+08	8.1053E+08	4.38	0.20	4.32	4.52	0.20	9.88	0.21	Standard
d18O_radio140515_Br3_paine@26	2.00	2.0138E-03	7.3749E-03	1.6226E+09	6.7910E-02	3.2677E+06	6.5738E-02	16:28	8.1055E+08	4.1039E+06	4.29	0.15	0.21	4.43	0.15	9.79	0.20	Standard
d18O_radio140515_Br3_paine@27	2.01	2.0139E-03	7.8518E-03	1.6245E+09	6.8367E-02	3.2714E+06	6.5860E-02	16:33	8.0845E+08		4.36	0.16		4.51	0.16	9.87	0.21	Standard
d18O_radio140515_Br3_paine@28	2.00	2.0137E-03	9.6395E-03	1.6249E+09	5.7790E-02	3.2721E+06	5.6906E-02	16:37	8.1335E+08		4.24	0.19		4.39	0.19	9.75	0.21	Standard
d18O_radio140515_Br3_paine@29	2.00	2.0142E-03	1.5898E-02	1.6114E+09	5.7144E-02	3.2457E+06	5.6851E-02	16:42	8.0747E+08		4.48	0.32		4.63	0.32	9.99	0.25	Standard
d18O_radio140515_Br3_paine@30	2.00	2.0138E-03	1.0493E-02	1.6223E+09	3.9456E-02	3.2671E+06	3.7203E-02	16:47	8.1240E+08		4.31	0.21		4.46	0.21	9.82	0.22	Standard
d18O_radio140515_Br3_paine@31	2.00	2.0135E-03	1.6753E-02	1.6213E+09	7.1055E-02	3.2649E+06	7.3036E-02	16:52	8.1090E+08		4.15	0.34		4.31	0.34	9.67	0.25	Standard

Table A2 Continued.

SIMS ANALYSES						Mount: BR4			Standard: UNIL-Q1 (Paine)	Analyse: $\delta^{18}O$			Value= 9.81±0.14 (VSMOW, 2σ)				Date: 15.04.2015	
	Beam	H'2/L'2 ($^{18}O/^{16}O$)		L'2 (^{18}O/Coeff)		H'2 (^{16}O/Coeff)		Time	Yield	Measurements (‰)		mean	Drift correction (‰)		Calibration (‰)			
	nA	*CPS*	*2SD*	*CPS*	*2SD*	*CPS*	*2SD*		CPS/nA	$\delta^{18}O$	*2SD int*	*2SD*	$\delta^{18}O$	*2SD*	$\delta^{18}O_{VSMOW}$	*2SD*	*Comment*	
pai netest@1	2.03	2.0128E-03	6.6115E-03	1.6665E+09	6.0345E-02	3.3541E+06	6.1440E-02	16:53	8.2107E+08	3.78	0.13	3.87					Standard	
pai netest@2	2.04	2.0135E-03	9.9076E-03	1.6795E+09	5.8593E-02	3.3813E+06	5.9778E-02	16:57	8.2462E+08	4.12	0.20	0.18					Standard	
pai netest@3	2.04	2.0128E-03	8.5675E-03	1.6707E+09	6.0638E-02	3.3628E+06	6.1744E-02	17:02	8.1719E+08	3.81	0.17						Standard	
pai netest@4	2.04	2.0129E-03	1.2050E-02	1.6703E+09	5.1319E-02	3.3623E+06	5.1232E-02	17:06	8.1840E+08	3.85	0.24						Standard	
pai netest@5	2.04	2.0125E-03	1.0420E-02	1.6687E+09	6.8309E-02	3.3584E+06	6.7110E-02	17:11	8.1805E+08	3.65	0.21						Standard	
pai netest@6	2.04	2.0134E-03	1.1243E-02	1.6710E+09	5.9893E-02	3.3641E+06	6.4247E-02	17:15	8.2070E+08	4.08	0.22						Standard	
pai netest@7	2.04	2.0125E-03	1.0240E-02	1.6690E+09	6.4622E-02	3.3581E+06	5.6129E-02	17:20	8.1875E+08	3.66	0.20						Standard	
pai netest@8	2.04	2.0133E-03	1.3648E-02	1.6759E+09	6.2192E-02	3.3741E+06	5.9052E-02	17:24	8.2077E+08	4.03	0.27						Standard	
d18O_radio140515_Br6_paine@1	2.01	2.0130E-03	1.2063E-02	1.6573E+09	5.7584E-02	3.3361E+06	5.8641E-02	18:13	8.2328E+08	3.87	0.24	3.81	3.82	0.24	9.80	0.19	Standard	
d18O_radio140515_Br6_paine@2	2.03	2.0126E-03	1.3146E-02	1.6583E+09	6.7066E-02	3.3374E+06	7.2164E-02	18:18	8.1787E+08	3.69	0.26	0.21	3.63	0.26	9.62	0.20	Standard	
d18O_radio140515_Br6_paine@3	2.03	2.0128E-03	1.0243E-02	1.6676E+09	6.4683E-02	3.3567E+06	6.5774E-02	18:22	8.2021E+08	3.77	0.20		3.72	0.20	9.70	0.18	Standard	
d18O_radio140515_Br6_paine@4	2.04	2.0129E-03	1.0343E-02	1.6716E+09	5.6885E-02	3.3648E+06	5.7190E-02	18:27	8.1937E+08	3.85	0.21		3.80	0.21	9.78	0.18	Standard	
d18O_radio140515_Br6_paine@5	2.04	2.0130E-03	7.0072E-03	1.6696E+09	6.0927E-02	3.3611E+06	5.7248E-02	18:31	8.1734E+08	3.89	0.14		3.84	0.14	9.82	0.16	Standard	
d18O_radio140515_Br6_paine@6	2.04	2.0125E-03	7.9833E-03	1.6723E+09	6.7213E-02	3.3655E+06	6.8291E-02	18:36	8.1943E+08	3.63	0.16		3.58	0.16	9.56	0.17	Standard	
d18O_radio140515_Br6_paine@7	2.04	2.0128E-03	6.2833E-03	1.6732E+09	5.9769E-02	3.3678E+06	5.9234E-02	18:40	8.2120E+08	3.81	0.13		3.75	0.13	9.74	0.16	Standard	
d18O_radio140515_Br6_paine@8	2.04	2.0131E-03	9.3588E-03	1.6707E+09	7.2400E-02	3.3633E+06	7.4907E-02	18:44	8.1884E+08	3.95	0.19		3.90	0.19	9.89	0.17	Standard	
d18O_radio150515_Br4_gr1@1	2.04	2.0126E-03	1.0713E-02	1.7466E+09	1.9396E-01	3.5153E+06	1.9457E-01	18:49	8.5588E+08	3.70	0.21	28.66					So28	Optical rejection
d18O_radio150515_Br4_gr1@2	2.05	2.0639E-03	1.0934E-02	1.6641E+09	7.8706E-02	3.4349E+06	7.9034E-02	18:53	8.1346E+08	29.30	0.22	1.31	29.25	0.22	35.38	0.19	So28	
d18O_radio150515_Br4_gr1@3	2.05	2.0622E-03	1.0006E-02	1.6176E+09	6.9460E-02	3.3359E+06	6.8421E-02	18:58	7.9054E+08	28.44	0.20		28.39	0.20	34.52	0.18	So28	
d18O_radio150515_Br4_gr1@4	2.04	2.0628E-03	1.1832E-02	1.6309E+09	8.6208E-02	3.3643E+06	9.0018E-02	19:02	8.0026E+08	28.72	0.24		28.68	0.24	34.81	0.19	So28	
d18O_radio150515_Br4_gr1@5	2.03	2.0635E-03	8.7081E-03	1.6403E+09	6.8295E-02	3.3844E+06	7.1627E-02	19:07	8.0623E+08	29.06	0.17		29.02	0.17	35.15	0.17	So28	
d18O_radio150515_Br4_gr1@6	2.03	2.0627E-03	8.6922E-03	1.6381E+09	9.4310E-02	3.3791E+06	9.5999E-02	19:11	8.0524E+08	28.66	0.17		28.62	0.17	34.75	0.17	So28	
d18O_radio150515_Br4_gr1@7	2.03	2.0618E-03	9.7494E-03	1.6533E+09	8.1503E-02	3.4090E+06	8.0144E-02	19:16	8.1268E+08	28.24	0.19		28.20	0.19	34.33	0.18	So28	
d18O_radio150515_Br4_gr1@8	2.04	2.0602E-03	6.5240E-03	1.6480E+09	1.0019E-01	3.3951E+06	9.8400E-02	19:20	8.0874E+08	27.41	0.13		27.36	0.13	33.49	0.16	So28	
d18O_radio150515_Br4_gr1@9	2.04	2.0643E-03	9.9301E-03	1.6524E+09	7.3786E-02	3.4107E+06	7.8049E-02	19:25	8.0879E+08	29.46	0.20		29.42	0.20	35.56	0.18	So28	
d18O_radio140515_Br6_paine@9	2.04	2.0131E-03	1.1790E-02	1.6703E+09	7.1457E-02	3.3626E+06	7.0241E-02	19:29	8.1938E+08	3.96	0.24	4.00	3.92	0.24	9.90	0.19	Standard	
d18O_radio140515_Br6_paine@10	2.04	2.0132E-03	1.0369E-02	1.6724E+09	5.7800E-02	3.3666E+06	6.0129E-02	19:33	8.1831E+08	3.97	0.21	0.10	3.93	0.21	9.91	0.18	Standard	
d18O_radio140515_Br6_paine@11	2.03	2.0132E-03	1.4134E-02	1.6672E+09	5.1836E-02	3.3566E+06	5.6460E-02	19:38	8.1961E+08	4.01	0.28		3.97	0.28	9.95	0.20	Standard	
d18O_radio140515_Br6_paine@12	2.03	2.0134E-03	9.9310E-03	1.6697E+09	7.1045E-02	3.3601E+06	6.3874E-02	19:42	8.2351E+08	4.07	0.20		4.03	0.20	10.01	0.18	Standard	
d18O_radio140515_Br6_gr2@1	2.03	2.0606E-03	7.5153E-03	1.6508E+09	8.5454E-02	3.4018E+06	8.6739E-02	19:47	8.1405E+08	27.64	0.15	26.58	27.60	0.15	33.73	0.17	So17	
d18O_radio140515_Br6_gr2@2	2.03	2.0610E-03	1.3998E-02	1.6299E+09	8.7293E-02	3.3592E+06	8.9474E-02	19:51	8.0145E+08	27.84	0.28	5.24	27.80	0.28	33.93	0.21	So17	
d18O_radio140515_Br6_gr2@3	2.04	2.0600E-03	1.1269E-02	1.6309E+09	7.3518E-02	3.3598E+06	7.9697E-02	19:56	8.0034E+08	27.35	0.23		27.32	0.23	33.44	0.19	So17	
d18O_radio140515_Br6_gr2@4	2.03	2.0452E-03	1.0559E-02	1.6003E+09	7.5922E-02	3.2728E+06	7.5878E-02	20:00	7.8638E+08	19.94	0.21		19.91	0.21	25.99	0.18	So17	
d18O_radio140515_Br6_gr2@5	2.03	2.0560E-03	9.8680E-03	1.6332E+09	4.9607E-02	3.3581E+06	5.0205E-02	20:05	8.0493E+08	25.34	0.20		25.30	0.20	31.42	0.18	So17	
d18O_radio140515_Br6_gr2@6	2.04	2.0603E-03	6.6486E-03	1.6284E+09	7.6420E-02	3.3549E+06	7.7954E-02	20:09	7.9976E+08	27.50	0.13		27.46	0.13	33.59	0.16	So17	
d18O_radio140515_Br6_gr2@7	2.03	2.0612E-03	8.4631E-03	1.6211E+09	6.7242E-02	3.3417E+06	6.8599E-02	20:13	7.9744E+08	27.92	0.17		27.88	0.17	34.01	0.17	So17	
d18O_radio140515_Br6_gr2@8	2.04	2.0617E-03	1.2065E-02	1.6050E+09	8.3643E-02	3.3089E+06	8.4944E-02	20:18	7.8769E+08	28.16	0.24		28.13	0.24	34.26	0.19	So17	
d18O_radio140515_Br6_gr2@9	2.03	2.0604E-03	8.5175E-03	1.6097E+09	7.1580E-02	3.3165E+06	7.1947E-02	20:22	7.9172E+08	27.53	0.17		27.49	0.17	33.62	0.17	So17	
d18O_radio140515_Br6_paine@13	2.03	2.0133E-03	1.0406E-02	1.6731E+09	7.0130E-02	3.3688E+06	7.1789E-02	20:27	8.2422E+08	4.06	0.21	3.97	4.03	0.21	10.01	0.18	Standard	
d18O_radio140515_Br6_paine@14	2.03	2.0131E-03	7.9494E-03	1.6718E+09	6.9382E-02	3.3652E+06	7.2143E-02	20:31	8.2281E+08	3.93	0.16	0.15	3.90	0.16	9.88	0.16	Standard	
d18O_radio140515_Br6_paine@15	2.03	2.0132E-03	6.4113E-03	1.6791E+09	7.4820E-02	3.3805E+06	7.5146E-02	20:36	8.2753E+08	3.99	0.13		3.96	0.13	9.95	0.16	Standard	
d18O_radio140515_Br6_paine@16	2.04	2.0130E-03	1.4092E-02	1.6802E+09	5.5541E-02	3.3812E+06	4.9147E-02	20:40	8.2420E+08	3.88	0.28		3.85	0.28	9.84	0.20	Standard	
d18O_radio140515_Br6_gr3@1	2.04	2.0547E-03	7.2567E-03	1.6311E+09	6.4278E-02	3.3516E+06	6.9380E-02	20:45	8.0093E+08	24.71	0.15	25.36	24.68	0.15	30.79	0.16	Ki39	
d18O_radio140515_Br6_gr3@2	2.04	2.0562E-03	6.0968E-03	1.6286E+09	6.4868E-02	3.3488E+06	6.6075E-02	20:49	7.9826E+08	25.42	0.12	1.06	25.39	0.12	31.51	0.16	Ki39	
d18O_radio140515_Br6_gr3@3	2.03	2.0573E-03	1.2111E-02	1.6200E+09	6.7266E-02	3.3329E+06	7.1486E-02	20:54	7.9772E+08	25.99	0.24		25.96	0.24	32.08	0.19	Ki39	
d18O_radio140515_Br6_gr3@4	2.03	2.0575E-03	9.4845E-03	1.6208E+09	6.9018E-02	3.3350E+06	6.4867E-02	20:58	7.9791E+08	26.07	0.19		26.04	0.19	32.16	0.18	Ki39	
d18O_radio140515_Br6_gr3@5	2.03	2.0542E-03	8.2619E-03	1.6161E+09	8.7287E-02	3.3198E+06	8.3911E-02	21:02	7.9673E+08	24.44	0.17		24.41	0.17	30.52	0.17	Ki39	
d18O_radio140515_Br6_gr3@6	2.04	2.0559E-03	6.9500E-03	1.6288E+09	8.6267E-02	3.3488E+06	8.5161E-02	21:07	7.9993E+08	25.30	0.14		25.27	0.14	31.39	0.16	Ki39	
d18O_radio140515_Br6_gr3@7	2.04	2.0565E-03	1.3798E-02	1.6427E+09	8.7269E-02	3.3779E+06	8.7515E-02	21:11	8.0614E+08	25.59	0.28		25.57	0.28	31.69	0.20	Ki39	
d18O_radio140515_Br6_gr3@8	2.04	2.0559E-03	7.5944E-03	1.6369E+09	8.8253E-02	3.3653E+06	8.9474E-02	21:16	8.0421E+08	25.26	0.15		25.24	0.15	31.35	0.17	Ki39	
d18O_radio140515_Br6_gr3@9	2.04	2.0563E-03	6.9231E-03	1.6517E+09	7.3132E-02	3.3960E+06	7.2204E-02	21:20	8.1042E+08	25.46	0.14		25.44	0.14	31.55	0.16	Ki39	
d18O_radio140515_Br6_paine@17	2.03	2.0128E-03	1.4981E-02	1.6804E+09	7.4403E-02	3.3827E+06	7.5310E-02	21:25	8.2612E+08	3.79	0.30	3.77	3.77	0.30	9.76	0.21	Standard	
d18O_radio140515_Br6_paine@18	2.04	2.0126E-03	1.1448E-02	1.6748E+09	5.9975E-02	3.3706E+06	6.3258E-02	21:29	8.2182E+08	3.68	0.23	0.20	3.65	0.23	9.64	0.18	Standard	
d18O_radio140515_Br6_paine@19	2.04	2.0130E-03	1.1013E-02	1.6734E+09	5.5880E-02	3.3686E+06	5.6228E-02	21:34	8.1936E+08	3.90	0.22		3.88	0.22	9.87	0.18	Standard	
d18O_radio140515_Br6_paine@20	2.04	2.0126E-03	7.5113E-03	1.6755E+09	5.9092E-02	3.3724E+06	5.8587E-02	21:38	8.2245E+08	3.70	0.15		3.68	0.15	9.67	0.16	Standard	
d18O_radio140515_Br6_gr4@1	2.03	2.0611E-03	1.2760E-02	1.6522E+09	5.9432E-02	3.4053E+06	6.0746E-02	21:43	8.1359E+08	27.88	0.26	28.16	27.86	0.26	33.99	0.20	So13	
d18O_radio140515_Br6_gr4@2	2.03	2.0618E-03	9.3055E-03	1.6402E+09	6.9547E-02	3.3816E+06	7.1132E-02	21:47	8.0792E+08	28.24	0.19	0.80	28.22	0.19	34.36	0.18	So13	
d18O_radio140515_Br6_gr4@3	2.03	2.0606E-03	1.1790E-02	1.6354E+09	6.7997E-02	3.3700E+06	6.9344E-02	21:51	8.0583E+08	27.63	0.24		27.62	0.24	33.74	0.19	So13	
d18O_radio140515_Br6_gr4@4	2.03	2.0628E-03	8.8919E-03	1.6310E+09	7.5209E-02	3.3646E+06	7.2690E-02	21:56	8.0326E+08	28.71	0.18		28.69	0.18	34.83	0.17	So13	
d18O_radio140515_Br6_gr4@5	2.03	2.0612E-03	6.5772E-03	1.6364E+09	7.3007E-02	3.3731E+06	7.0941E-02	22:00	8.0417E+08	27.92	0.13		27.91	0.13	34.04	0.16	So13	
d18O_radio140515_Br6_gr4@6	2.03	2.0614E-03	1.3608E-02	1.6427E+09	7.5065E-02	3.3863E+06	7.8724E-02	22:05	8.0762E+08	28.02	0.27		28.00	0.27	34.13	0.20	So13	
d18O_radio140515_Br6_gr4@7	2.04	2.0610E-03	1.0066E-02	1.6356E+09	8.0492E-02	3.3708E+06	7.9730E-02	22:09	8.0171E+08	27.85	0.20		27.83	0.20	33.96	0.18	So13	
d18O_radio140515_Br6_gr4@8	2.04	2.0629E-03	6.0910E-03	1.6272E+09	5.9428E-02	3.3567E+06	5.8503E-02	22:14	7.9857E+08	28.78	0.12		28.77	0.12	34.90	0.16	So13	
d18O_radio140515_Br6_gr4@9	2.04	2.0622E-03	1.0600E-02	1.6241E+09	6.3944E-02	3.3496E+06	6.3582E-02	22:18	7.9780E+08	28.41	0.21		28.40	0.21	34.53	0.18	So13	
d18O_radio140515_Br6_paine@21	2.03	2.0134E-03	1.3811E-02	1.6781E+09	6.5189E-02	3.3787E+06	6.6906E-02	22:23	8.2643E+08	4.10	0.28	3.88	4.09	0.28	10.07	0.20	Standard	
d18O_radio140515_Br6_paine@22	2.03	2.0126E-03	9.6559E-03	1.6764E+09	7.5909E-02	3.3740E+06	7.7536E-02	22:27	8.2428E+08	3.70	0.19	0.33	3.69	0.19	9.67	0.17	Standard	
d18O_radio140515_Br6_paine@23	2.04	2.0130E-03	7.5023E-03	1.6745E+09	6.8699E-02	3.3710E+06	6.5879E-02	22:31	8.2069E+08	3.89	0.15		3.88	0.15	9.87	0.16	Standard	
d18O_radio140515_Br6_paine@24	2.04	2.0129E-03	7.8080E-03	1.6712E+09	6.6718E-02	3.3627E+06	6.3211E-02	22:36	8.1830E+08	3.83	0.16		3.82	0.16	9.80	0.16	Standard	

Table A2 Continued.

SIMS ANALYSES						Mount: BR4			Standard: UNIL-QI (Paine)		Analyse: $\delta^{18}O$			Value= 9.81±0.14 (VSMOW, 2σ)				Date: 15.04.2015
	Beam	H'2/L'2 ($^{18}O/^{16}O$)		L'2 (^{18}O/Coeff)		H'2 (^{16}O/Coeff)		Time	Yield		Measurements (‰)		mean	Drift correction (‰)		Calibration (‰)		
	nA	*CPS*	*2SD*	*CPS*	*2SD*	*CPS*	*2SD*		CPS/nA		$\delta^{18}O$	*2SD int*	*2SD*	$\delta^{18}O$	*2SD*	$\delta^{18}O_{(VSMOW)}$	*2SD*	*Comment*
d18O_radio140515_Br6_gr5@1	2.04	2.0525E-03	9.9192E-03	1.6439E+09	4.7133E-02	3.3743E+06	4.4173E-02	22:40	8.0608E+08	8.0381E+08	23.59	0.20	22.46	23.58	0.20	29.68	0.18	Go 73
d18O_radio140515_Br6_gr5@2	2.03	2.0470E-03	8.9851E-03	1.6326E+09	7.0408E-02	3.3421E+06	7.3858E-02	22:45	8.0303E+08	8.0914E+06	20.87	0.18	1.98	20.86	0.18	26.95	0.17	Go 73
d18O_radio140515_Br6_gr5@3	2.03	2.0506E-03	6.7719E-03	1.6380E+09	5.2645E-02	3.3588E+06	5.4022E-02	22:49	8.0575E+08		22.62	0.14		22.61	0.14	28.71	0.16	Go 73
d18O_radio140515_Br6_gr5@4	2.03	2.0495E-03	7.5490E-03	1.6389E+09	6.0033E-02	3.3587E+06	6.3272E-02	22:54	8.0722E+08		22.11	0.15		22.10	0.15	28.20	0.17	Go 73
d18O_radio140515_Br6_gr5@5	2.04	2.0511E-03	8.9839E-03	1.6210E+09	5.8196E-02	3.3247E+06	6.0297E-02	22:58	7.9528E+08		22.87	0.18		22.86	0.18	28.96	0.17	Go 73
d18O_radio140515_Br6_gr5@6	2.04	2.0471E-03	8.6845E-03	1.6341E+09	5.6994E-02	3.3454E+06	5.7484E-02	23:03	8.0161E+08		20.88	0.17		20.88	0.17	26.96	0.17	Go 73
d18O_radio140515_Br6_gr5@7	2.04	2.0518E-03	9.3622E-03	1.6354E+09	6.1400E-02	3.3556E+06	6.3598E-02	23:07	8.0360E+08		23.24	0.19		23.23	0.19	29.33	0.17	Go 73
d18O_radio140515_Br6_gr5@8	2.04	2.0511E-03	1.0948E-02	1.6473E+09	4.6602E-02	3.3789E+06	4.6857E-02	23:11	8.0930E+08		22.90	0.22		22.90	0.22	29.00	0.18	Go 73
d18O_radio140515_Br6_gr5@9	2.03	2.0515E-03	1.1724E-02	1.6306E+09	6.6403E-02	3.3448E+06	6.8572E-02	23:16	8.0241E+08		23.09	0.23		23.09	0.23	29.19	0.19	Go 73
d18O_radio140515_Br6_paine@25	2.03	2.0128E-03	6.8165E-03	1.6575E+09	7.2023E-02	3.3361E+06	7.5977E-02	23:20	8.1572E+08	8.2451E+08	3.78	0.14	3.78	3.78	0.14	9.76	0.16	Standard
d18O_radio140515_Br6_paine@26	2.03	2.0131E-03	1.0038E-02	1.6657E+09	7.3176E-02	3.3532E+06	7.2728E-02	23:25	8.1998E+08	2.4027E+07	3.94	0.20	0.24	3.94	0.20	9.93	0.18	Standard
d18O_radio140515_Br6_paine@27	2.04	2.0126E-03	8.9633E-03	1.6692E+09	6.2025E-02	3.3593E+06	6.3903E-02	23:29	8.2007E+08		3.67	0.18		3.67	0.18	9.65	0.17	Standard
d18O_radio140515_Br6_paine@28	2.03	2.0127E-03	1.0576E-02	1.7129E+09	3.9317E-01	3.4476E+06	3.9562E-01	23:34	8.4227E+08		3.72	0.21		3.72	0.21	9.70	0.18	Standard
d18O_radio140515_Br6_gr6@1	2.08	2.0569E-03	8.6139E-03	1.6499E+09	6.1225E-02	3.3934E+06	6.0493E-02	23:38	7.9379E+08	8.1007E+08	25.76	0.17	25.56	25.76	0.17	31.88	0.17	Ki40
d18O_radio140515_Br6_gr6@2	2.03	2.0560E-03	1.1792E-02	1.6580E+09	7.2280E-02	3.4088E+06	7.1059E-02	23:43	8.1492E+08	2.0046E+07	25.35	0.24	1.22	25.35	0.24	31.46	0.19	Ki40
d18O_radio140515_Br6_gr6@3	2.03	2.0577E-03	7.7751E-03	1.6545E+09	6.3783E-02	3.4041E+06	6.7496E-02	23:47	8.1517E+08		26.16	0.16		26.16	0.16	32.28	0.17	Ki40
d18O_radio140515_Br6_gr6@4	2.03	2.0567E-03	1.1418E-02	1.6706E+09	6.6511E-02	3.4358E+06	6.2533E-02	23:52	8.2397E+08		25.67	0.23		25.68	0.23	31.79	0.19	Ki40
d18O_radio140515_Br6_gr6@5	2.06	2.0573E-03	1.0457E-02	1.6438E+09	6.2807E-02	3.3819E+06	6.0193E-02	23:56	7.9717E+08		26.00	0.21		26.00	0.21	32.12	0.18	Ki40
d18O_radio140515_Br6_gr6@6	2.04	2.0565E-03	1.3010E-02	1.6476E+09	4.0814E-02	3.3878E+06	3.7466E-02	0:01	8.0598E+08		25.59	0.26		25.59	0.26	31.71	0.20	Ki40
d18O_radio140515_Br6_gr6@7	2.04	2.0567E-03	9.9386E-03	1.6460E+09	6.9676E-02	3.3856E+06	6.7519E-02	0:05	8.0579E+08		25.67	0.20		25.68	0.20	31.79	0.18	Ki40
d18O_radio140515_Br6_gr6@8	2.04	2.0570E-03	7.2394E-03	1.6395E+09	4.4224E-02	3.3723E+06	4.4000E-02	0:09	8.0534E+08		25.82	0.14		25.82	0.14	31.94	0.16	Ki40
d18O_radio140515_Br6_gr6@9	2.03	2.0532E-03	1.2171E-02	1.6655E+09	5.7576E-02	3.4196E+06	5.9742E-02	0:14	8.2024E+08		23.94	0.24		23.95	0.24	30.06	0.19	Ki40
d18O_radio140515_Br6_gr6@10	2.04	2.0566E-03	8.1340E-03	1.6658E+09	5.2508E-02	3.4248E+06	4.6906E-02	0:18	8.1837E+08		25.64	0.16		25.64	0.16	31.76	0.17	Ki40
d18O_radio140515_Br6_paine@29	2.04	2.0131E-03	7.7599E-03	1.6811E+09	5.5309E-02	3.3841E+06	5.4268E-02	0:23	8.2469E+08	8.2486E+08	3.94	0.16	3.84	3.94	0.16	9.93	0.16	Standard
d18O_radio140515_Br6_paine@30	2.04	2.0129E-03	1.0935E-02	1.6801E+09	6.2244E-02	3.3819E+06	6.8602E-02	0:27	8.2455E+08	2.3284E+06	3.86	0.22	0.15	3.87	0.22	9.86	0.18	Standard
d18O_radio140515_Br6_paine@31	2.03	2.0128E-03	9.9995E-03	1.6744E+09	6.5245E-02	3.3701E+06	6.5109E-02	0:32	8.2371E+08		3.77	0.20		3.78	0.20	9.77	0.18	Standard
d18O_radio140515_Br6_paine@32	2.03	2.0128E-03	9.5395E-03	1.6800E+09	7.8006E-02	3.3813E+06	7.9009E-02	0:36	8.2648E+08		3.78	0.19		3.79	0.19	9.78	0.17	Standard
d18O_radio140515_Br6_gr7@1	2.04	2.0645E-03	1.0391E-02	1.6652E+09	5.3227E-02	3.4378E+06	5.5013E-02	0:41	8.1560E+08	8.2039E+08	29.59	0.21	29.14	29.60	0.21	35.74	0.18	So25
d18O_radio140515_Br6_gr7@2	2.04	2.0641E-03	1.2728E-02	1.6695E+09	7.1093E-02	3.4462E+06	7.4626E-02	0:45	8.1914E+08	8.1707E+06	29.35	0.25	0.65	29.36	0.25	35.50	0.20	So25
d18O_radio140515_Br6_gr7@3	2.04	2.0635E-03	9.8006E-03	1.6681E+09	5.8688E-02	3.4421E+06	5.9999E-02	0:50	8.1861E+08		29.08	0.20		29.09	0.20	35.23	0.18	So25
d18O_radio140515_Br6_gr7@4	2.03	2.0628E-03	9.4296E-03	1.6657E+09	6.9193E-02	3.4359E+06	7.0098E-02	0:54	8.1959E+08		28.73	0.19		28.74	0.19	34.88	0.18	So25
d18O_radio140515_Br6_gr7@5	2.03	2.0629E-03	1.3748E-02	1.6751E+09	6.8349E-02	3.4555E+06	6.3326E-02	0:59	8.2524E+08		28.77	0.27		28.78	0.27	34.91	0.20	So25
d18O_radio140515_Br6_gr7@6	2.03	2.0639E-03	8.3532E-03	1.6715E+09	5.6673E-02	3.4499E+06	5.5875E-02	1:03	8.2307E+08		29.29	0.17		29.31	0.17	35.45	0.17	So25
d18O_radio140515_Br6_gr7@7	2.03	2.0628E-03	9.0524E-03	1.6831E+09	7.0948E-02	3.4717E+06	7.0958E-02	1:08	8.2771E+08		28.74	0.18		28.76	0.18	34.89	0.17	So25
d18O_radio140515_Br6_gr7@8	2.03	2.0640E-03	9.1899E-03	1.6632E+09	6.0975E-02	3.4327E+06	6.1198E-02	1:12	8.1806E+08		29.35	0.18		29.36	0.18	35.50	0.17	So25
d18O_radio140515_Br6_gr7@9	2.04	2.0641E-03	1.0231E-02	1.6616E+09	6.7873E-02	3.4297E+06	6.8461E-02	1:16	8.1645E+08		29.39	0.20		29.41	0.20	35.55	0.18	So25
d18O_radio140515_Br6_paine@33	2.04	2.0129E-03	1.0114E-02	1.6741E+09	5.7104E-02	3.3695E+06	6.0851E-02	1:21	8.2187E+08	8.2496E+08	3.83	0.20	3.78	3.85	0.20	9.83	0.18	Standard
d18O_radio140515_Br6_paine@34	2.04	2.0126E-03	1.0055E-02	1.6809E+09	6.4429E-02	3.3831E+06	6.4582E-02	1:25	8.2545E+08	4.9991E+06	3.71	0.20	0.28	3.73	0.20	9.71	0.18	Standard
d18O_radio140515_Br6_paine@35	2.03	2.0125E-03	1.2008E-02	1.6772E+09	5.9848E-02	3.3751E+06	5.8759E-02	1:30	8.2459E+08		3.64	0.24		3.66	0.24	9.64	0.19	Standard
d18O_radio140515_Br6_paine@36	2.03	2.0131E-03	8.7266E-03	1.6816E+09	7.3801E-02	3.3852E+06	7.5762E-02	1:34	8.2793E+08		3.96	0.17		3.98	0.17	9.97	0.17	Standard
d18O_radio140515_Br6_g8@1	2.03	2.0560E-03	1.2459E-02	1.6640E+09	6.2323E-02	3.4211E+06	6.6347E-02	1:39	8.1857E+08	8.2294E+08	25.33	0.25	25.23	25.35	0.25	31.46	0.19	Ki41
d18O_radio140515_Br6_g8@2	2.03	2.0580E-03	7.8959E-03	1.6689E+09	5.6224E-02	3.4347E+06	5.5084E-02	1:43	8.2386E+08	1.1542E+07	26.35	0.16	1.54	26.37	0.16	32.49	0.17	Ki41
d18O_radio140515_Br6_g8@3	2.03	2.0557E-03	9.1606E-03	1.6804E+09	8.5850E-02	3.4545E+06	8.8395E-02	1:48	8.2970E+08		25.20	0.18		25.22	0.18	31.33	0.17	Ki41
d18O_radio140515_Br6_g8@4	2.03	2.0567E-03	7.7263E-03	1.6768E+09	5.8464E-02	3.4488E+06	6.0128E-02	1:52	8.2770E+08		25.70	0.15		25.72	0.15	31.84	0.17	Ki41
d18O_radio140515_Br6_g8@5	2.03	2.0529E-03	9.5368E-03	1.6730E+09	8.5429E-02	3.4343E+06	8.6683E-02	1:57	8.2287E+08		23.78	0.19		23.81	0.19	29.91	0.18	Ki41
d18O_radio140515_Br6_g8@6	2.03	2.0537E-03	9.0134E-03	1.6493E+09	5.2726E-02	3.3874E+06	5.6799E-02	2:01	8.1057E+08		24.21	0.18		24.23	0.18	30.34	0.17	Ki41
d18O_radio140515_Br6_g8@7	2.03	2.0556E-03	1.0172E-02	1.6617E+09	7.1631E-02	3.4159E+06	7.3094E-02	2:06	8.1781E+08		25.14	0.20		25.16	0.20	31.28	0.18	Ki41
d18O_radio140515_Br6_g8@8	2.03	2.0569E-03	9.4115E-03	1.6718E+09	6.9062E-02	3.4387E+06	6.7582E-02	2:10	8.2503E+08		25.76	0.19		25.79	0.19	31.90	0.18	Ki41
d18O_radio140515_Br6_g8@9	2.03	2.0553E-03	1.0145E-02	1.6761E+09	7.3415E-02	3.4447E+06	7.4823E-02	2:15	8.2712E+08		25.00	0.20		25.02	0.20	31.14	0.18	Ki41
d18O_radio140515_Br6_g8@10	2.03	2.0570E-03	9.6903E-03	1.6793E+09	6.9951E-02	3.4543E+06	7.4507E-02	2:19	8.2616E+08		25.82	0.19		25.85	0.19	31.96	0.18	Ki41
d18O_radio140515_Br6_paine@37	2.03	2.0129E-03	7.2914E-03	1.6884E+09	6.5959E-02	3.3986E+06	6.8471E-02	2:24	8.3076E+08	8.2501E+08	3.86	0.15	3.73	3.89	0.15	9.88	0.16	Standard
d18O_radio140515_Br6_paine@38	2.04	2.0123E-03	1.3103E-02	1.6781E+09	6.4507E-02	3.3772E+06	6.2111E-02	2:28	8.2319E+08	7.6752E+06	3.53	0.26	0.47	3.56	0.26	9.54	0.19	Standard
d18O_radio140515_Br6_paine@39	2.03	2.0132E-03	6.4785E-03	1.6724E+09	5.4989E-02	3.3671E+06	5.3187E-02	2:33	8.2285E+08		4.00	0.13		4.03	0.13	10.02	0.16	Standard
d18O_radio140515_Br6_paine@40	2.03	2.0123E-03	9.8918E-03	1.6701E+09	6.8308E-02	3.3608E+06	7.1730E-02	2:37	8.2324E+08		3.55	0.20		3.58	0.20	9.56	0.18	Standard
d18O_radio140515_Br6_gr9@1	2.03	2.0639E-03	1.1245E-02	1.6708E+09	5.6669E-02	3.4482E+06	5.7050E-02	2:42	8.2448E+08	8.2269E+08	29.25	0.22	29.06	29.28	0.22	35.42	0.19	So31
d18O_radio140515_Br6_gr9@2	2.04	2.0632E-03	9.6273E-03	1.6758E+09	6.5172E-02	3.4574E+06	6.5107E-02	2:46	8.2266E+08	6.9887E+06	28.92	0.19	0.56	28.95	0.19	35.09	0.18	So31
d18O_radio140515_Br6_gr9@3	2.03	2.0645E-03	7.6299E-03	1.6640E+09	4.9439E-02	3.4353E+06	5.2569E-02	2:50	8.1847E+08		29.59	0.15		29.62	0.15	35.76	0.17	So31
d18O_radio140515_Br6_gr9@4	2.03	2.0628E-03	1.0990E-02	1.6715E+09	8.1053E-02	3.4480E+06	8.2205E-02	2:55	8.2245E+08		28.70	0.22		28.74	0.22	34.87	0.19	So31
d18O_radio140515_Br6_gr9@5	2.03	2.0628E-03	1.2228E-02	1.6741E+09	7.3456E-02	3.4534E+06	7.4855E-02	2:59	8.2483E+08		28.73	0.24		28.77	0.24	34.90	0.19	So31
d18O_radio140515_Br6_gr9@6	2.03	2.0632E-03	9.5657E-03	1.6748E+09	7.6589E-02	3.4551E+06	8.1301E-02	3:04	8.2635E+08		28.92	0.19		28.96	0.19	35.10	0.18	So31
d18O_radio140515_Br6_gr9@7	2.03	2.0634E-03	9.1334E-03	1.6743E+09	7.8146E-02	3.4547E+06	7.9450E-02	3:08	8.2500E+08		29.02	0.18		29.06	0.18	35.19	0.17	So31
d18O_radio140515_Br6_gr9@8	2.03	2.0638E-03	7.7889E-03	1.6753E+09	7.4662E-02	3.4574E+06	7.7046E-02	3:13	8.2438E+08		29.24	0.16		29.28	0.16	35.42	0.17	So31
d18O_radio140515_Br6_gr9@9	2.04	2.0636E-03	1.1822E-02	1.6617E+09	6.4215E-02	3.4292E+06	6.5094E-02	3:17	8.1559E+08		29.15	0.24		29.19	0.24	35.32	0.19	So31

Table A2 Continued.

	SIMS ANALYSES				Mount: BR4		Standard: UNIL-Q1 (Paine)		Analyse: $\delta^{18}O$			Value=9.81±0.14 (VSMOW, 2σ)			Date: 15.04.2015	
	Beam	$1^{16}2^{1}/2^{1}(^{18}O/^{16}O)$		$1^{1}2^{1}(^{18}O/Ceff)$		$1^{1}2^{1}(^{18}O/Ceff)$	Time	Yield		Measurements (‰)		mean	Drift correction (‰)		Calibration (‰)		*Comment*
	n.i	*CPS*	*2SD*	*CPS*	*2SD*	*CPS*		*CPS/nA*		$\delta^{18}O$	*2SD int*	*2SD*	$\delta^{18}O$	*2SD*	$\delta^{18}O_{(VSMOW)}$	*2SD*	
d18O_radio140515_Bt6_paine@41	2.03	2.0128E-03	9.4529E-03	1.6693E+09	5.6510E-02	3.3603E+06	3:22	8.2374E+08	8.2356E+08	3.80	0.19	3.75	3.83	0.19	9.82	0.17	Standard
d18O_radio140515_Bt6_paine@42	2.02	2.0124E-03	1.1556E-02	1.6689E+09	6.9823E-02	3.3585E+06	3:26	8.2425E+08	1.0853E+06	3.58	0.23	0.26	3.62	0.23	9.60	0.18	Standard
d18O_radio140515_Bt6_paine@43	2.03	2.0130E-03	6.5448E-03	1.6689E+09	6.0907E-02	3.3597E+06	3:31	8.2310E+08		3.89	0.13		3.93	0.13	9.91	0.16	Standard
d18O_radio140515_Bt6_paine@44	2.03	2.0127E-03	1.1426E-02	1.6739E+09	5.5716E-02	3.3693E+06	3:35	8.2315E+08		3.73	0.23		3.77	0.23	9.76	0.18	Standard
d18O_radio140515_Bt6_gr10@1	2.03	2.0569E-03	1.2726E-02	1.6393E+09	7.8974E-02	3.3720E+06	3:40	8.0672E+08	8.1658E+08	25.80	0.25	17.93	25.84	0.25	31.96	0.20	S.s21	
d18O_radio140515_Bt6_gr10@02	2.03	2.0560E-03	8.6852E-03	1.7008E+09	1.0990E-01	3.4968E+06	3:44	8.3935E+08	2.0905E+07	25.33	0.17	19.67	25.37	0.17	31.49	0.17	S.s21	
d18O_radio140515_Bt6_gr10@03	2.04	2.0363E-03	1.4335E-02	1.6862E+09	6.6989E-02	3.4335E+06	3:49	8.2744E+08		15.52	0.29						S.s21	Optical rejection
d18O_radio140515_Bt6_gr10@04	2.05	2.0605E-03	7.7522E-03	1.6728E+09	6.7246E-02	3.4468E+06	3:53	8.1767E+08		27.57	0.16		27.62	0.16	33.75	0.17	S.s21	
d18O_radio140515_Bt6_gr10@05	2.04	2.0136E-03	8.8607E-03	1.6799E+09	6.1452E-02	3.3825E+06	3:58	8.2334E+08		4.19	0.18						S.s21	Optical rejection
d18O_radio140515_Bt6_gr10@06	2.03	2.0128E-03	1.5543E-02	1.6625E+09	8.5399E-02	3.3463E+06	4:02	8.1888E+08		3.77	0.31						S.s21	Optical rejection
d18O_radio140515_Bt6_gr10@07	2.03	2.0235E-03	9.8608E-03	1.6563E+09	1.5207E-01	3.3515E+06	4:07	8.1449E+08		9.10	0.20						S.s21	Optical rejection
d18O_radio140515_Bt6_gr10@08	2.04	2.0558E-03	1.3207E-02	1.6496E+09	1.0729E-01	3.3911E+06	4:11	8.0846E+08		25.23	0.26		25.27	0.26	31.39	0.20	S.s21	
d18O_radio140515_Bt6_gr10@09	2.04	2.0562E-03	9.9306E-03	1.6634E+09	1.0450E-01	3.4204E+06	4:16	8.1393E+08		25.45	0.20		25.50	0.20	31.62	0.18	S.s21	
d18O_radio140515_Bt6_gr10@10	2.04	2.0593E-03	1.2063E-02	1.6390E+09	7.4060E-02	3.3751E+06	4:20	8.0425E+08		26.97	0.24		27.02	0.24	33.15	0.19	S.s21	
d18O_radio140515_Bt6_gr10@11	2.03	2.0218E-03	1.4269E-02	1.6421E+09	6.7430E-02	3.3199E+06	4:25	8.0779E+08		8.27	0.29						S.s21	Optical rejection
d18O_radio140515_Bt6_paine@45	2.03	2.0125E-03	1.0628E-02	1.6738E+09	5.6629E-02	3.3687E+06	4:29	8.2387E+08	8.2606E+08	3.62	0.21	3.73	3.67	0.21	9.65	0.18	Standard	
d18O_radio140515_Bt6_paine@46	2.03	2.0127E-03	1.2121E-02	1.6810E+09	7.8859E-02	3.3833E+06	4:34	8.2699E+08	3.3265E+06	3.72	0.24	0.19	3.77	0.24	9.76	0.19	Standard	
d18O_radio140515_Bt6_paine@47	2.04	2.0123E-03	9.1256E-03	1.6765E+09	6.7367E-02	3.3736E+06	4:38	8.2308E+08		3.55	0.18		3.60	0.18	9.58	0.17	Standard	
d18O_radio140515_Bt6_paine@48	2.04	2.0128E-03	1.2353E-02	1.6848E+09	6.5180E-02	3.3916E+06	4:42	8.2769E+08		3.80	0.25		3.85	0.25	9.84	0.19	Standard	
d18O_radio140515_Bt6_paine@49	2.04	2.0129E-03	9.3673E-03	1.6881E+09	5.5538E-02	3.3976E+06	4:47	8.2693E+08		3.82	0.19		3.87	0.19	9.86	0.17	Standard	
d18O_radio140515_Bt6_paine@50	2.04	2.0127E-03	1.4054E-02	1.6846E+09	7.3290E-02	3.3906E+06	4:51	8.2614E+08		3.75	0.28		3.81	0.28	9.79	0.20	Standard	
d18O_radio140515_Bt6_paine@51	2.04	2.0127E-03	1.3301E-02	1.6849E+09	5.3908E-02	3.3916E+06	4:56	8.2679E+08		3.74	0.27		3.80	0.27	9.79	0.20	Standard	
d18O_radio140515_Bt6_paine@52	2.03	2.0128E-03	6.0676E-03	1.6806E+09	7.0343E-02	3.3830E+06	5:00	8.2699E+08		3.81	0.12		3.86	0.12	9.85	0.16	Standard	

Table A2 Continued.

SIMS ANALYSES						Mount: BR6			Standard: UNIL-QI (Paine)		Analyse: $\delta^{18}O$			Value= 9.81±0.14 (VSMOW, 2σ)				Date: 15.04.2015	
	Beam	H'2/L'2 ($^{18}O/^{16}O$)		L'2 (^{18}O/Coeff)		H'2 (^{18}O/Coeff)		Time	Yield		Measurements (‰)		mean	Drift correction (‰)		Calibration (‰)		Comment	
	nA	CPS	2SD	CPS	2SD	CPS	2SD		CPS/nA		$\delta^{18}O$	2SD int	2SD	$\delta^{18}O$	2SD	$\delta^{18}O_{(VSMOW)}$	2SD		
testpaine@1	2.05	2.0139E-03	1.7593E-02	1.4957E+09	4.6252E-02	3.0125E+06	4.5186E-02	8:15	7.2869E+08		4.36	0.35	4.24					Standard	
testpaine@2	2.06	2.0137E-03	1.2930E-02	1.4918E+09	6.7964E-02	3.0041E+06	6.1349E-02	8:20	7.2263E+08		4.23	0.26	0.32					Standard	
testpaine@3	2.06	2.0139E-03	9.5934E-03	1.5001E+09	2.9258E-02	3.0215E+06	3.6290E-02	8:24	7.2681E+08		4.32	0.19						Standard	
testpaine@4	2.07	2.0137E-03	1.4276E-02	1.5032E+09	8.1637E-02	3.0270E+06	8.1922E-02	8:29	7.2788E+08		4.24	0.29						Standard	
testpaine@5	2.07	2.0130E-03	1.0186E-02	1.5219E+09	2.1353E-02	3.0644E+06	2.8967E-02	8:34	7.3450E+08		3.88	0.20						Standard	
testpaine@6	2.07	2.0141E-03	1.2309E-02	1.5401E+09	7.0213E-02	3.1016E+06	6.7331E-02	8:38	7.4357E+08		4.42	0.25						Standard	
testpaine@7	2.08	2.0137E-03	1.7440E-02	1.5446E+09	6.4726E-02	3.1102E+06	6.3247E-02	8:43	7.4340E+08		4.23	0.35						Standard	
testpaine@8	2.07	2.0136E-03	8.3634E-03	1.5143E+09	4.3275E-02	3.0494E+06	4.2236E-02	8:48	7.3175E+08		4.21	0.17						Standard	
d18O_radio140515_Br6_paine@1	2.05	2.0132E-03	1.1915E-02	1.6203E+09	9.1067E-02	3.2616E+06	9.5347E-02	9:30	7.9053E+08		3.97	0.24	3.78	3.84	0.24	10.00	0.20	Standard	
d18O_radio140515_Br6_paine@2	2.06	2.0127E-03	6.1710E-03	1.6238E+09	9.9510E-02	3.2681E+06	1.0080E-01	9:34	7.8800E+08		3.72	0.12	0.32	3.59	0.12	9.75	0.17	Standard	
d18O_radio140515_Br6_paine@3	2.06	2.0129E-03	1.2560E-02	1.6247E+09	9.2470E-02	3.2704E+06	9.3494E-02	9:39	7.8716E+08		3.85	0.25		3.72	0.25	9.88	0.20	Standard	
d18O_radio140515_Br6_paine@4	2.07	2.0123E-03	1.0069E-02	1.6274E+09	8.0125E-02	3.2750E+06	8.4921E-02	9:43	7.8728E+08		3.56	0.20		3.44	0.20	9.59	0.19	Standard	
d18O_radio140515_Br6_paine@5	2.06	2.0126E-03	8.9395E-03	1.6332E+09	9.2634E-02	3.2870E+06	9.1676E-02	9:48	7.9116E+08		3.71	0.18		3.59	0.18	9.75	0.18	Standard	
d18O_radio140515_Br6_paine@6	2.07	2.0127E-03	9.3132E-03	1.6346E+09	8.9973E-02	3.2896E+06	8.8676E-02	9:53	7.9017E+08		3.73	0.19		3.61	0.19	9.77	0.18	Standard	
d18O_radio140515_Br6_paine@7	2.07	2.0133E-03	8.6549E-03	1.6374E+09	9.0309E-02	3.2965E+06	9.2172E-02	9:57	7.9178E+08		4.02	0.17		3.91	0.17	10.07	0.18	Standard	
d18O_radio140515_Br6_paine@8	2.07	2.0125E-03	7.0161E-03	1.6358E+09	9.4975E-02	3.2923E+06	9.4991E-02	10:02	7.8989E+08		3.65	0.14		3.55	0.14	9.70	0.17	Standard	
d18O_radio140515_Br6_gr1@1	2.06	2.0621E-03	8.9128E-03	1.6031E+09	8.4729E-02	3.3056E+06	8.8328E-02	10:07	7.7727E+08		28.38	0.18	28.45	28.27	0.18	34.58	0.18	So15	
d18O_radio140515_Br6_gr1@2	2.06	2.0629E-03	9.4579E-03	1.5975E+09	9.7854E-02	3.2958E+06	9.8009E-02	10:11	7.7719E+08		28.78	0.19	1.08	28.67	0.19	34.99	0.19	So15	
d18O_radio140515_Br6_gr1@3	2.06	2.0633E-03	9.9792E-03	1.6160E+09	1.0567E-01	3.3343E+06	1.0196E-01	10:16	7.8489E+08		28.97	0.20		28.87	0.20	35.18	0.19	So15	
d18O_radio140515_Br6_gr1@4	2.06	2.0608E-03	1.3238E-02	1.6160E+09	9.8559E-02	3.3302E+06	9.9441E-02	10:21	7.8478E+08		27.72	0.26		27.62	0.26	33.92	0.21	So15	
d18O_radio140515_Br6_gr1@5	2.06	2.0612E-03	1.0345E-02	1.6019E+09	1.0103E-01	3.3018E+06	1.0063E-01	10:25	7.7792E+08		27.91	0.21		27.81	0.21	34.12	0.19	So15	
d18O_radio140515_Br6_gr1@6	2.05	2.0632E-03	1.1117E-02	1.5966E+09	8.7404E-02	3.2938E+06	8.1651E-02	10:30	7.7715E+08		28.93	0.22		28.84	0.22	35.15	0.20	So15	
d18O_radio140515_Br6_gr2@1	2.05	1.9283E-03	1.9667E-01	5.4155E+07	5.1049E-02	1.0430E+05	1.7469E-01	10:35	2.6398E+07		-38.35	3.93	18.29					Ki48	
d18O_radio140515_Br6_gr2@2	2.05	2.0520E-03	1.0316E-02	1.5900E+09	1.0269E-01	3.2627E+06	1.0207E-01	10:40	7.7439E+08		23.36	0.21	1.84	23.27	0.21	29.55	0.19	Ki48	
d18O_radio140515_Br6_gr2@3	2.06	2.0556E-03	9.5755E-03	1.5935E+09	9.9016E-02	3.2755E+06	1.0056E-01	10:44	7.7274E+08		25.12	0.19		25.04	0.19	31.33	0.19	Ki48	
d18O_radio140515_Br6_gr2@4	2.06	2.0547E-03	9.0162E-03	1.5920E+09	1.0913E-01	3.2707E+06	1.1372E-01	10:49	7.7308E+08		24.69	0.18		24.61	0.18	30.90	0.18	Ki48	
d18O_radio140515_Br6_gr2@5	2.06	1.9352E-03	4.0611E-01	5.0912E+07	1.7019E-01	9.8523E+04	3.9726E-01	10:54	2.4774E+07		-34.91	8.12						Ki48	Yield rejection
d18O_radio140515_Br6_gr2@6	2.05	2.0241E-03	1.1963E-02	1.5707E+09	5.9758E-02	3.1791E+06	6.0775E-02	10:58	7.6585E+08		9.43	0.24						Ki48	Optical rejection
d18O_radio140515_Br6_paine@9	2.05	2.0130E-03	1.1705E-02	1.6333E+09	1.0300E-01	3.2879E+06	1.0464E-01	11:03	7.9709E+08		3.90	0.23	3.75	3.83	0.23	9.99	0.19	Standard	
d18O_radio140515_Br6_paine@10	2.06	2.0131E-03	8.1153E-03	1.6378E+09	9.3133E-02	3.2969E+06	9.9071E-02	11:08	7.9694E+08		3.92	0.16	0.36	3.85	0.16	10.01	0.18	Standard	
d18O_radio140515_Br6_paine@11	2.05	2.0124E-03	1.0659E-02	1.6314E+09	8.8680E-02	3.2832E+06	9.4583E-02	11:12	7.9539E+08		3.59	0.21		3.52	0.21	9.68	0.19	Standard	
d18O_radio140515_Br6_paine@12	2.04	2.0124E-03	1.2528E-02	1.6316E+09	9.2831E-02	3.2837E+06	1.0001E-01	11:17	7.9833E+08		3.60	0.25		3.54	0.25	9.70	0.20	Standard	
d18O_radio140515_Br6_gr3@1	2.04	2.0621E-03	1.0108E-02	1.5740E+09	8.4365E-02	3.2454E+06	8.4911E-02	11:22	7.7084E+08		28.36	0.20	27.76	28.30	0.20	34.61	0.19	So23	
d18O_radio140515_Br6_gr3@2	2.04	2.0610E-03	8.0251E-03	1.5743E+09	8.8386E-02	3.2446E+06	8.9124E-02	11:26	7.7198E+08		27.82	0.16	1.20	27.76	0.16	34.06	0.18	So23	
d18O_radio140515_Br6_gr3@3	2.04	2.0585E-03	9.9781E-03	1.5723E+09	9.3612E-02	3.2363E+06	9.5834E-02	11:31	7.7155E+08		26.60	0.20		26.55	0.20	32.85	0.19	So23	
d18O_radio140515_Br6_gr3@4	2.04	2.0615E-03	8.4235E-03	1.5705E+09	8.3251E-02	3.2377E+06	8.1275E-02	11:36	7.7032E+08		28.07	0.17		28.01	0.17	34.32	0.18	So23	
d18O_radio140515_Br6_gr3@5	2.04	2.0611E-03	8.1492E-03	1.5673E+09	1.0586E-01	3.2307E+06	1.1067E-01	11:40	7.6865E+08		27.89	0.16		27.84	0.16	34.15	0.18	So23	
d18O_radio140515_Br6_gr3@6	2.04	2.0610E-03	8.4231E-03	1.5701E+09	7.9481E-02	3.2359E+06	7.9874E-02	11:45	7.6865E+08		27.82	0.17		27.77	0.17	34.07	0.18	So23	
d18O_radio140515_Br6_gr4@1	2.04	2.0558E-03	1.2551E-02	1.5758E+09	9.5302E-02	3.2396E+06	9.9914E-02	11:50	7.7254E+08		25.22	0.25	25.05	25.18	0.25	31.47	0.20	Ki43s	
d18O_radio140515_Br6_gr4@2	2.04	2.0560E-03	7.1512E-03	1.5658E+09	8.3894E-02	3.2193E+06	8.2917E-02	11:54	7.6701E+08		25.32	0.14	0.86	25.28	0.14	31.57	0.17	Ki43s	
d18O_radio140515_Br6_gr4@3	2.04	2.0553E-03	1.1215E-02	1.5602E+09	6.9223E-02	3.2067E+06	6.9353E-02	11:59	7.6648E+08		25.00	0.22		24.96	0.22	31.25	0.20	Ki43s	
d18O_radio140515_Br6_gr4@4	2.03	2.0559E-03	1.0795E-02	1.5519E+09	9.8114E-02	3.1903E+06	9.8963E-02	12:04	7.6341E+08		25.26	0.22		25.23	0.22	31.52	0.19	Ki43s	
d18O_radio140515_Br6_gr4@5	2.03	2.0537E-03	9.1853E-03	1.5467E+09	8.2495E-02	3.1768E+06	8.5077E-02	12:08	7.6051E+08		24.21	0.18		24.17	0.18	30.46	0.18	Ki43s	
d18O_radio140515_Br6_gr4@6	2.04	2.0559E-03	9.6891E-03	1.5760E+09	1.0189E-01	3.2399E+06	1.0479E-01	12:13	7.7415E+08		25.30	0.19		25.27	0.19	31.56	0.19	Ki43s	
d18O_radio140515_Br6_paine@13	2.13	2.0128E-03	1.1931E-02	1.6354E+09	2.0230E-01	3.2913E+06	2.0002E-01	12:18	7.6771E+08		3.77	0.24	3.67	3.74	0.24	9.90	0.20	Standard	
d18O_radio140515_Br6_paine@14	2.04	2.0126E-03	1.2097E-02	1.6277E+09	1.1435E-01	3.2764E+06	1.1916E-01	12:23	7.9905E+08		3.67	0.24	0.17	3.65	0.24	9.80	0.20	Standard	
d18O_radio140515_Br6_paine@15	2.03	2.0125E-03	9.1071E-03	1.6208E+09	9.8747E-02	3.2621E+06	9.8133E-02	12:27	7.9714E+08		3.66	0.18		3.64	0.18	9.80	0.18	Standard	
d18O_radio140515_Br6_paine@16	2.03	2.0123E-03	1.5538E-02	1.6213E+09	9.5483E-02	3.2626E+06	9.4056E-02	12:32	7.9933E+08		3.56	0.31		3.54	0.31	9.70	0.22	Standard	
d18O_radio140515_Br6_gr5@1	2.03	2.0187E-03	1.4905E-02	1.4510E+09	4.1803E-01	2.9294E+06	4.0498E-01	12:37	7.1340E+08		6.74	0.30	14.20					Ki20	Optical rejection
d18O_radio140515_Br6_gr5@2	2.04	2.0319E-03	1.0360E-02	1.5447E+09	8.3110E-02	3.1390E+06	8.3679E-02	12:41	7.5638E+08		13.32	0.21	7.97	13.31	0.21	19.52	0.19	Ki20	
d18O_radio140515_Br6_gr5@3	2.04	2.0361E-03	1.3058E-02	1.5538E+09	7.7325E-02	3.1637E+06	7.1454E-02	12:46	7.6070E+08		15.39	0.26		15.38	0.26	21.61	0.21	Ki20	
d18O_radio140515_Br6_gr5@4	2.04	2.0364E-03	1.3753E-02	1.6184E+09	4.0052E-02	3.2966E+06	3.4498E-02	12:51	7.9139E+08		15.57	0.28		15.56	0.28	21.79	0.21	Ki20	
d18O_radio140515_Br6_gr5@5	2.04	2.0371E-03	1.1959E-02	1.5578E+09	9.5179E-02	3.1735E+06	9.0099E-02	12:55	7.6321E+08		15.92	0.24		15.91	0.24	22.14	0.20	Ki20	
d18O_radio140515_Br6_gr5@6	2.05	2.0419E-03	1.0489E-02	1.5766E+09	1.0723E-01	3.2191E+06	1.1302E-01	13:00	7.7060E+08		18.29	0.21		18.29	0.21	24.53	0.19	Ki20	
d18O_radio140515_Br6_gr6@1	2.05	2.0539E-03	8.7792E-03	2.1220E+09	2.0405E-01	4.3587E+06	1.9792E-01	13:05	1.0360E+09		24.31	0.18	24.35					So29	SEM rejection
d18O_radio140515_Br6_gr6@2	2.05	2.0537E-03	1.2637E-02	2.0202E+09	2.7549E-01	4.1489E+06	2.7047E-01	13:09	9.8587E+08		24.19	0.25	0.90					So29	SEM rejection
d18O_radio140515_Br6_gr6@3	2.04	2.0524E-03	1.1417E-02	2.1118E+09	2.2198E-01	4.3342E+06	2.1548E-01	13:14	1.0340E+09		23.56	0.23						So29	SEM rejection
d18O_radio140515_Br6_gr6@4	2.04	2.0546E-03	1.1355E-02	2.0779E+09	2.2026E-01	4.2691E+06	2.0921E-01	13:19	1.0188E+09		24.64	0.23						So29	SEM rejection
d18O_radio140515_Br6_gr6@5	2.04	2.0549E-03	1.0585E-02	2.1258E+09	2.0366E-01	4.3683E+06	2.0263E-01	13:23	1.0399E+09		24.80	0.21						So29	SEM rejection
d18O_radio140515_Br6_gr6@6	2.05	2.0546E-03	1.1793E-02	2.0132E+09	9.3889E-02	4.1364E+06	9.2734E-02	13:28	9.8238E+08		24.61	0.24						So29	SEM rejection
d18O_radio140515_Br6_paine@17	2.05	2.0124E-03	1.1103E-02	1.6330E+09	9.4529E-02	3.2862E+06	9.4052E-02	13:33	7.9782E+08		3.59	0.22	3.63	3.60	0.22	9.76	0.19	Standard	
d18O_radio140515_Br6_paine@18	2.04	2.0123E-03	9.5256E-03	1.6321E+09	8.2464E-02	3.2843E+06	8.1430E-02	13:37	7.9923E+08		3.55	0.19	0.15	3.57	0.19	9.73	0.18	Standard	
d18O_radio140515_Br6_paine@19	2.04	2.0127E-03	1.1824E-02	1.6369E+09	8.7225E-02	3.2945E+06	8.9616E-02	13:42	8.0045E+08		3.72	0.24		3.74	0.24	9.90	0.20	Standard	
d18O_radio140515_Br6_paine@20	2.05	2.0125E-03	9.8187E-03	1.6400E+09	9.8772E-02	3.3007E+06	1.0070E-01	13:47	7.9976E+08		3.65	0.20		3.67	0.20	9.83	0.18	Standard	
d18O_radio140515_Br6_gr7@1	2.05	2.0104E-03	1.2609E-02	1.5538E+09	4.3540E-02	3.1253E+06	3.1498E-02	13:52	7.5835E+08	5.0592E+08	2.61	0.25	-0.62					ki12s	Optical rejection
d18O_radio140515_Br6_gr7@2	2.05	2.0226E-03	1.0613E-02	1.4540E+09	1.1038E-01	2.9409E+06	1.0563E-01	13:56	7.0946E+08	5.6035E+08	8.69	0.21	15.52					ki12s	Optical rejection
d18O_radio140515_Br6_gr7@3	2.04	2.0167E-03	1.3620E-02	1.4269E+09	4.8856E-01	2.8775E+06	4.8737E-01	14:01	6.9926E+08		5.74	0.27						ki12s	Optical rejection
d18O_radio140515_Br6_gr7@4	2.03	1.9889E-03	4.5630E-02	3.4231E+08	4.9852E-01	6.8117E+05	5.3033E-01	14:06	1.6821E+08		-8.13	0.91						ki12s	Optical rejection
d18O_radio140515_Br6_gr7@5	2.04	1.9833E-03	4.6421E-02	2.8736E+08	2.9607E+00	5.6978E+05	2.9917E+00	14:10	1.4111E+08		-10.93	0.93						ki12s	Optical rejection
d18O_radio140515_Br6_gr7@6	2.04	2.0018E-03	1.3235E-02	1.1399E+09	5.5299E-01	2.2816E+06	5.4686E-01	14:15	5.5915E+08		-1.69	0.26						ki12s	Optical rejection

Table A2 Continued.

	SIMS ANALYSES				Mount: BR6		Standard: UNIL-Q1 (Paine)		Analyse: $\delta^{18}O$			Value= 9.81±0.14 (VSMOW, 2σ)			Date: 15.04.2015
	Beam	H^+2/L^+2 ($^{18}O/^{16}O$)		L^+2 ($^{18}OCoeff$)		H^+2 ($^{18}OCoeff$)	Time	Yield	Measurements (‰)		mean	Diff correction (‰)		Calibration (‰)	
	n.A	*CPS*	*2SD*	*CPS*	*2SD*	*CPS*		*CPS/nA*	$\delta^{18}O$	*2SD int*	*2SD*	$\Delta^{18}O$	*2SD*	$\delta^{18}O_{(VSMOW)}$	*2SD*	*Comment*
d18O_radio140515_Br6_gr6@1	2.04	2.0627E-03	9.8599E-03	1.6296E+09	9.8020E-02	3.3613E+06	14:20	7.9940E+08	8.0161E+08	28.67	0.20	28.76	28.71	0.20	35.03	0.19	So26
d18O_radio140515_Br6_gr6@2	2.04	2.0623E-03	8.9823E-03	1.6240E+09	9.5548E-02	3.3491E+06	14:24	7.9640E+08	7.8550E+06	28.49	0.18	0.55	28.54	0.18	34.85	0.18	So26
d18O_radio140515_Br6_gr6@3	2.04	2.0624E-03	9.9467E-03	1.6371E+09	1.2179E-01	3.3763E+06	14:29	8.0410E+08		28.53	0.20		28.58	0.20	34.89	0.19	So26
d18O_radio140515_Br6_gr6@4	2.04	2.0638E-03	1.1112E-02	1.6444E+09	8.8016E-02	3.3938E+06	14:34	8.0672E+08		29.25	0.22		29.30	0.22	35.62	0.20	So26
d18O_radio140515_Br6_gr6@5	2.04	2.0629E-03	1.0914E-02	1.6333E+09	8.2686E-02	3.3693E+06	14:38	8.0036E+08		28.78	0.22		28.84	0.22	35.15	0.19	So26
d18O_radio140515_Br6_gr6@6	2.04	2.0630E-03	9.2247E-03	1.6370E+09	1.1487E-01	3.3774E+06	14:43	8.0167E+08		28.84	0.18		28.90	0.18	35.22	0.18	So26
d18O_radio140515_Br6_paine@21	2.04	2.0126E-03	9.5532E-03	1.6277E+09	9.1938E-02	3.2760E+06	14:48	8.9063E+08	7.9804E+08	3.71	0.19	3.57	3.77	0.19	9.93	0.18	Standard
d18O_radio140515_Br6_paine@22	2.04	2.0124E-03	1.0529E-02	1.6347E+09	1.0899E-01	3.2898E+06	14:52	8.0031E+08	7.9745E+08	3.60	0.21	0.37	3.67	0.21	9.83	0.19	Standard
d18O_radio140515_Br6_paine@23	2.06	2.0118E-03	9.4764E-03	1.6317E+09	8.6866E-02	3.2827E+06	14:57	7.9389E+08	7.9320E+08	3.30	0.19		3.37	0.19	9.53	0.18	Standard
d18O_radio140515_Br6_paine@24	2.05	2.0126E-03	6.1522E-03	1.6339E+09	8.7112E-02	3.2885E+06	15:02	7.9758E+08	7.9483E+08	3.68	0.12		3.75	0.12	9.91	0.17	Standard
d18O_radio140515_Br6_gr9@1	2.05	2.0624E-03	8.0225E-03	1.6290E+09	1.1587E-01	3.3600E+06	15:06	7.9511E+08	7.9483E+08	28.54	0.16	28.52	28.62	0.16	34.93	0.18	So12
d18O_radio140515_Br6_gr9@2	2.04	2.0629E-03	1.0816E-02	1.6147E+09	9.1531E-02	3.3311E+06	15:11	7.9120E+08	7.5463E+06	28.80	0.22	0.96	28.88	0.22	35.19	0.19	So12
d18O_radio140515_Br6_gr9@3	2.04	2.0606E-03	1.3828E-02	1.6191E+09	1.1003E-01	3.3361E+06	15:16	7.9519E+08		27.63	0.28		27.71	0.28	34.01	0.21	So12
d18O_radio140515_Br6_gr9@4	2.04	2.0627E-03	7.7437E-03	1.6132E+09	8.8812E-02	3.3275E+06	15:20	7.9173E+08		28.66	0.15		28.74	0.15	35.05	0.18	So12
d18O_radio140515_Br6_gr9@5	2.01	2.0634E-03	7.6818E-03	1.6122E+09	1.1141E-01	3.3268E+06	15:42	8.0173E+08		29.03	0.15		29.13	0.15	35.44	0.18	So12
d18O_radio140515_Br6_gr9@6	2.03	2.0623E-03	9.7393E-03	1.6116E+09	9.5404E-02	3.3238E+06	15:47	7.9402E+08		28.48	0.19		28.58	0.19	34.90	0.19	So12
d18O_radio140515_Br6_gr10@1	2.03	2.0467E-03	1.2809E-02	1.6129E+09	9.1036E-02	3.3010E+06	15:51	7.9351E+08	7.9021E+08	20.70	0.26	20.17	20.80	0.26	27.06	0.20	Go68
d18O_radio140515_Br6_gr10@2	2.04	2.0444E-03	9.4878E-03	1.6037E+09	1.0684E-01	3.2788E+06	15:56	7.8477E+08	1.0067E+07	19.53	0.19	1.13	19.63	0.19	25.89	0.18	Go68
d18O_radio140515_Br6_gr10@3	2.04	2.0453E-03	8.3673E-03	1.6034E+09	9.2715E-02	3.2792E+06	16:01	7.8699E+08		20.02	0.17		20.13	0.17	26.39	0.18	Go68
d18O_radio140515_Br6_gr10@4	2.04	2.0455E-03	1.2785E-02	1.6043E+09	1.0075E-01	3.2815E+06	16:06	7.8626E+08		20.10	0.26		20.21	0.26	26.47	0.20	Go68
d18O_radio140515_Br6_gr10@5	2.04	2.0447E-03	9.0250E-03	1.6268E+09	1.0585E-01	3.3263E+06	16:10	7.9553E+08		19.69	0.18		19.80	0.18	26.06	0.18	Go68
d18O_radio140515_Br6_gr10@6	2.05	2.0473E-03	8.3613E-03	1.6303E+09	9.2747E-02	3.3374E+06	16:15	7.9523E+08		20.98	0.17		21.09	0.17	27.36	0.18	Go68
d18O_radio140515_Br6_paine@25	2.05	2.0118E-03	1.0292E-02	1.6288E+09	8.3739E-02	3.2771E+06	16:20	7.9446E+08	7.9513E+08	3.30	0.20	3.49	3.42	0.20	9.57	0.19	Standard
d18O_radio140515_Br6_paine@26	2.04	2.0127E-03	8.2003E-03	1.6238E+09	1.0693E-01	3.2683E+06	16:24	7.9408E+08	2.3748E+06	3.75	0.16	0.37	3.87	0.16	10.03	0.18	Standard
d18O_radio140515_Br6_paine@27	2.04	2.0121E-03	7.8594E-03	1.6228E+09	1.0413E-01	3.2651E+06	16:29	7.9520E+08		3.45	0.16		3.57	0.16	9.73	0.17	Standard
d18O_radio140515_Br6_paine@28	2.05	2.0122E-03	8.3880E-03	1.6296E+09	9.4821E-02	3.2792E+06	16:34	7.9676E+08		3.49	0.17		3.62	0.17	9.77	0.18	Standard

Table A2 Continued.

SIMS ANALYSES						Mount: BR7			Standard: UNIL-Q1 (Paine)		Analyse: $\delta^{18}O$			Value= 9.81±0.14 (VSMOW, 2σ)				Date: 13.04.2015
	Beam	H'2/L'2 ($^{18}O/^{16}O$)		L'2 (^{16}O/Coeff)		H'2 (^{16}O/Coeff)		Time	Yield	Measurements (‰)		mean	Drift correction (‰)		Calibration (‰)		Comment
	nA	CPS	2SD	CPS	2SD	CPS	2SD		CPS/nA	$\delta^{18}O$	2SD int	2SD	$\delta^{18}O$	2SD	$\delta^{18}O_{VSMOW}$	2SD	
130415_paine@1	2.03	2.0156E-03	7.8906E-03	1.5494E+09	1.0101E-01	3.1228E+06	1.0130E-01	12:46	7.6258E+08	5.21	0.16	5.26					Standard
130415_paine@2	2.04	2.0151E-03	9.4127E-03	1.5814E+09	1.0882E-01	3.1871E+06	1.1154E-01	12:50	7.7628E+08	4.94	0.19	1.82					Standard
130415_paine@3	2.03	2.0157E-03	1.2454E-02	1.5910E+09	7.0947E-02	3.2071E+06	7.0409E-02	12:54	7.8302E+08	5.22	0.25						Standard
130415_paine@4	2.03	2.0158E-03	1.0970E-02	1.5925E+09	1.4901E-01	3.2098E+06	1.4968E-01	12:59	7.8491E+08	5.27	0.22						Standard
130415_paine@5	2.03	2.0166E-03	7.0652E-03	1.5157E+09	1.3474E-01	3.0567E+06	1.3233E-01	13:03	7.4605E+08	5.66	0.14						Standard
130415_paine@6	2.03	2.0162E-03	9.1504E-03	1.5383E+09	6.8801E-02	3.1019E+06	6.5965E-02	13:07	7.5718E+08	5.50	0.18						Standard
130415_paine@7	2.03	2.0167E-03	1.1013E-02	1.5199E+09	7.2171E-02	3.0650E+06	7.3476E-02	13:11	7.4896E+08	5.71	0.22						Standard
130415_paine@9	1.99	2.0170E-03	1.2067E-02	1.5135E+09	1.3627E-01	3.0527E+06	1.3241E-01	13:25	7.6155E+08	5.90	0.24						Standard
130415_paine@10	1.99	2.0167E-03	1.3572E-02	1.5321E+09	8.0729E-02	3.0897E+06	8.3999E-02	13:29	7.6895E+08	5.73	0.27						Standard
130415_paine@11	2.00	2.0163E-03	1.1614E-02	1.5304E+09	7.1198E-02	3.0857E+06	7.1665E-02	13:33	7.6621E+08	5.54	0.23						Standard
130415_paine@12	1.99	2.0171E-03	1.0455E-02	1.5319E+09	5.3360E-02	3.0889E+06	4.5523E-02	13:37	7.6908E+08	5.96	0.21						Standard
130415_paine@13	2.00	2.0174E-03	1.0641E-02	1.5045E+09	8.9284E-02	3.0350E+06	9.0106E-02	13:42	7.5318E+08	6.10	0.21						Standard
130415_paine@15	1.97	2.0180E-03	1.0980E-02	1.3095E+09	2.8252E-02	2.6426E+06	3.0618E-02	14:09	6.6623E+08	6.39	0.22						Standard
130415_paine@16	1.97	2.0184E-03	8.4364E-03	1.3326E+09	1.5886E-01	2.6898E+06	1.5578E-01	14:13	6.7607E+08	6.56	0.17						Standard
130415_paine@17	1.97	2.0179E-03	1.0718E-02	1.3416E+09	1.4828E-01	2.7075E+06	1.4874E-01	14:17	6.8276E+08	6.34	0.21						Standard
130415_paine@18	1.96	2.0188E-03	1.3141E-02	1.3274E+09	1.1918E-01	2.6798E+06	1.1447E-01	14:21	6.7566E+08	6.79	0.26						Standard
130415_paine@19	1.96	2.0183E-03	9.0536E-03	1.3304E+09	1.2245E-01	2.6852E+06	1.2228E-01	14:26	6.7741E+08	6.54	0.18						Standard
130415_paine@20	1.93	2.0162E-03	1.1624E-02	1.3349E+09	4.1606E-02	2.6910E+06	4.3800E-02	14:41	6.9288E+08	5.49	0.23						Standard
130415_paine@21	1.93	2.0165E-03	1.3010E-02	1.3168E+09	2.7791E-02	2.6554E+06	3.1095E-02	14:46	6.8206E+08	5.65	0.26						Standard
130415_paine@22	1.94	2.0157E-03	1.6604E-02	1.3108E+09	2.0965E-02	2.6420E+06	2.6607E-02	14:50	6.7723E+08	5.22	0.33						Standard
130415_paine@23	1.94	2.0155E-03	1.5079E-02	1.3108E+09	1.6958E-02	2.6417E+06	2.0658E-02	14:54	6.7525E+08	5.15	0.30						Standard
130415_paine@24	1.94	2.0163E-03	1.4509E-02	1.3067E+09	5.2514E-02	2.6348E+06	5.7951E-02	14:58	6.7459E+08	5.53	0.29						Standard
130415_paine@25	1.93	2.0159E-03	1.3068E-02	1.2995E+09	4.0062E-02	2.6194E+06	4.3406E-02	15:03	6.7227E+08	5.34	0.26						Standard
130415_paine@26	1.93	2.0163E-03	1.5462E-02	1.3004E+09	2.8943E-02	2.6217E+06	2.8061E-02	15:07	6.7435E+08	5.56	0.31						Standard
130415_paine@27	1.93	2.0158E-03	1.2187E-02	1.3057E+09	4.1994E-02	2.6318E+06	4.2313E-02	15:11	6.7624E+08	5.28	0.24						Standard
130415_paine@28	1.92	2.0133E-03	1.6687E-02	1.4918E+09	5.7281E-02	3.0034E+06	6.3561E-02	15:17	7.7561E+08	4.02	0.33						Standard
130415_paine@29	1.93	2.0129E-03	6.9970E-03	1.4888E+09	4.7319E-02	2.9972E+06	4.9858E-02	15:21	7.7006E+08	3.86	0.14						Standard
130415_paine@30	1.93	2.0130E-03	8.8625E-03	1.5390E+09	8.4649E-02	3.0979E+06	7.9960E-02	15:25	7.9794E+08	3.88	0.18						Standard
130415_paine@31	2.00	2.0128E-03	1.0751E-02	1.5583E+09	5.4511E-02	3.1365E+06	5.7148E-02	15:30	7.7771E+08	3.79	0.22						Standard
130415_paine@32	2.02	2.0126E-03	9.1744E-03	1.5627E+09	3.5377E-02	3.1450E+06	4.0030E-02	15:34	7.7182E+08	3.69	0.18						Standard
130415_paine@33	2.04	2.0130E-03	1.2464E-02	1.5871E+09	6.8061E-02	3.1965E+06	5.9685E-02	15:38	7.7830E+08	3.90	0.25						Standard
130415_paine@34	2.05	2.0132E-03	1.2983E-02	1.5984E+09	6.4136E-02	3.2175E+06	6.8171E-02	15:42	7.8004E+08	3.97	0.26						Standard
130415_paine@35	2.04	2.0129E-03	9.9295E-03	1.6026E+09	4.8911E-02	3.2261E+06	5.3946E-02	15:47	7.8405E+08	3.83	0.20						Standard
130415_Br7_paine@1	2.04	2.0127E-03	1.0806E-02	1.5596E+09	7.6244E-02	3.1391E+06	7.7670E-02	16:56	7.6634E+08	3.76	0.22	3.96	3.71	0.22	9.64	0.20	Standard
130415_Br7_paine@2	2.04	2.0133E-03	1.4296E-02	1.5709E+09	4.3052E-02	3.1629E+06	5.0097E-02	17:00	7.6842E+08	4.04	0.29	0.37	3.99	0.29	9.92	0.22	Standard
130415_Br7_paine@3	2.05	2.0128E-03	1.0913E-02	1.5752E+09	3.8583E-02	3.1702E+06	3.1134E-02	17:04	7.6663E+08	3.79	0.22		3.74	0.22	9.67	0.20	Standard
130415_Br7_paine@4	2.05	2.0132E-03	1.1310E-02	1.5816E+09	3.4133E-02	3.1854E+06	3.2646E-02	17:08	7.6993E+08	4.01	0.23		3.96	0.23	9.89	0.20	Standard
130415_Br7_paine@5	2.06	2.0127E-03	1.3649E-02	1.5863E+09	3.4680E-02	3.1927E+06	3.6680E-02	17:13	7.6956E+08	3.72	0.27		3.67	0.27	9.60	0.22	Standard
130415_Br7_paine@6	2.06	2.0129E-03	1.2716E-02	1.5639E+09	4.3366E-02	3.1476E+06	3.6962E-02	17:17	7.6098E+08	3.84	0.25		3.80	0.25	9.72	0.21	Standard
130415_Br7_paine@7	2.06	2.0138E-03	1.2409E-02	1.5734E+09	3.7702E-02	3.1684E+06	3.5322E-02	17:21	7.6457E+08	4.30	0.25		4.26	0.25	10.18	0.21	Standard
130415_Br7_paine@8	2.06	2.0131E-03	6.2288E-03	1.5904E+09	2.8036E-01	3.2015E+06	2.7970E-01	17:26	7.7191E+08	3.92	0.12		3.87	0.12	9.80	0.18	Standard
130415_Br7_paine@9	2.06	2.0134E-03	1.2815E-02	1.5918E+09	4.2764E-02	3.2048E+06	5.1509E-02	17:30	7.7332E+08	4.08	0.26		4.04	0.26	9.96	0.21	Standard
130415_Br7_paine@10	2.06	2.0135E-03	7.8612E-03	1.6008E+09	2.3403E-01	3.2232E+06	2.2951E-01	17:34	7.7731E+08	4.14	0.16		4.09	0.16	10.02	0.19	Standard
130415_Br7_grl1@1	2.06	2.0296E-03	1.4368E-02	1.9304E+09	2.3080E-01	3.9185E+06	2.3554E-01	17:38	9.3679E+08	12.18	0.29	13.80	12.14	0.29	18.12	0.22	Go74
130415_Br7_grl1@2	2.05	2.0326E-03	1.1081E-02	1.9359E+09	9.5799E-02	3.9350E+06	9.4847E-02	17:43	9.4235E+08	13.67	0.22	1.50	13.62	0.22	19.61	0.21	Go74
130415_Br7_grl1@3	2.05	2.0344E-03	1.1562E-02	1.9158E+09	9.3487E-02	3.8994E+06	8.4114E-02	17:47	9.3509E+08	14.54	0.23		14.50	0.23	20.49	0.21	Go74
130415_Br7_grl1@4	2.05	2.0321E-03	6.3894E-03	1.9441E+09	1.7510E-01	3.9509E+06	1.7558E-01	17:51	9.4681E+08	13.42	0.13		13.38	0.13	19.36	0.18	Go74
130415_Br7_grl1@5	2.06	2.0317E-03	7.5554E-03	1.8609E+09	1.5122E-01	3.7808E+06	1.4849E-01	17:56	9.0356E+08	13.22	0.15		13.18	0.15	19.16	0.19	Go74
130415_Br7_grl1@6	2.06	2.0334E-03	7.0346E-03	1.8874E+09	9.0756E-02	3.8380E+06	9.3422E-02	18:00	9.1553E+08	14.08	0.14		14.04	0.14	20.03	0.19	Go74
130415_Br7_grl1@7	2.06	2.0343E-03	9.5619E-03	1.8607E+09	3.6216E-02	3.7852E+06	4.0130E-02	18:04	9.0457E+08	14.50	0.19		14.46	0.19	20.45	0.20	Go74
130415_Br7_grl1@8	2.05	2.0332E-03	5.6310E-03	1.9362E+09	2.4568E-01	3.9369E+06	2.4437E-01	18:09	9.4401E+08	13.94	0.11		13.90	0.11	19.89	0.18	Go74
130415_Br7_grl1@9	2.05	2.0347E-03	1.0881E-02	1.8324E+09	1.1271E-01	3.7288E+06	1.1570E-01	18:13	8.9261E+08	14.70	0.22		14.66	0.22	20.65	0.20	Go74
130415_Br7_grl1@10	2.05	2.0328E-03	8.3452E-03	1.9256E+09	1.6175E-01	3.9144E+06	1.6020E-01	18:17	9.3808E+08	13.75	0.17		13.71	0.17	19.70	0.19	Go74
130415_Br7_paine@11	2.05	2.0133E-03	1.4886E-02	1.6115E+09	3.3702E-02	3.2445E+06	4.1020E-02	18:22	7.8505E+08	4.03	0.30	4.03	3.99	0.30	9.92	0.23	Standard
130415_Br7_paine@12	2.06	2.0137E-03	9.0543E-03	1.6097E+09	4.1832E-02	3.2420E+06	4.0076E-02	18:26	7.8187E+08	4.22	0.18	0.23	4.18	0.18	10.11	0.19	Standard
130415_Br7_paine@13	2.06	2.0132E-03	7.8793E-03	1.6044E+09	3.9902E-02	3.2291E+06	4.9710E-02	18:30	7.7830E+08	3.99	0.16		3.96	0.16	9.89	0.19	Standard
130415_Br7_paine@14	2.05	2.0132E-03	1.0807E-02	1.5991E+09	4.4087E-02	3.2192E+06	4.6435E-02	18:35	7.7905E+08	4.01	0.22		3.98	0.22	9.90	0.20	Standard
130415_Br7_paine@15	2.04	2.0130E-03	1.3452E-02	1.5957E+09	3.1639E-02	3.2119E+06	4.1065E-02	18:39	7.8059E+08	3.91	0.27		3.87	0.27	9.80	0.22	Standard
130415_Br7_gr5@1	2.05	2.0549E-03	1.4851E-02	1.5525E+09	5.4170E-02	3.1915E+06	6.9134E-02	18:43	7.5786E+08	24.78	0.30		24.74	0.30	30.79	0.23	Ki34s
130415_Br7_grl@1	2.05	2.0534E-03	1.1258E-02	1.5689E+09	8.0312E-02	3.2216E+06	7.9699E-02	18:48	7.6619E+08	24.04	0.23	24.57	24.01	0.23	30.05	0.21	Ki08c
130415_Br7_grl@2	2.06	2.0545E-03	8.9694E-03	1.5899E+09	4.7702E-02	3.2663E+06	4.8381E-02	18:52	7.7362E+08	24.56	0.18	2.03	24.53	0.18	30.58	0.20	Ki08c
130415_Br7_grl@3	2.06	2.0587E-03	1.0989E-02	1.5780E+09	3.6569E-02	3.2486E+06	3.9260E-02	18:56	7.6675E+08	26.69	0.22		26.66	0.22	32.72	0.21	Ki08c
130415_Br7_grl@4	2.06	2.0518E-03	1.1445E-02	1.5609E+09	8.7924E-02	3.2027E+06	8.2422E-02	19:01	7.5735E+08	23.24	0.23		23.21	0.23	29.25	0.21	Ki08c
130415_Br7_grl@5	2.05	2.0551E-03	1.5309E-02	1.5641E+09	4.3248E-02	3.2153E+06	4.1565E-02	19:05	7.6201E+08	24.90	0.31		24.87	0.31	30.92	0.23	Ki08c
130415_Br7_grl@6	2.05	2.0519E-03	1.0145E-02	1.5665E+09	5.9554E-02	3.2146E+06	6.4200E-02	19:09	7.6297E+08	23.28	0.20		23.25	0.20	29.30	0.20	Ki08c
130415_Br7_grl@7	2.05	2.0547E-03	9.3874E-03	1.5573E+09	2.2510E-02	3.1999E+06	2.6416E-02	19:13	7.6043E+08	24.68	0.19		24.65	0.19	30.70	0.20	Ki08c
130415_Br7_grl@8	2.05	2.0560E-03	1.0537E-02	1.5596E+09	4.0982E-02	3.2056E+06	4.8363E-02	19:18	7.5937E+08	25.33	0.21		25.30	0.21	31.35	0.20	Ki08c
130415_Br7_grl@9	2.06	2.0551E-03	1.0745E-02	1.5483E+09	2.6274E-02	3.1819E+06	2.8286E-02	19:22	7.5075E+08	24.88	0.21		24.85	0.21	30.90	0.21	Ki08c
130415_Br7_grl@10	2.06	2.0535E-03	1.3231E-02	1.5592E+09	6.6022E-02	3.2017E+06	6.7189E-02	19:26	7.5617E+08	24.07	0.26		24.04	0.26	30.08	0.22	Ki08c

Table A2 Continued.

SIMS ANALYSES					Mount: BR7					Analyse: $\delta^{18}O$			Value= 9.81±0.14 (VSMOW, 2σ)				Date: 13.04.2015	
130415_Br7_paine@16	2.06	2.0133E-03	9.9864E-03	1.6134E+09	6.4524E-02	3.2482E+06	6.1102E-02	19:31	7.8493E+08	4.02	0.20	3.88	3.99	0.20	9.92	0.20	Standard	
130415_Br7_paine@17	2.06	2.0129E-03	6.1700E-03	1.6248E+09	5.2735E-02	3.2706E+06	5.2544E-02	19:35	7.8979E+08	3.84	0.12	0.17	3.81	0.12	9.74	0.18	Standard	
130415_Br7_paine@18	2.06	2.0129E-03	1.4825E-02	1.6259E+09	4.7767E-02	3.2728E+06	5.4556E-02	19:39	7.8890E+08	3.86	0.30		3.83	0.30	9.76	0.23	Standard	
130415_Br7_paine@19	2.06	2.0129E-03	9.5201E-03	1.6287E+09	5.5131E-02	3.2785E+06	6.2063E-02	19:43	7.9131E+08	3.85	0.19		3.82	0.19	9.75	0.20	Standard	
130415_Br7_paine@20	2.06	2.0128E-03	6.1613E-03	1.6290E+09	5.5855E-02	3.2789E+06	5.5126E-02	19:48	7.8930E+08	3.81	0.12		3.79	0.12	9.71	0.18	Standard	
130415_Br7_gr2@1	2.07	2.0577E-03	9.5340E-03	1.5811E+09	3.7022E-02	3.2535E+06	3.6536E-02	19:52	7.6516E+08	26.16	0.19	25.38	26.14	0.19	32.20	0.20	Ki42	
130415_Br7_gr2@2	2.06	2.0557E-03	9.1871E-03	1.5577E+09	4.7364E-02	3.2019E+06	4.7538E-02	19:56	7.5686E+08	25.17	0.18	0.95	25.15	0.18	31.20	0.20	Ki42	
130415_Br7_gr2@3	2.06	2.0546E-03	1.2620E-02	1.5505E+09	7.3477E-02	3.1856E+06	7.6874E-02	20:01	7.5302E+08	24.64	0.25		24.61	0.25	30.66	0.22	Ki42	
130415_Br7_gr2@4	2.06	2.0551E-03	9.0504E-03	1.5706E+09	9.0269E-02	3.2275E+06	8.6779E-02	20:05	7.6412E+08	24.91	0.18		24.89	0.18	30.94	0.20	Ki42	
130415_Br7_gr2@5	2.06	2.0550E-03	1.0185E-02	1.5665E+09	4.0353E-02	3.2192E+06	4.3887E-02	20:09	7.5909E+08	24.85	0.20		24.83	0.20	30.88	0.20	Ki42	
130415_Br7_gr2@6	2.07	2.0570E-03	9.2942E-03	1.5488E+09	5.0414E-02	3.1858E+06	5.3561E-02	20:13	7.4882E+08	25.82	0.19		25.79	0.19	31.85	0.20	Ki42	
130415_Br7_gr2@7	2.06	2.0563E-03	9.3062E-03	1.5546E+09	5.4166E-02	3.1955E+06	4.6993E-02	20:18	7.5352E+08	25.48	0.19		25.46	0.19	31.51	0.20	Ki42	
130415_Br7_gr2@8	2.07	2.0564E-03	7.7441E-03	1.5436E+09	3.0539E-02	3.1743E+06	2.9880E-02	20:22	7.4667E+08	25.53	0.15		25.51	0.15	31.57	0.19	Ki42	
130415_Br7_gr2@9	2.06	2.0567E-03	1.0821E-02	1.5721E+09	7.9637E-02	3.2348E+06	7.1863E-02	20:26	7.6231E+08	25.69	0.22		25.67	0.22	31.73	0.21	Ki42	
130415_Br7_gr2@10	2.07	2.0564E-03	7.8830E-03	1.5536E+09	6.1468E-02	3.1946E+06	6.7371E-02	20:31	7.5230E+08	25.52	0.16		25.50	0.16	31.56	0.19	Ki42	
130415_Br7_paine@21	2.06	2.0135E-03	8.2644E-03	1.6395E+09	2.9975E-02	3.3004E+06	3.9715E-02	20:35	7.9542E+08	4.14	0.17	3.82	4.12	0.17	10.05	0.19	Standard	
130415_Br7_paine@22	2.07	2.0127E-03	1.0541E-02	1.6386E+09	6.2560E-02	3.2978E+06	6.3786E-02	20:39	7.9236E+08	3.72	0.21	0.41	3.70	0.21	9.62	0.20	Standard	
130415_Br7_paine@23	2.07	2.0130E-03	1.0813E-02	1.6413E+09	4.8296E-02	3.3039E+06	5.0713E-02	20:43	7.9121E+08	3.89	0.22		3.87	0.22	9.80	0.20	Standard	
130415_Br7_paine@24	2.07	2.0126E-03	7.8604E-03	1.6408E+09	4.0344E-02	3.3023E+06	3.9668E-02	20:48	7.9402E+08	3.71	0.16		3.70	0.16	9.62	0.19	Standard	
130415_Br7_paine@25	2.07	2.0125E-03	9.1706E-03	1.6240E+09	3.9576E-02	3.2685E+06	3.9593E-02	20:52	7.8483E+08	3.63	0.18		3.61	0.18	9.54	0.19	Standard	
130415_Br7_gr3@1	2.06	2.0537E-03	9.9265E-03	1.5711E+09	4.7466E-02	3.2263E+06	4.8092E-02	20:56	7.6296E+08	24.21	0.20	24.42	24.19	0.20	30.24	0.20	Ki03c	
130415_Br7_gr3@2	2.07	2.0550E-03	9.3157E-03	1.5448E+09	6.5358E-02	3.1743E+06	6.3441E-02	21:01	7.4770E+08	24.83	0.19	1.36	24.81	0.19	30.87	0.20	Ki03c	
130415_Br7_gr3@3	2.07	2.0543E-03	6.2825E-03	1.5344E+09	4.1491E-02	3.1516E+06	4.5539E-02	21:05	7.4098E+08	24.47	0.13		24.45	0.13	30.50	0.19	Ki03c	
130415_Br7_gr3@4	2.07	2.0560E-03	1.0020E-02	1.5543E+09	5.0174E-02	3.1956E+06	5.1811E-02	21:09	7.5043E+08	25.33	0.20		25.32	0.20	31.37	0.20	Ki03c	
130415_Br7_gr3@5	2.07	2.0534E-03	1.6693E-02	1.5466E+09	2.4248E-02	3.1764E+06	2.9871E-02	21:13	7.4871E+08	24.06	0.33		24.04	0.33	30.09	0.24	Ki03c	
130415_Br7_gr3@6	2.06	2.0539E-03	8.9509E-03	1.5508E+09	6.4003E-02	3.1855E+06	6.5277E-02	21:18	7.5303E+08	24.28	0.18		24.26	0.18	30.31	0.20	Ki03c	
130415_Br7_gr3@7	2.06	2.0561E-03	1.2948E-02	1.5577E+09	3.7181E-02	3.2035E+06	3.7255E-02	21:22	7.5509E+08	25.36	0.26		25.35	0.26	31.40	0.22	Ki03c	
130415_Br7_gr3@8	2.07	2.0527E-03	1.1367E-02	1.5531E+09	5.4693E-02	3.1880E+06	5.8873E-02	21:26	7.5171E+08	23.66	0.23		23.65	0.23	29.70	0.21	Ki03c	
130415_Br7_gr3@9	2.07	2.0548E-03	8.4085E-03	1.5557E+09	2.3984E-02	3.1966E+06	2.3769E-02	21:31	7.5168E+08	24.74	0.17		24.73	0.17	30.78	0.19	Ki03c	
130415_Br7_gr3@10	2.07	2.0518E-03	6.2550E-03	1.5495E+09	2.4479E-02	3.1792E+06	2.5309E-02	21:35	7.4879E+08	23.23	0.13		23.22	0.13	29.26	0.18	Ki03c	
130415_Br7_paine@26	2.06	2.0133E-03	1.0319E-02	1.6243E+09	5.5448E-02	3.2699E+06	5.8223E-02	21:39	7.8960E+08	4.03	0.21	3.83	4.02	0.21	9.94	0.20	Standard	
130415_Br7_paine@27	2.05	2.0126E-03	7.6468E-03	1.6159E+09	5.8938E-02	3.2525E+06	6.0901E-02	21:44	7.8657E+08	3.70	0.15	0.25	3.69	0.15	9.62	0.19	Standard	
130415_Br7_paine@28	2.06	2.0127E-03	1.1305E-02	1.6212E+09	5.3563E-02	3.2639E+06	4.5590E-02	21:48	7.8877E+08	3.76	0.23		3.75	0.23	9.68	0.20	Standard	
130415_Br7_paine@29	2.06	2.0130E-03	9.3745E-03	1.6257E+09	7.3638E-02	3.2723E+06	7.0757E-02	21:52	7.8898E+08	3.88	0.19		3.87	0.19	9.80	0.19	Standard	
130415_Br7_paine@30	2.06	2.0128E-03	1.1083E-02	1.6261E+09	4.9226E-02	3.2729E+06	4.8042E-02	21:56	7.8905E+08	3.79	0.22		3.78	0.22	9.71	0.20	Standard	
130415_Br7_gr4@1	2.06	2.0418E-03	1.2718E-02	1.5370E+09	3.6428E-02	3.1383E+06	3.6716E-02	22:01	7.4791E+08	18.27	0.25	19.85	18.26	0.25	24.27	0.22	Ki57	
130415_Br7_gr4@2	2.06	2.0468E-03	1.1904E-02	1.5337E+09	4.1215E-02	3.1393E+06	4.5267E-02	22:05	7.4490E+08	20.75	0.24	6.32	20.75	0.24	26.78	0.21	Ki57	
130415_Br7_gr4@3	2.06	2.0298E-03	1.6670E-02	1.5830E+09	9.4649E-02	3.2132E+06	9.4160E-02	22:09	7.6971E+08	12.27	0.33						Ki57	Optical rejection
130415_Br7_gr4@4	2.06	2.0482E-03	8.9288E-03	1.5427E+09	3.2754E-02	3.1595E+06	3.1420E-02	22:14	7.4833E+08	21.43	0.18		21.42	0.18	27.45	0.20	Ki57	
130415_Br7_gr4@5	2.07	2.0455E-03	1.0884E-02	1.5673E+09	4.2129E-02	3.2057E+06	4.7898E-02	22:18	7.5758E+08	20.11	0.22		20.10	0.22	26.13	0.21	Ki57	
130415_Br7_gr4@6	2.06	2.0524E-03	8.9179E-03	1.5764E+09	4.1225E-02	3.2345E+06	4.7880E-02	22:22	7.6548E+08	23.52	0.18		23.52	0.18	29.56	0.20	Ki57	
130415_Br7_gr4@7	2.07	2.0494E-03	9.4479E-03	1.5644E+09	6.2714E-02	3.2064E+06	5.8429E-02	22:27	7.5622E+08	22.06	0.19		22.05	0.19	28.09	0.20	Ki57	
130415_Br7_gr4@8	2.06	2.0426E-03	1.1356E-02	1.5558E+09	5.7892E-02	3.1778E+06	6.1339E-02	22:31	7.5380E+08	18.63	0.23		18.63	0.23	24.64	0.21	Ki57	
130415_Br7_gr4@9	2.07	2.0500E-03	1.3074E-02	1.5618E+09	3.3990E-02	3.2016E+06	3.8277E-02	22:35	7.5467E+08	22.33	0.26		22.33	0.26	28.36	0.22	Ki57	
130415_Br7_gr4@10	2.07	2.0436E-03	9.3365E-03	1.5385E+09	3.3097E-02	3.1439E+06	3.1000E-02	22:39	7.4468E+08	19.15	0.19		19.15	0.19	25.16	0.20	Ki57	
130415_Br7_paine@31	2.06	2.0127E-03	1.2704E-02	1.6355E+09	4.3566E-02	3.2923E+06	4.0634E-02	22:44	7.9246E+08	3.73	0.25	3.91	3.73	0.25	9.65	0.21	Standard	
130415_Br7_paine@32	2.06	2.0131E-03	6.1475E-03	1.6364E+09	4.8020E-02	3.2939E+06	4.7674E-02	22:48	7.9332E+08	3.94	0.12	0.28	3.94	0.12	9.87	0.18	Standard	
130415_Br7_paine@33	2.06	2.0132E-03	1.3488E-02	1.6398E+09	4.4770E-02	3.3013E+06	4.8020E-02	22:52	7.9605E+08	4.00	0.27		4.01	0.27	9.93	0.22	Standard	
130415_Br7_paine@34	2.06	2.0134E-03	1.0335E-02	1.6373E+09	5.2963E-02	3.2961E+06	5.3691E-02	22:57	7.9440E+08	4.07	0.21		4.07	0.21	10.00	0.20	Standard	
130415_Br7_paine@35	2.06	2.0128E-03	1.1630E-02	1.6344E+09	5.1662E-02	3.2886E+06	4.9216E-02	23:01	7.9251E+08	3.81	0.23		3.81	0.23	9.74	0.21	Standard	
130415_Br7_gr6@1	2.06	2.0409E-03	6.2150E-03	1.5784E+09	3.1588E-02	3.2216E+06	3.3336E-02	23:05	7.6522E+08	17.82	0.12	18.89	17.82	0.12	23.83	0.18	Ki34s	
130415_Br7_gr6@2	2.06	2.0478E-03	1.0634E-02	1.5464E+09	4.5610E-02	3.1664E+06	4.5263E-02	23:10	7.5072E+08	21.26	0.21	6.36	21.26	0.21	27.29	0.20	Ki34s	
130415_Br7_gr6@3	2.05	2.0443E-03	1.4171E-02	1.5584E+09	3.6849E-02	3.1850E+06	4.8582E-02	23:14	7.6028E+08	19.48	0.28		19.48	0.28	25.50	0.23	Ki34s	
130415_Br7_gr6@4	2.05	2.0453E-03	1.0290E-02	1.5412E+09	5.5255E-02	3.1520E+06	5.9955E-02	23:18	7.5074E+08	19.98	0.21		19.98	0.21	26.00	0.20	Ki34s	
130415_Br7_gr6@5	2.06	2.0491E-03	1.4270E-02	1.5255E+09	5.5228E-02	3.1260E+06	5.4152E-02	23:23	7.4195E+08	21.91	0.29		21.91	0.29	27.94	0.23	Ki34s	
130415_Br7_gr6@6	2.06	2.0275E-03	1.2054E-02	1.5431E+09	5.5999E-02	3.1297E+06	4.4519E-02	23:27	7.4904E+08	11.12	0.24						Ki34s	Optical rejection
130415_Br7_gr6@7	2.06	2.0420E-03	1.2947E-02	1.5812E+09	3.1247E-02	3.2287E+06	3.3753E-02	23:31	7.6575E+08	18.33	0.26		18.34	0.26	24.35	0.22	Ki34s	
130415_Br7_gr6@8	2.06	2.0459E-03	9.3083E-03	1.5531E+09	3.6190E-02	3.1769E+06	4.5820E-02	23:35	7.5285E+08	20.28	0.19		20.29	0.19	26.31	0.20	Ki34s	
130415_Br7_gr6@9	2.06	2.0450E-03	9.8072E-03	1.5632E+09	2.0241E-01	3.1965E+06	2.0242E-01	23:40	7.5951E+08	19.87	0.20		19.88	0.20	25.90	0.20	Ki34s	
130415_Br7_paine@36	2.06	2.0132E-03	1.0386E-02	1.6526E+09	2.1380E-01	3.3269E+06	2.1489E-01	23:44	8.0411E+08	3.97	0.21	3.87	3.97	0.21	9.90	0.20	Standard	
130415_Br7_paine@37	2.06	2.0127E-03	6.7732E-03	1.6447E+09	5.8738E-02	3.3106E+06	6.1652E-02	23:48	7.9692E+08	3.74	0.14	0.27	3.75	0.14	9.68	0.18	Standard	
130415_Br7_paine@38	2.17	2.0129E-03	8.1895E-03	1.6499E+09	2.1244E-01	3.3163E+06	1.6864E-01	23:53	7.5996E+08	3.82	0.16		3.83	0.16	9.76	0.19	Standard	
130415_Br7_paine@39	2.07	2.0133E-03	1.1682E-02	1.6326E+09	7.2361E-02	3.2867E+06	7.6305E-02	23:57	7.8849E+08	4.06	0.23		4.07	0.23	10.00	0.21	Standard	
130415_Br7_paine@40	2.07	2.0128E-03	7.6518E-03	1.6279E+09	6.6299E-02	3.2764E+06	6.5476E-02	0:01	7.8583E+08	3.78	0.15		3.79	0.15	9.72	0.19	Standard	

Table A2 Continued.

SIMS ANALYSES						Mount: BR7						Analyse: $\delta^{18}O$			Value= 9.81±0.14 (VSMOW, 2σ)			Date: 13.04.2015
130415_Br7_gr7@1	2.07	2.0413E-03	8.8205E-03	1.5661E+09	5.8303E-02	3.1966E+06	5.6438E-02	0:06	7.5792E+08	18.02	0.18	17.96	18.03	0.18	24.04	0.19	Pe01
130415_Br7_gr7@2	2.06	2.0410E-03	1.0961E-02	1.5958E+09	6.4633E-02	3.2569E+06	6.6764E-02	0:10	7.7412E+08	17.84	0.22	0.34	17.85	0.22	23.86	0.21	Pe01
130415_Br7_gr7@3	2.07	2.0412E-03	9.8403E-03	1.5723E+09	4.5831E-02	3.2091E+06	5.1200E-02	0:14	7.5918E+08	17.95	0.20		17.96	0.20	23.97	0.20	Pe01
130415_Br7_gr7@4	2.07	2.0412E-03	1.1121E-02	1.5746E+09	4.8306E-02	3.2144E+06	5.3019E-02	0:18	7.6133E+08	17.96	0.22		17.98	0.22	23.99	0.21	Pe01
130415_Br7_gr7@5	2.07	2.0406E-03	1.2653E-02	1.5985E+09	4.8293E-02	3.2618E+06	5.1178E-02	0:23	7.7276E+08	17.64	0.25		17.66	0.25	23.67	0.22	Pe01
130415_Br7_gr7@6	2.07	2.0415E-03	9.3514E-03	1.6024E+09	4.4068E-02	3.2716E+06	4.4293E-02	0:27	7.7561E+08	18.12	0.19		18.14	0.19	24.15	0.20	Pe01
130415_Br7_gr7@7	2.07	2.0408E-03	1.0383E-02	1.6000E+09	6.6089E-02	3.2653E+06	6.7677E-02	0:31	7.7443E+08	17.76	0.21		17.78	0.21	23.79	0.20	Pe01
130415_Br7_gr7@8	2.06	2.0415E-03	1.1854E-02	1.6001E+09	5.6244E-02	3.2655E+06	6.4100E-02	0:36	7.7765E+08	18.13	0.24		18.14	0.24	24.15	0.21	Pe01
130415_Br7_gr7@9	2.06	2.0414E-03	1.0626E-02	1.6122E+09	4.0327E-02	3.2912E+06	4.1317E-02	0:40	7.8135E+08	18.05	0.21		18.06	0.21	24.07	0.20	Pe01
130415_Br7_gr7@10	2.08	2.0416E-03	1.1729E-02	1.6019E+09	4.0470E-02	3.2706E+06	4.0700E-02	0:44	7.7115E+08	18.15	0.23		18.16	0.23	24.18	0.21	Pe01
130415_Br7_paine@41	2.07	2.0128E-03	1.3816E-02	1.6287E+09	5.9794E-02	3.2783E+06	6.2528E-02	0:49	7.8652E+08	3.78	0.28	3.77	3.80	0.28	9.73	0.22	Standard
130415_Br7_paine@42	2.07	2.0126E-03	7.5271E-03	1.6392E+09	4.5352E-02	3.2993E+06	4.7950E-02	0:53	7.9292E+08	3.71	0.15	0.19	3.72	0.15	9.65	0.19	Standard
130415_Br7_paine@43	2.07	2.0128E-03	9.2617E-03	1.6376E+09	5.8778E-02	3.2960E+06	5.9020E-02	0:57	7.9138E+08	3.79	0.19		3.81	0.19	9.74	0.19	Standard
130415_Br7_paine@44	2.07	2.0130E-03	9.7547E-03	1.6455E+09	3.9894E-02	3.3121E+06	3.7300E-02	1:01	7.9671E+08	3.91	0.20		3.93	0.20	9.86	0.20	Standard
130415_Br7_paine@45	2.07	2.0126E-03	8.6098E-03	1.6485E+09	6.6983E-02	3.3179E+06	6.9927E-02	1:06	7.9613E+08	3.67	0.17		3.69	0.17	9.61	0.19	Standard
130415_Br7_gr8@1	2.06	2.0532E-03	8.5815E-03	1.6223E+09	4.9841E-02	3.3308E+06	5.3542E-02	1:10	7.8637E+08	23.92	0.17	24.14	23.94	0.17	29.98	0.19	Ki32
130415_Br7_gr8@2	2.06	2.0541E-03	1.1149E-02	1.6078E+09	5.2423E-02	3.3033E+06	4.6199E-02	1:14	7.8098E+08	24.36	0.22	1.85	24.39	0.22	30.43	0.21	Ki32
130415_Br7_gr8@3	2.06	2.0520E-03	7.9640E-03	1.6277E+09	3.8489E-02	3.3393E+06	4.3619E-02	1:19	7.8876E+08	23.35	0.16		23.37	0.16	29.41	0.19	Ki32
130415_Br7_gr8@4	2.07	2.0543E-03	1.0085E-02	1.6220E+09	2.5417E-02	3.3322E+06	2.4774E-02	1:23	7.8536E+08	24.48	0.20		24.50	0.20	30.55	0.20	Ki32
130415_Br7_gr8@5	2.07	2.0506E-03	1.2488E-02	1.6669E+09	7.7570E-02	3.4182E+06	7.7270E-02	1:27	8.0500E+08	22.63	0.25		22.65	0.25	28.69	0.22	Ki32
130415_Br7_gr8@6	2.07	2.0531E-03	9.1190E-03	1.6428E+09	5.5861E-02	3.3731E+06	5.4879E-02	1:32	7.9195E+08	23.89	0.18		23.92	0.18	29.96	0.20	Ki32
130415_Br7_gr8@7	2.07	2.0541E-03	1.1963E-02	1.6495E+09	4.1713E-02	3.3881E+06	4.4912E-02	1:36	7.9814E+08	24.37	0.24		24.39	0.24	30.44	0.21	Ki32
130415_Br7_gr8@8	2.07	2.0578E-03	1.0719E-02	1.6624E+09	4.3636E-02	3.4206E+06	4.5450E-02	1:40	8.0384E+08	26.21	0.21		26.24	0.21	32.30	0.21	Ki32
130415_Br7_gr8@9	2.07	2.0530E-03	1.0507E-02	1.6278E+09	5.7073E-02	3.3430E+06	5.3047E-02	1:45	7.8554E+08	23.84	0.21		23.87	0.21	29.92	0.20	Ki32
130415_Br7_gr8@10	2.07	2.0541E-03	1.2091E-02	1.6262E+09	2.8954E-02	3.3406E+06	2.7718E-02	1:49	7.8523E+08	24.37	0.24		24.40	0.24	30.45	0.21	Ki32
130415_Br7_paine@46	2.07	2.0131E-03	1.2332E-02	1.6530E+09	5.8693E-02	3.3280E+06	5.7706E-02	1:53	7.9834E+08	3.94	0.25	3.98	3.97	0.25	9.89	0.21	Standard
130415_Br7_paine@47	2.07	2.0131E-03	1.1541E-02	1.6508E+09	5.7534E-02	3.3235E+06	5.9458E-02	1:58	7.9616E+08	3.95	0.23	0.19	3.97	0.23	9.90	0.21	Standard
130415_Br7_paine@48	2.08	2.0135E-03	1.3465E-02	1.6573E+09	6.4496E-02	3.3366E+06	7.0916E-02	2:02	7.9825E+08	4.12	0.27		4.15	0.27	10.08	0.22	Standard
130415_Br7_paine@49	2.08	2.0133E-03	7.7254E-03	1.6574E+09	4.1213E-02	3.3368E+06	4.0021E-02	2:06	7.9871E+08	4.04	0.15		4.07	0.15	10.00	0.19	Standard
130415_Br7_paine@50	2.07	2.0130E-03	1.2734E-02	1.6527E+09	4.0470E-02	3.3269E+06	4.2480E-02	2:10	7.9723E+08	3.88	0.25		3.91	0.25	9.84	0.21	Standard
130415_Br7_gr9@1	2.06	2.0564E-03	1.1235E-02	1.6054E+09	5.6043E-02	3.3015E+06	5.2745E-02	2:15	7.7760E+08	25.54	0.22	26.49	25.57	0.22	31.63	0.21	ki46
130415_Br7_gr9@2	2.07	2.0538E-03	9.3720E-03	1.5845E+09	2.4793E-02	3.2544E+06	2.5093E-02	2:19	7.6501E+08	24.24	0.19	3.14	24.27	0.19	30.32	0.20	ki46
130415_Br7_gr9@3	2.07	2.0580E-03	1.0464E-02	1.6183E+09	5.8910E-02	3.3305E+06	5.7868E-02	2:23	7.8278E+08	26.34	0.21		26.37	0.21	32.43	0.20	ki46
130415_Br7_gr9@4	2.07	2.0582E-03	7.5584E-03	1.6106E+09	4.7902E-02	3.3150E+06	4.9974E-02	2:28	7.7664E+08	26.41	0.15		26.45	0.15	32.51	0.19	ki46
130415_Br7_gr9@5	2.08	2.0626E-03	1.1232E-02	1.6063E+09	4.5119E-02	3.3132E+06	4.6286E-02	2:32	7.7397E+08	28.64	0.22		28.67	0.22	34.75	0.21	ki46
130415_Br7_gr9@6	2.08	2.0580E-03	6.8604E-03	1.5841E+09	2.9735E-02	3.2602E+06	3.0569E-02	2:36	7.6223E+08	26.32	0.14		26.35	0.14	32.41	0.19	ki46
130415_Br7_gr9@7	2.07	2.0581E-03	8.7777E-03	1.6002E+09	4.0477E-02	3.2936E+06	4.2022E-02	2:41	7.7308E+08	26.37	0.18		26.41	0.18	32.47	0.20	ki46
130415_Br7_gr9@8	2.06	2.0556E-03	1.1961E-02	1.5942E+09	3.3051E-02	3.2762E+06	4.3569E-02	2:45	7.7219E+08	25.11	0.24		25.15	0.24	31.20	0.21	ki46
130415_Br7_gr9@9	2.07	2.0579E-03	9.9090E-03	1.6120E+09	4.3813E-02	3.3174E+06	4.5560E-02	2:49	7.7981E+08	26.29	0.20		26.32	0.20	32.38	0.20	ki46
130415_Br7_gr9@10	2.07	2.0645E-03	9.0001E-03	1.6200E+09	3.7845E-02	3.3436E+06	4.1604E-02	2:54	7.8237E+08	29.58	0.18		29.62	0.18	35.70	0.20	ki46
130415_Br7_paine@51	2.06	2.0125E-03	1.1195E-02	1.6448E+09	4.5930E-02	3.3101E+06	4.4786E-02	2:58	7.9722E+08	3.66	0.22	3.88	3.69	0.22	9.62	0.20	Standard
130415_Br7_paine@52	2.07	2.0127E-03	1.1705E-02	1.6522E+09	4.8040E-02	3.3257E+06	4.9590E-02	3:02	7.9950E+08	3.72	0.23	0.41	3.76	0.23	9.69	0.21	Standard
130415_Br7_paine@53	2.07	2.0135E-03	9.2992E-03	1.6541E+09	4.6044E-02	3.3297E+06	4.1375E-02	3:07	8.0069E+08	4.12	0.19		4.16	0.19	10.09	0.19	Standard
130415_Br7_paine@54	2.07	2.0129E-03	7.9538E-03	1.6585E+09	5.4004E-02	3.3396E+06	4.9118E-02	3:11	8.0312E+08	3.84	0.16		3.87	0.16	9.80	0.19	Standard
130415_Br7_paine@55	2.07	2.0133E-03	6.1137E-03	1.6545E+09	4.8793E-02	3.3311E+06	5.0242E-02	3:15	7.9990E+08	4.05	0.12		4.09	0.12	10.02	0.18	Standard
130415_Br7_gr10@1	2.07	2.0510E-03	1.0000E-02	1.6475E+09	5.5959E-02	3.3790E+06	5.7198E-02	3:20	7.9631E+08	22.83	0.20	24.82	22.87	0.20	28.91	0.20	Ki01
130415_Br7_gr10@2	2.07	2.0542E-03	9.2442E-03	1.6333E+09	4.1036E-02	3.3560E+06	3.8015E-02	3:24	7.8940E+08	24.44	0.18	2.75	24.48	0.18	30.53	0.20	Ki01
130415_Br7_gr10@3	2.07	2.0543E-03	6.6651E-03	1.6308E+09	4.7081E-02	3.3505E+06	4.9811E-02	3:28	7.8900E+08	24.50	0.13		24.54	0.13	30.59	0.19	Ki01
130415_Br7_gr10@4	2.07	2.0557E-03	6.4748E-03	1.6357E+09	4.9818E-02	3.3625E+06	4.8193E-02	3:33	7.9026E+08	25.19	0.13		25.23	0.13	31.29	0.19	Ki01
130415_Br7_gr10@5	2.07	2.0559E-03	1.2957E-02	1.6463E+09	6.8035E-02	3.3844E+06	6.9672E-02	3:37	7.9599E+08	25.29	0.26		25.33	0.26	31.38	0.22	Ki01
130415_Br7_gr10@6	2.07	2.0551E-03	1.2335E-02	1.6492E+09	4.5291E-02	3.3881E+06	5.5411E-02	3:41	7.9534E+08	24.88	0.25		24.92	0.25	30.97	0.21	Ki01
130415_Br7_gr10@7	2.07	2.0617E-03	8.6618E-03	1.6357E+09	5.3595E-02	3.3723E+06	5.3639E-02	3:46	7.9131E+08	28.19	0.17		28.23	0.17	34.30	0.20	Ki01
130415_Br7_gr10@8	2.07	2.0540E-03	1.1271E-02	1.6328E+09	5.5840E-02	3.3539E+06	6.0428E-02	3:50	7.8762E+08	24.36	0.23		24.40	0.23	30.45	0.21	Ki01
130415_Br7_gr10@9	2.07	2.0531E-03	1.0015E-02	1.6296E+09	4.5858E-02	3.3447E+06	5.5887E-02	3:54	7.8910E+08	23.87	0.20		23.92	0.20	29.96	0.20	Ki01
130415_Br7_gr10@10	2.07	2.0546E-03	1.0142E-02	1.6624E+09	7.1304E-02	3.4159E+06	7.5395E-02	3:59	8.0425E+08	24.63	0.20		24.67	0.20	30.72	0.20	Ki01
130415_Br7_paine@56	2.07	2.0132E-03	1.3634E-02	1.6603E+09	4.6575E-02	3.3425E+06	4.7470E-02	4:03	8.0166E+08	4.01	0.27	3.86	4.06	0.27	9.99	0.22	Standard
130415_Br7_paine@57	2.07	2.0128E-03	1.2699E-02	1.6424E+09	5.0568E-02	3.3058E+06	5.7074E-02	4:07	7.9180E+08	3.79	0.25	0.39	3.83	0.25	9.76	0.21	Standard
130415_Br7_paine@58	2.07	2.0132E-03	1.2540E-02	1.6405E+09	4.5179E-02	3.3017E+06	4.9661E-02	4:12	7.9153E+08	4.01	0.25		4.06	0.25	9.99	0.21	Standard
130415_Br7_paine@59	2.07	2.0135E-03	1.2256E-02	1.6461E+09	5.1195E-02	3.3145E+06	5.4455E-02	4:16	7.9400E+08	4.12	0.25		4.17	0.25	10.10	0.21	Standard
130415_Br7_paine@60	2.07	2.0130E-03	8.9796E-03	1.6371E+09	2.9047E-02	3.2954E+06	3.1532E-02	4:20	7.9010E+08	3.87	0.18		3.92	0.18	9.85	0.19	Standard
130415_Br7_paine@61	2.07	2.0129E-03	1.0915E-02	1.6307E+09	5.8448E-02	3.2828E+06	5.7201E-02	4:25	7.8927E+08	3.86	0.22		3.91	0.22	9.84	0.20	Standard
130415_Br7_paine@62	2.07	2.0126E-03	6.7828E-03	1.6309E+09	4.9124E-02	3.2829E+06	5.0105E-02	4:29	7.8616E+08	3.70	0.14		3.75	0.14	9.68	0.18	Standard
130415_Br7_paine@63	2.07	2.0122E-03	9.6890E-03	1.6269E+09	2.7193E-02	3.2740E+06	3.2466E-02	4:33	7.8647E+08	3.50	0.19		3.55	0.19	9.48	0.20	Standard

SIMS を用いた中生代放散虫岩の酸素同位体分析

Maximilien BÔLE・池田　昌之・Peter O. BAUMGARTNER・堀　利栄・
Anne-Sophie BOUVIER・Duje KUKOČ

要　旨

化石殻の炭酸カルシウムの酸素同位体比（$\delta^{18}O$）を用いた古海洋研究が広く用いられているが，珪質化石殻については分析の制約や同位体分別の不確定性等のため，古海洋研究への適用例は限られている．本論では，二次イオン質量分析計（SIMS）によって測定した日本，イタリア，スイス，ルーマニアの中生代チャートに含まれる放散虫化石 $\delta^{18}O$ 変動の古海洋指標としての有用性について報告する．53 試料 507 点の測定の結果，放散虫殻 $\delta^{18}O$ は 19.8 ～ 35.3 ‰で，現世及び新生代の放散虫殻の値と調和的であり，標準試料 UNIL-Q1 の繰り返し測定誤差 0.3 ‰以上に 1 チャート試料中の $\delta^{18}O$ 変化がみられる．このことから，続成作用（セグリゲーション）の影響による均一化は完全ではなく，初生的な値が保存されている可能性を支持する．さらに，予察的な放散虫化石の $\delta^{18}O$ 記録は低解像度にもかかわらず，1,000 万年スケールではコノドントのアパタイトや低 Mg 炭酸塩殻に確認される前期－中期三畳紀の正のシフトや後期三畳紀の安定した高い値と調和的であるが，前期ジュラ紀のパンサラッサ海遠洋域における放散虫化石 $\delta^{18}O$ の約 8 ‰の負のシフトはテチス海沿岸域の低 Mg 炭酸塩殻には確認されない．さらに高解像度で他指標と比較することで，放散虫化石の $\delta^{18}O$ 記録の古海洋学的意義をより深く理解できると期待される．